

Optimal Stopping and Switching Problems with Financial Applications

Zheng Wang

Submitted in partial fulfillment of the
requirements for the degree
of Doctor of Philosophy
in the Graduate School of Arts and Sciences

COLUMBIA UNIVERSITY

2017

©2016

Zheng Wang

All Rights Reserved

ABSTRACT

Optimal Stopping and Switching Problems with Financial Applications

Zheng Wang

This dissertation studies a collection of problems on trading assets and derivatives over finite and infinite horizons. In the first part, we analyze an optimal switching problem with transaction costs that involves an infinite sequence of trades. The investor's value functions and optimal timing strategies are derived when prices are driven by an exponential Ornstein-Uhlenbeck (XOU) or Cox-Ingersoll-Ross (CIR) process. We compare the findings to the results from the associated optimal double stopping problems and identify the conditions under which the double stopping and switching problems admit the same optimal entry and/or exit timing strategies.

Our results show that when prices are driven by a CIR process, optimal strategies for the switching problems are of the classic buy-low-sell-high type. On the other hand, under XOU price dynamics, the investor should refrain from entering the market if the current price is very close to zero. As a result, the continuation (waiting) region for entry is disconnected. In both models, we provide numerical examples to illustrate the dependence of timing strategies on model parameters.

In the second part, we study the problem of trading futures with transaction costs when the underlying spot price is mean-reverting. Specifically, we model the spot dynamics by the OU, CIR or XOU model. The futures term structure is derived and its connection to futures price dynamics is examined.

For each futures contract, we describe the evolution of the roll yield, and compute explicitly the expected roll yield. For the futures trading problem, we incorporate the investor's timing options to enter and exit the market, as well as a chooser option to long or short a futures upon entry. This leads us to formulate and solve the corresponding optimal double stopping problems to determine the optimal trading strategies. Numerical results are presented to illustrate the optimal entry and exit boundaries under different models. We find that the option to choose between a long or short position induces the investor to delay market entry, as compared to the case where the investor pre-commits to go either long or short.

Finally, we analyze the optimal risk-averse timing to sell a risky asset. The investor's risk preference is described by the exponential, power or log utility. Two stochastic models are considered for the asset price – the geometric Brownian motion (GBM) and XOU models to account for, respectively, the trending and mean-reverting price dynamics. In all cases, we derive the optimal thresholds and certainty equivalents to sell the asset, and compare them across models and utilities, with emphasis on their dependence on asset price, risk aversion, and quantity. We find that the timing option may render the investor's value function and certainty equivalent non-concave in price even though the utility function is concave in wealth. Numerical results are provided to illustrate the investor's optimal strategies and the premia associated with optimally timing to sell with different utilities under different price dynamics.

Table of Contents

List of Figures	iv
List of Tables	v
1 Introduction	1
1.1 Optimal Switching under XOU and CIR Dynamics with Transaction Costs	1
1.2 Speculative Futures Trading under Mean Reversion	5
1.3 Optimal Risk Averse Timing of an Asset Sale	8
2 Optimal Switching under XOU and CIR Dynamics with Transaction Costs	12
2.1 Problem Overview	13
2.1.1 Optimal Double Stopping Problem	14
2.1.2 Optimal Switching Problem	16
2.2 Summary of Analytical Results	17
2.2.1 XOU Model	17
2.2.2 CIR model	26
2.3 Methods of Solution and Proofs	34
2.3.1 Optimal Switching Timing under the XOU Model	34
2.3.2 Optimal Switching Timing under the CIR Model	46

3	Speculative Futures Trading under Mean Reversion	48
3.1	Futures Prices and Term Structures	49
3.1.1	OU and CIR Spot Models	49
3.1.2	XOU Spot Model	53
3.2	Roll Yield	58
3.2.1	OU and CIR Spot Models	60
3.2.2	XOU Spot Model	61
3.3	Optimal Timing to Trade Futures	63
3.3.1	Optimal Double Stopping Approach	64
3.3.2	Variational Inequalities & Optimal Trading Strategies	66
3.4	Conclusion	73
4	Optimal Risk Averse Timing of an Asset Sale	75
4.1	Problem Overview	76
4.2	Optimal Timing Strategies	79
4.2.1	The GBM Model	79
4.2.2	The XOU Model	84
4.3	Certainty Equivalents	89
4.4	Methods of Solution and Proofs	95
4.4.1	GBM Model	95
4.4.2	XOU Model	101
	Bibliography	108
	A Appendix for GBM Example	117
	B Appendix for Chapter 2	119
B.1	Proof of Lemma 2.2.5 (Bounds of \tilde{J}^ξ and \tilde{V}^ξ)	119
B.2	Proof of Lemma 2.2.12 (Bounds of \tilde{J}^x and \tilde{V}^x)	120

C Appendix for Chapter 3	122
C.1 Numerical Implementation	122

List of Figures

2.1	The optimal levels vs speed of mean reversion under XOU model	24
2.2	The optimal levels vs transaction cost c_b under XOU model . .	25
2.3	A sample XOU path with optimal levels	27
2.4	The optimal levels vs speed of mean reversion under CIR model	34
2.5	A sample CIR path with optimal levels	35
3.1	Calibration of VIX futures prices	57
3.2	Optimal boundaries for futures trading under the CIR model .	69
3.3	Comparison of optimal boundaries under the CIR model . . .	70
3.4	Optimal boundaries with transaction costs under OU and XOU models	71
3.5	The value functions \mathcal{P} , \mathcal{A} , and \mathcal{B} vs spot price	72
4.1	Value functions and utilities under the GBM model	82
4.2	Optimal selling thresholds under the GBM model vs quantity	82
4.3	Value functions and optimal selling thresholds under the XOU model	88
4.4	Certainty equivalent vs price	93
4.5	Liquidation premium $L(z, \nu)$ under the XOU model	94

List of Tables

4.1 Optimal thresholds for asset sale 89

Acknowledgments

I wish to express the deepest gratitude to my advisor, Professor Tim Leung, for his mentorship. This dissertation would not be possible without Professor Leung's constant support and guidance over the past five years. Pursuing a doctoral degree is a challenging endeavor and Professor Leung was beside me every step of the way. His passion, confidence and optimism has greatly inspired me. I am very fortunate to be able to work with him.

I am grateful for the wonderful opportunity to study at the Department of Industrial Engineering and Operations Research at Columbia University. I worked alongside exceptional academic researchers and forged friendships with some of the most brilliant people whom I have had the privilege of knowing. The courses I have taken at Columbia enriched my education and equipped me with the skills and knowledge to undertake doctoral research. I have also had the pleasure of serving as a teaching assistant for many graduate courses. I thank Professor David Yao, Professor Donald Goldfarb, Professor Cliff Stein, Professor Tim Leung, Professor Ioannis Karatzas, Professor Mark Brown, Professor Karl Sigman and Professor Xuedong He for these valuable experiences that will benefit me throughout my future career. I would like to express my great appreciations to Professor Karl Sigman, Professor Jose Blanchet, Professor Agostino Capponi and Professor Yuchong Zhang for serving on my dissertation committee and taking the time to peruse my thesis. I am also grateful to Professor Jay Sethuraman, director of the PhD program, for his support and assistance.

The doctoral students at the Department of Industrial Engineering and Operations Research form a close-knit family, my friends here have given me countless happy memories that I will greatly treasure. For this I thank Jing Guo, Cun Mu, Chun Ye, Linan Yang, Anran Li, Itai Feigenbaum, Di Xiao, Fei He, Ningyuan Chen, Yin Lu, Bo Huang, Xinyun Chen, Juan Li, Chun Wang, Jing Dong, Yupeng Chen, Chen Chen, Zhen Qiu, Shuheng Zheng, Marco Santoli and Jinbeom Kim. I also wish to make special mention of Jiao Li from the Department of Applied Physics and Applied Mathematics for making significant contributions to Chapter 3.

Most importantly, I wish to thank my parents Yiping Wang and Huanqun Zheng, my sister Kexin Wang and my wife Xin Li. My parents have provided me with unconditional support over the years and have nurtured me into the person I am today. I am thankful to my sixteen year old sister Kexin Wang for giving me much laughter and joy. I hope my life experience can be a useful guide for her future pursuits. I am deeply grateful to my wife Xin Li who has weathered both rain and shine with me. I could not have asked for a better life companion and I wish to share this accomplishment with her.

To my parents Yiping Wang
and Huanqun Zheng,
my sister Kexin Wang
and my wife Xin Li

Chapter 1

Introduction

Many trading and investment decisions involve choosing when to buy and/or sell an asset. Concomitant to this central problem are the following questions:

1. How is optimality defined? 2. How does price dynamics affect the optimal strategies? 3. What happens when one optimizes over an infinite sequence of trading decisions? 4. How to trade derivatives over a finite horizon? 5. How does the investor's optimal trading strategies depend on his/her risk preference?

In this dissertation, we seek to address these questions using optimal stopping theory. In the subsequent sections, we describe the motivation and methodology for each chapter in this thesis.

1.1 Optimal Switching under XOU and CIR Dynamics with Transaction Costs

The fluctuation of prices about constant values, a phenomenon known as mean reversion, has been witnessed in many assets. Evidence of mean-reverting behaviors have been identified in equities (see Poterba and Summers [1988]; Malliaropulos and Priestley [1999]; Balvers et al. [2000]; Gropp [2004]), for-

foreign exchange rates (see Engel and Hamilton [1989]; Anthony and MacDonald [1998]; Larsen and Sørensen [2007]), commodities (see Schwartz [1997]) and volatility indices (see Metcalf and Hassett [1995], Bessembinder et al. [1995], Casassus and Collin-Dufresne [2005], and references therein).

Schwartz [1997] proposed the XOU process as a way to model commodity prices. Since then, the XOU model has become a favored choice for modeling mean-reverting price processes due to its analytic tractability. Moreover, it serves as the foundation for more complex mean-reverting models. Another popular choice for modeling mean reversion is the CIR process, it is first introduced in Cox et al. [1985] as an extension of the Vasicek (OU) model and is commonly used to model short interest rates. The CIR process has also been used to model volatility (see Heston [1993]), energy prices (see Ribeiro and Hodges [2004]) and as a model for project values in real options literature. For example, Carmona and León [2007] study an irreversible investment problem where the interest rate follows a CIR process. In Ewald and Wang [2010], the authors model the project value as a CIR process and solve a Dixit and Pindyck type investment problem.

In the first part of this thesis, we consider an *optimal switching* problem where the investor is assumed to alternate between market entry and exit actions for an infinite number of times. This is in contrast to *optimal double stopping* problems where the investor cannot re-enter the market after exit. The optimal entry and exit timings will depend on the asset price dynamics, in particular if the price process is a super/sub-martingale, then the problem is greatly simplified and it is optimal to either exit the market immediately or hold the asset forever. For example, this happens in the case of an underlying asset with a geometric Brownian motion (GBM) price process (see Example A and Shiryaev et al. [2008]). On the other hand, as a result of the signature swinging movements, assets which demonstrate mean reversion are natural

candidates for carrying out buy-low-sell-high investment strategies. In Chapter 2, we study the optimal timing of trades subject to fixed transaction costs under the XOU or CIR model. Building on earlier studies of double stopping problems (see Leung et al. [2015] and Leung et al. [2014]), we use the optimal structures of the buy/sell/wait regions to infer a similar solution structure for the optimal switching problems and verify using variational inequalities. Subsequently, we compare the solution of the optimal switching problem to that of the optimal double stopping problem.

For the XOU model, it is optimal to sell when the asset price is sufficiently high under both double stopping and switching scenarios. However, the exact values of the upper thresholds differ for the two problems. When it comes to market entry, we observe that under some circumstances, it is optimal to never enter. In this case, the optimal switching problem for an investor with a long position degenerates into an optimal stopping problem. In the alternate case, it is optimal under both optimal double stopping and optimal switching problems for the investor to only enter the market when the asset price first descends into a band above zero. Precisely, the continuation region for entry takes the form $(0, A) \cup (B, +\infty)$, with critical price levels A and B (for details refer to Theorems 2.2.4 and 2.2.7). In other words, the continuation region is *disconnected*. This interesting observation is a result of fixed transaction costs. In the presence of only proportional costs, it is always optimal to enter when the price is low enough (see Zhang and Zhang [2008]).

For trading problems under the CIR model, we find that it is optimal to liquidate when the asset price is high enough. As in the XOU model, the exit levels differ for double stopping and switching problems. Moreover, for the switching problem, we identify necessary and sufficient conditions under which it is optimal to never enter. In this case, the optimal switching problem for an investor with a long position is identical to an optimal single stopping

problem. Chapter 2 is built on Leung et al. [2015] and Leung et al. [2014].

In a closely related study, Zervos et al. [2013] consider an optimal switching problem with fixed transaction costs under a class of time-homogeneous diffusions which encompasses the GBM, CEV and other models. Their findings, however, cannot be applied to the XOU model as it violates Assumption 4 of their paper (see Remark 2.3.2 below). Specifically, their model assumptions restrict the optimal entry region to be defined by a single critical level, whereas we show that in the XOU model the optimal entry region is actually a band strictly above zero.

Song et al. [2009] solve for optimal buy-low-sell-high strategies over a finite horizon by way of a numerical stochastic approximation scheme. Song and Zhang [2013] analyze the optimal switching problem with stop-loss under OU price dynamics. In a similar setting, Zhang and Zhang [2008] and Kong and Zhang [2010] study the infinite sequential buying and selling/shorting problem under XOU price dynamics with proportional transaction costs. In contrast to these studies, we study optimal switching problems under both XOU and CIR models with fixed transaction costs. In particular, the optimal entry timing under XOU model with fixed costs is characteristically different from that with proportional costs.

In addition to the works mentioned above, portfolio construction and hedging problems involving mean reverting assets have also been studied. For instance, Benth and Karlsen [2005] consider the optimization problem of an investor who has to allocate his wealth between a risk-free asset and a risky asset that follows an XOU process. Jurek and Yang [2007] analyze a finite horizon portfolio optimization problem concerning an OU spread where risk preferences are characterized by the power utility and Epstein-Zin recursive utility. Chiu and Wong [2012] consider the optimal trading of co-integrated assets with a mean-variance portfolio selection criterion. Tourin and Yan [2013]

derive the dynamic trading strategy for a pair of co-integrated stocks with the objective of maximizing the expected terminal utility of wealth over a fixed horizon. In the case of exponential utility, they simplify the associated Hamilton-Jacobi-Bellman equation and obtain a closed-form solution.

1.2 Speculative Futures Trading under Mean Reversion

Futures are an integral part of the universe of derivatives. In 2015, the total volume of futures and options traded on exchanges worldwide rose by 13.5% from 21.83 billion contracts in 2014 to 24.78 billion contracts. The largest growth is in Asia-Pacific, where the combined volume increased by a remarkable 33.7%. Number of futures contracts traded globally grew substantially by 19.3% to 14.48 billion from 12.14 billion a year prior. The CME group and the National Stock Exchange of India (NSE) are the largest futures and options exchanges. The 2015 combined trading volume of CME group with its subsidiary exchanges, Chicago Mercantile Exchange, Chicago Board of Trade and New York Mercantile Exchange was 3.53 billion contracts, while NSE had a volume of 3.03 billion contracts.¹

A futures is a contract that requires the buyer to purchase (seller to sell) a fixed quantity of an asset, such as a commodity, at a fixed price to be paid for on a pre-specified future date. Commonly traded on exchanges, there are futures written on various underlying assets or references, including commodities, interest rates, equity indices, and volatility indices. Many futures stipulate physical delivery of the underlying asset, with notable examples of agricultural, energy, and metal futures. However, some, like the VIX futures, are settled in cash.

¹Statistics taken from Acworth [2016].

Futures are often used as a hedging instrument, but they are also popular among speculative investors. In fact, they are seldom traded with the intention of holding it to maturity as less than 1% of futures traded ever reach physical delivery.² This motivates the question of optimal timing to trade a futures.

In chapter 3, we investigate the speculative trading of futures under mean-reverting spot price dynamics. Mean reversion is commonly observed for the spot price in many futures markets, ranging from commodities and interest rates to currencies and volatility indices, as studied in many empirical studies (see, among others, Bessembinder et al. [1995], Irwin et al. [1996], Schwartz [1997], Casassus and Collin-Dufresne [2005], Geman [2007], Bali and Demirtas [2008], Wang and Daigler [2011]). For volatility futures as an example, Grübichler and Longstaff [1996] and Zhang and Zhu [2006] model the S&P500 volatility index (VIX) by the CIR process and provide a formula for the futures price. We start by deriving the price functions and dynamics of the futures under the OU, CIR, and XOU models. Futures prices are computed under the risk-neutral measure, but its evolution over time is described by the historical measure. Thus, the investor's optimal timing to trade depends on both measures.

Moreover, we incorporate the investor's timing option to enter and subsequently exit the market. Before entering the market, the investor faces two possible strategies: long or short a futures first, then close the position later. In the first strategy, an investor is expected to establish the long position when the price is sufficiently low, and then exits when the price is high. The opposite is expected for the second strategy. In both cases, the presence of transaction costs expands the waiting region, indicating the investor's desire for better prices. In addition, the waiting region expands drastically near expiry since transaction costs discourage entry when futures is very close to maturity. Fi-

²See p.615 of Elton et al. [2009] for a discussion.

nally, the main feature of our trading problem approach is to combine these two related problems and analyze the optimal strategy when an investor has the freedom to choose between either a *long-short* or a *short-long* position. Among our results, we find that when the investor has the right to choose, she delays market entry to wait for better prices compared to the individual standalone problems.

Our model is a variation of the theoretical arbitrage model proposed by Dai et al. [2011], who also incorporate the timing options to enter and exit the market, as well as the choice between opposite positions upon entry. Their sole underlying traded process is the stochastic *basis* representing the difference between the index and futures values, which is modeled by a Brownian bridge. In an earlier study, Brennan and Schwartz [1990] formulate a similar optimal stopping problem for trading futures where the underlying basis is a Brownian bridge. In comparison to these two models, we model directly the spot price process, which allows for calibration of futures prices and provide a no-arbitrage link between the (risk-neutral) pricing and (historical) trading problems, as opposed to a priori assuming the existence of arbitrage opportunities, and modeling the basis that is neither calibrated nor shown to be consistent with the futures curves. A similar timing strategy for pairs trading has been studied by Cartea et al. [2015] as an extension of the buy-low-sell-high strategy used in Leung and Li [2015].

In addition, we study the distribution and dynamics of *roll yield*, an important concept in futures trading. Following the literature and industry practice, we define roll yield as the difference between changes in futures price and changes in the underlying price (see e.g. Moskowitz et al. [2012], Gorton et al. [2013]). For traders, roll yield is a useful gauge for deciding to invest in the spot asset or associated futures. In essence, roll yield defined herein represents the net cost and/or benefit of owning futures over the spot asset. Therefore,

even for an investor who trades futures only, the corresponding roll yield is a useful reference and can affect her trading decisions. Chapter 3 is based on Leung et al. [2016].

1.3 Optimal Risk Averse Timing of an Asset Sale

In chapter 4 we consider a risk-averse investor who seeks to sell an asset by selecting a timing strategy that maximizes the expected utility resulting from the sale. At any point in time, the investor can either decide to sell immediately, or wait for a potentially better opportunity in the future. Naturally, the investor's decision to sell should depend on the investor's risk aversion and the price evolution of the risky asset. To better understand their effects, we model the investor's risk preference by the exponential, power, or log utility. In addition, we consider two contrasting models for the asset price – the GBM and XOU models – to account for, respectively, the trending and mean-reverting price dynamics. The choice of multiple utilities and stochastic models allows for a comprehensive comparison analysis of all six possible settings.

We analyze a number of optimal stopping problems faced by the investor under different models and utilities. The investor's value functions and the corresponding optimal timing strategies are solved analytically. In particular, we identify the scenarios where the optimal strategies are trivial. These arise in the GBM model with exponential and power utilities, but not with log utility or under the XOU model with any utility. The non-trivial optimal timing strategies are shown to be of threshold type. The optimal threshold represents the critical price at which the investor is willing to sell the asset and forgo future sale opportunities. In most cases, the optimal threshold is determined from an implicit equation, though under the GBM model with log

utility the optimal threshold is explicit. Moreover, intuitively the investor's optimal timing strategy should depend, not only on risk aversion and price dynamics, but also the quantity of assets to be sold simultaneously. In general, we find that the dependence is neither linear nor explicit. Nevertheless, under the GBM model with log utility, the optimal price to sell is inversely proportional to quantity so that the sale will always result in the same total revenue regardless of quantity. In contrast, under the XOU model with power utility, the optimal threshold is independent of quantity, and thus the total revenue scales linearly with quantity.

While all utility functions considered herein are concave, the timing option to sell may render the investor's value functions and certainty equivalents non-concave in price under different models. For instance, under the GBM model with log utility the value function can be convex in the continuation (waiting) region and concave when the value function coincides with the utility function for sufficiently high asset price. Under the XOU model, we observe that the value functions are in general neither concave nor convex in price. If the time of asset sale is pre-determined and fixed, then the value functions are always concave. Therefore, the phenomenon of non-concavity arises due to the timing option to sell. Mathematically, the reason lies in the fact that the value functions are constructed using convex functions that are the general solutions to the PDE associated with the underlying GBM or XOU process.

To better understand the investor's perceived value of the risky asset with the timing option to sell, we analyze the certainty equivalent associated with each utility maximization problem. With analytic formulas, we illustrate the properties of the certainty equivalents. In all cases, the certainty equivalent dominates the current asset price, and the difference indicates the premium of the timing option. The gap typically widens as the underlying price increases before eventually diminishing to zero for sufficiently high price. As a conse-

quence, the certainty equivalents are in general neither concave nor convex in price. If the optimal strategy is trivial, the certainty equivalent is simply a linear function of asset price. Chapter 4 is adapted from Leung and Wang [2016].

In the literature, Henderson [2007] considers a risk-averse manager with a negative exponential utility who seeks to optimally time the investment in a project while trading in a correlated asset as a partial hedge. Under the GBM model, the manager's optimal timing strategy is to either invest according to a finite threshold or postpone indefinitely. In comparison, the investor in our exponential utility case under the GBM model may either sell immediately or at a finite threshold, but will never find it optimal to wait indefinitely. Evans et al. [2008] also study a mixed stochastic control/optimal stopping problem with the objective of determining the optimal time to sell a non-traded asset where the investor has a power utility. In our paper, we show that the optimal timing with power utility is either to sell immediately or wait indefinitely under the GBM model, but the threshold-type strategy is optimal under the XOU model.

Our study focuses on the GBM and XOU models for the asset price. A related paper by Leung et al. [2015] analyzes optimal stopping and switching problems under the XOU model. Their results are applicable to our case with power utility under the same model. Other mean-reverting price models, such as the OU model (see e.g. Ekström et al. [2011]) and Cox-Ingersoll-Ross (CIR) model (see e.g. Ewald and Wang [2010]; Leung et al. [2014]), have been used to analyze various optimal timing problems. The recent work by Ekström and Vaicenavicius [2016] investigates the optimal timing to sell an asset when its price process follows a GBM-like process with a random drift. All these studies do not incorporate risk aversion.

Alternative risk criteria can also be used to study the asset sale timing

problem. Inspired by prospect theory, Henderson [2012] considers an S-shape (piecewise power) utility function of gain/loss relative to the initial price. Under the GBM model, the investor may find it optimal to sell at a loss. Pedersen and Peskir [2016] solve for the optimal selling strategy under the mean-variance risk criterion. Instead of maximizing expected utility, one can also incorporate alternative risk penalties to the optimal timing problems. Leung and Shirai [2015] study this problem under both GBM and XOU models with shortfall and quadratic penalties. Other than asset sale, the problem of optimal time to sell and/or buy derivatives by a risk-averse investor has been studied by Henderson and Hobson [2011]; Leung and Ludkovski [2012], among others.

Chapter 2

Optimal Switching under XOUP and CIR Dynamics with Transaction Costs

In this chapter, we analyze an optimal switching problem that involves an infinite sequence of trades, when prices are driven by an XOUP or CIR process. We compare the results with earlier works on optimal double stopping problems and identify the conditions under which the double stopping and switching problems admit the same optimal entry and/or exit timing strategies. In the CIR case, the investor's optimal strategy is characterized by a lower level for entry and an upper level for exit. However, in the XOUP case, we find that the investor enters only when the current price is in a band strictly above zero. In other words, the continuation (waiting) region for entry is *disconnected*. Numerical results are provided to illustrate the dependence of timing strategies on model parameters and transaction costs.

In Section 2.1, we formulate both the optimal double stopping and optimal switching problems. Then, we present our analytical and numerical results in Section 2.2. The proofs of our main results are detailed in Section 2.3. Finally,

Appendix B contains the proofs for a number of lemmas.

2.1 Problem Overview

In the background, we fix a probability space $(\Omega, \mathcal{F}, \mathbb{P})$, where \mathbb{P} is the historical probability measure. In this section, we provide an overview of our optimal double stopping and switching problems, which will involve an exponential Ornstein-Uhlenbeck (XOU) process. The XOU process $(\xi_t)_{t \geq 0}$ is defined by

$$\xi_t = e^{X_t}, \quad dX_t = \mu(\theta - X_t) dt + \sigma dB_t. \quad (2.1.1)$$

Here, X is an OU process driven by a standard Brownian motion B , with constant parameters $\mu, \sigma > 0$, $\theta \in \mathbb{R}$. In other words, X is the log-price of the positive XOU process ξ .

Another process considered herein is the CIR process Y that satisfies

$$dY_t = \mu(\theta - Y_t) dt + \sigma \sqrt{Y_t} dB_t, \quad (2.1.2)$$

with constants $\mu, \theta, \sigma > 0$. If $2\mu\theta \geq \sigma^2$ holds, which is often referred to as the Feller condition (see Feller [1951]), then the level 0 is inaccessible by Y . If the initial value $Y_0 > 0$, then Y stays strictly positive at all times almost surely. Nevertheless, if $Y_0 = 0$, then Y will enter the interior of the state space immediately and stays positive thereafter almost surely. If $2\mu\theta < \sigma^2$, then the level 0 is a reflecting boundary. This means that once Y reaches 0, it immediately returns to the interior of the state space and continues to evolve. For a detailed categorization of boundaries for diffusion processes, we refer to Chapter 2 of Borodin and Salminen [2002] and Chapter 15 of Karlin and Taylor [1981].

2.1.1 Optimal Double Stopping Problem

Optimal double stopping problems under XOU and CIR models have been studied in detail in Leung et al. [2015] and Leung et al. [2014] respectively. In this chapter, we will compare the optimal strategies of double stopping problems with that of switching problems. For convenience, we shall restate the definitions of optimal double stopping problems under XOU and CIR models below.

Given a risky asset with an XOU price process, we first consider the optimal timing to sell. If the share of the asset is sold at some time τ , then the investor will receive the value $\xi_\tau = e^{X_\tau}$ and pay a constant transaction cost $c_s > 0$. Denote by \mathbb{F} the filtration generated by B , and \mathcal{T} the set of all \mathbb{F} -stopping times. To maximize the expected discounted value, the investor solves the optimal stopping problem

$$V^\xi(x) = \sup_{\tau \in \mathcal{T}} \mathbb{E}_x \{ e^{-r\tau} (e^{X_\tau} - c_s) \}, \quad (2.1.3)$$

where $r > 0$ is the constant discount rate, and $\mathbb{E}_x \{ \cdot \} \equiv \mathbb{E} \{ \cdot | X_0 = x \}$.

The value function $V^\xi(x)$ represents the expected liquidation value associated with ξ . On the other hand, the current price plus the transaction cost constitute the total cost to enter the trade. Before even holding the risky asset, the investor can always choose the optimal timing to start the trade, or not to enter at all. This leads us to analyze the entry timing inherent in the trading problem. Precisely, we solve

$$J^\xi(x) = \sup_{\nu \in \mathcal{T}} \mathbb{E}_x \{ e^{-r\nu} (V^\xi(X_\nu) - e^{X_\nu} - c_b) \}, \quad (2.1.4)$$

with the constant transaction cost $c_b > 0$ incurred at the time of purchase. In other words, the trader seeks to maximize the expected difference between the value function $V^\xi(X_\nu)$ and the current e^{X_ν} , minus transaction cost c_b . The value function $J^\xi(x)$ represents the maximum expected value of the investment

opportunity in the price process ξ , with transaction costs c_b and c_s incurred, respectively, at entry and exit. For our analysis, the transaction costs c_b and c_s can be different. To facilitate presentation, we denote the functions

$$h_s^\xi(x) = e^x - c_s \quad \text{and} \quad h_b^\xi(x) = e^x + c_b. \quad (2.1.5)$$

If it turns out that $J^\xi(X_0) \leq 0$ for some initial value X_0 , then the investor will not start to trade X (see Appendix A below). In view of the example in Appendix A, it is important to identify the trivial cases under any given dynamics. Under the XOUC model, since $\sup_{x \in \mathbb{R}} (V^\xi(x) - h_b^\xi(x)) \leq 0$ implies that $J^\xi(x) \leq 0$ for $x \in \mathbb{R}$, we shall therefore focus on the case with

$$\sup_{x \in \mathbb{R}} (V^\xi(x) - h_b^\xi(x)) > 0, \quad (2.1.6)$$

and solve for the non-trivial optimal timing strategy.

Alternatively, under the CIR price dynamics, the optimal exit and entry problems are defined, respectively, as

$$V^X(y) = \sup_{\tau \in \mathcal{T}} \mathbb{E}_y \{ e^{-r\tau} h_s^X(Y_\tau) \}, \quad (2.1.7)$$

$$J^X(y) = \sup_{\nu \in \mathcal{T}} \mathbb{E}_y \{ e^{-r\nu} (V^X(Y_\nu) - h_b^X(Y_\nu)) \}, \quad (2.1.8)$$

where

$$h_s^X(y) = y - c_s, \quad \text{and} \quad h_b^X(y) = y + c_b. \quad (2.1.9)$$

If it turns out that $J^X(Y_0) \leq 0$ for some initial value Y_0 , then it is optimal not to start at all. Therefore, it is important to identify the trivial cases. Under the CIR model, since $\sup_{y \in \mathbb{R}_+} (V^X(y) - h_b(y)) \leq 0$ implies that $J^X(y) = 0$ for $y \in \mathbb{R}_+$, we shall therefore focus on the case with

$$\sup_{y \in \mathbb{R}_+} (V^X(y) - h_b(y)) > 0, \quad (2.1.10)$$

and solve for the non-trivial optimal timing strategy.

2.1.2 Optimal Switching Problem

Under the optimal switching approach, the investor is assumed to commit to an infinite number of trades. The sequential trading times are modeled by the stopping times $\nu_1, \tau_1, \nu_2, \tau_2, \dots \in \mathcal{T}$ such that

$$0 \leq \nu_1 \leq \tau_1 \leq \nu_2 \leq \tau_2 \leq \dots$$

A share of the risky asset is bought and sold, respectively, at times ν_i and τ_i , $i \in \mathbb{N}$. The investor's optimal timing to trade would depend on the initial position. Precisely, under the XOU model, if the investor starts with a zero position, then the first trading decision is when to *buy* and the corresponding optimal switching problem is

$$\tilde{J}^\xi(x) = \sup_{\Lambda_0} \mathbb{E}_x \left\{ \sum_{n=1}^{\infty} [e^{-r\tau_n} h_s^\xi(X_{\tau_n}) - e^{-r\nu_n} h_b^\xi(X_{\nu_n})] \right\}, \quad (2.1.11)$$

with the set of admissible stopping times $\Lambda_0 = (\nu_1, \tau_1, \nu_2, \tau_2, \dots)$, and the reward functions h_s^ξ and h_b^ξ defined in (2.1.5). On the other hand, if the investor is initially holding a share of the asset, then the investor first determines when to *sell* and solves

$$\tilde{V}^\xi(x) = \sup_{\Lambda_1} \mathbb{E}_x \left\{ e^{-r\tau_1} h_s^\xi(X_{\tau_1}) + \sum_{n=2}^{\infty} [e^{-r\tau_n} h_s^\xi(X_{\tau_n}) - e^{-r\nu_n} h_b^\xi(X_{\nu_n})] \right\}, \quad (2.1.12)$$

with $\Lambda_1 = (\tau_1, \nu_2, \tau_2, \nu_3, \dots)$.

Under CIR price dynamics, the optimal switching problems are similarly defined as

$$\tilde{J}^X(y) = \sup_{\Lambda_0} \mathbb{E}_y \left\{ \sum_{n=1}^{\infty} [e^{-r\tau_n} h_s^X(Y_{\tau_n}) - e^{-r\nu_n} h_b^X(Y_{\nu_n})] \right\}, \quad (2.1.13)$$

$$\tilde{V}^X(y) = \sup_{\Lambda_1} \mathbb{E}_y \left\{ e^{-r\tau_1} h_s^X(Y_{\tau_1}) + \sum_{n=2}^{\infty} [e^{-r\tau_n} h_s^X(Y_{\tau_n}) - e^{-r\nu_n} h_b^X(Y_{\nu_n})] \right\}, \quad (2.1.14)$$

where the reward functions h_s^X and h_b^X and are defined in (2.1.9).

In summary, the optimal double stopping and switching problems differ in the number of trades. Observe that any strategy for the double stopping problems (2.1.3) and (2.1.4) (resp. (2.1.7) and (2.1.8)) are also candidate strategies for the switching problems (2.1.12) and (2.1.11) (resp. (2.1.13) and (2.1.14)) respectively. Therefore, it follows that $V^\xi(x) \leq \tilde{V}^\xi(x)$ (resp. $V^\chi(y) \leq \tilde{V}^\chi(y)$) and $J^\xi(x) \leq \tilde{J}^\xi(x)$ (resp. $J^\chi(y) \leq \tilde{J}^\chi(y)$). Our objective is to derive and compare the corresponding optimal timing strategies under these two approaches.

2.2 Summary of Analytical Results

We first summarize our analytical results and illustrate the optimal trading strategies. For completeness, we shall restate the main results concerning optimal double stopping problems in Leung et al. [2015] and Leung et al. [2014] without proof. The method of solutions and proofs of the optimal switching problems will be discussed in Section 2.3.

2.2.1 XOU Model

We begin with the optimal stopping problems (2.1.3) and (2.1.4) under the XOU model. Denote the infinitesimal generator of the OU process X in (2.1.1) by

$$\mathcal{L} = \frac{\sigma^2}{2} \frac{d^2}{dx^2} + \mu(\theta - x) \frac{d}{dx}. \quad (2.2.1)$$

Recall that the classical solutions of the differential equation

$$\mathcal{L}u(x) = ru(x),$$

for $x \in \mathbb{R}$, are (see e.g. p.542 of Borodin and Salminen [2002] and Prop. 2.1 of Alili et al. [2005]):

$$\begin{aligned} F(x) &\equiv F(x; r) := \int_0^\infty u^{\frac{r}{\mu}-1} e^{\sqrt{\frac{2\mu}{\sigma^2}}(x-\theta)u - \frac{u^2}{2}} du, \\ G(x) &\equiv G(x; r) := \int_0^\infty u^{\frac{r}{\mu}-1} e^{\sqrt{\frac{2\mu}{\sigma^2}}(\theta-x)u - \frac{u^2}{2}} du. \end{aligned}$$

Direct differentiation yields that $F'(x) > 0$, $F''(x) > 0$, $G'(x) < 0$ and $G''(x) > 0$. Hence, we observe that both $F(x)$ and $G(x)$ are strictly positive and convex, and they are, respectively, strictly increasing and decreasing.

Define the first passage time of X to some level κ by $\tau_\kappa = \inf\{t \geq 0 : X_t = \kappa\}$. As is well known, F and G admit the probabilistic expressions (see Itô and McKean [1965] and Rogers and Williams [2000]):

$$\mathbb{E}_x\{e^{-r\tau_\kappa}\} = \begin{cases} \frac{F(x)}{F(\kappa)} & \text{if } x \leq \kappa, \\ \frac{G(x)}{G(\kappa)} & \text{if } x \geq \kappa. \end{cases}$$

2.2.1.1 Optimal Double Stopping Problem

We now present the result for the optimal exit timing problem under the XOU model. First, we obtain a bound for the value function V^ξ .

Lemma 2.2.1. *There exists a positive constant K^ξ such that, for all $x \in \mathbb{R}$, $0 \leq V^\xi(x) \leq e^x + K^\xi$.*

Theorem 2.2.2. *The optimal liquidation problem (2.1.3) admits the solution*

$$V^\xi(x) = \begin{cases} \frac{e^{b^\xi} - c_s}{F(b^\xi)} F(x) & \text{if } x < b^\xi, \\ e^x - c_s & \text{if } x \geq b^\xi, \end{cases} \quad (2.2.2)$$

where the optimal log-price level b^ξ for liquidation is uniquely found from the equation

$$e^b F(b) = (e^b - c_s) F'(b). \quad (2.2.3)$$

The optimal liquidation time is given by

$$\tau^{\xi^*} = \inf\{t \geq 0 : X_t \geq b^{\xi^*}\} = \inf\{t \geq 0 : \xi_t \geq e^{b^{\xi^*}}\}.$$

We now turn to the optimal entry timing problem, and give a bound on the value function J^ξ .

Lemma 2.2.3. *There exists a positive constant \hat{K}^ξ such that, for all $x \in \mathbb{R}$, $0 \leq J^\xi(x) \leq \hat{K}^\xi$.*

Theorem 2.2.4. *Under the XOU model, the optimal entry timing problem (2.1.4) admits the solution*

$$J^\xi(x) = \begin{cases} P^\xi F(x) & \text{if } x \in (-\infty, a^{\xi^*}), \\ V^\xi(x) - (e^x + c_b) & \text{if } x \in [a^{\xi^*}, d^{\xi^*}], \\ Q^\xi G(x) & \text{if } x \in (d^{\xi^*}, +\infty), \end{cases}$$

with the constants

$$P^\xi = \frac{V^\xi(a^{\xi^*}) - (e^{a^{\xi^*}} + c_b)}{F(a^{\xi^*})}, \quad Q^\xi = \frac{V^\xi(d^{\xi^*}) - (e^{d^{\xi^*}} + c_b)}{G(d^{\xi^*})},$$

and the critical levels a^{ξ^*} and d^{ξ^*} satisfying, respectively,

$$\begin{aligned} F(a)(V^{\xi'}(a) - e^a) &= F'(a)(V^\xi(a) - (e^a + c_b)), \\ G(d)(V^{\xi'}(d) - e^d) &= G'(d)(V^\xi(d) - (e^d + c_b)). \end{aligned} \tag{2.2.4}$$

The optimal entry time is given by

$$\nu_{a^{\xi^*}, d^{\xi^*}} := \inf\{t \geq 0 : X_t \in [a^{\xi^*}, d^{\xi^*}]\}.$$

In summary, the investor should exit the market as soon as the price reaches the upper level $e^{b^{\xi^*}}$. In contrast, the optimal entry timing is the first time that the XOU price ξ enters the interval $[e^{a^{\xi^*}}, e^{d^{\xi^*}}]$. In other words, it is optimal to wait if the current price ξ_t is too close to zero, i.e. if $\xi_t < e^{a^{\xi^*}}$. Moreover, the interval $[e^{a^{\xi^*}}, e^{d^{\xi^*}}]$ is contained in $(0, e^{b^{\xi^*}})$, and thus, the continuation region for market entry is *disconnected*.

2.2.1.2 Optimal Switching Problem

We now turn to the optimal switching problems defined in (2.1.11) and (2.1.12) under the XOU model. To facilitate the presentation, we denote

$$\begin{aligned} f_s(x) &:= (\mu\theta + \frac{1}{2}\sigma^2 - r) - \mu x + rc_s e^{-x}, \\ f_b(x) &:= (\mu\theta + \frac{1}{2}\sigma^2 - r) - \mu x - rc_b e^{-x}. \end{aligned}$$

Applying the operator \mathcal{L} (see (2.2.1)) to h_s^ξ and h_b^ξ (see (2.1.5)), it follows that $(\mathcal{L} - r)h_s^\xi(x) = e^x f_s(x)$ and $(\mathcal{L} - r)h_b^\xi(x) = e^x f_b(x)$. Therefore, f_s (resp. f_b) preserves the sign of $(\mathcal{L} - r)h_s^\xi$ (resp. $(\mathcal{L} - r)h_b^\xi$). It can be shown that $f_s(x) = 0$ has a unique root, denoted by x_s . However,

$$f_b(x) = 0 \tag{2.2.5}$$

may have no root, a single root, or two distinct roots, denoted by x_{b1} and x_{b2} , if they exist. The following observations will also be useful:

$$f_s(x) \begin{cases} > 0 & \text{if } x < x_s, \\ < 0 & \text{if } x > x_s, \end{cases} \quad \text{and} \quad f_b(x) \begin{cases} < 0 & \text{if } x \in (-\infty, x_{b1}) \cup (x_{b2}, +\infty), \\ > 0 & \text{if } x \in (x_{b1}, x_{b2}). \end{cases} \tag{2.2.6}$$

We first obtain bounds for the value functions \tilde{J}^ξ and \tilde{V}^ξ .

Lemma 2.2.5. *There exists positive constants C_1 and C_2 such that*

$$\begin{aligned} 0 &\leq \tilde{J}^\xi(x) \leq C_1, \\ 0 &\leq \tilde{V}^\xi(x) \leq e^x + C_2. \end{aligned}$$

The optimal switching problems have two different sets of solutions depending on the problem data.

Theorem 2.2.6. *The optimal switching problem (2.1.11)-(2.1.12) admits the solution*

$$\tilde{J}^\xi(x) = 0, \text{ for } x \in \mathbb{R}, \quad \text{and} \quad \tilde{V}^\xi(x) = \begin{cases} \frac{e^{b^\xi} - c_s}{F(b^\xi)} F(x) & \text{if } x < b^\xi, \\ e^x - c_s & \text{if } x \geq b^\xi, \end{cases} \quad (2.2.7)$$

where b^ξ satisfies (2.2.3), if any of the following mutually exclusive conditions holds:

(i) *There is no root or a single root to equation (2.2.5).*

(ii) *There are two distinct roots to (2.2.5). Also*

$$\exists \tilde{a}^* \in (x_{b1}, x_{b2}) \quad \text{such that} \quad F(\tilde{a}^*)e^{\tilde{a}^*} = F'(\tilde{a}^*)(e^{\tilde{a}^*} + c_b), \quad (2.2.8)$$

and

$$\frac{e^{\tilde{a}^*} + c_b}{F(\tilde{a}^*)} \geq \frac{e^{b^\xi} - c_s}{F(b^\xi)}. \quad (2.2.9)$$

(iii) *There are two distinct roots to (2.2.5) but (2.2.8) does not hold.*

In Theorem 2.2.6, $\tilde{J}^\xi = 0$ means that it is optimal not to enter the market at all. On the other hand, if one starts with a unit of the underlying asset, the optimal switching problem reduces to a problem of optimal single stopping. Indeed, the investor will never re-enter the market after exit. This is identical to the optimal liquidation problem (2.1.3) where there is only a single (exit) trade. The optimal strategy in this case is the same as V^ξ in (2.2.2) – it is optimal to exit the market as soon as the log-price X reaches the threshold b^ξ .

We also address the remaining case when none of the conditions in Theorem 2.2.6 hold. As we show next, the optimal strategy will involve both entry and exit thresholds.

Theorem 2.2.7. *If there are two distinct roots to (2.2.5), x_{b1} and x_{b2} , and there exists a number $\tilde{a}^* \in (x_{b1}, x_{b2})$ satisfying (2.2.8) such that*

$$\frac{e^{\tilde{a}^*} + c_b}{F(\tilde{a}^*)} < \frac{e^{b^{\xi^*}} - c_s}{F(b^{\xi^*})}, \quad (2.2.10)$$

then the optimal switching problem (2.1.11)-(2.1.12) admits the solution

$$\tilde{J}^\xi(x) = \begin{cases} \tilde{P}F(x) & \text{if } x \in (-\infty, \tilde{a}^*), \\ \tilde{K}F(x) - (e^x + c_b) & \text{if } x \in [\tilde{a}^*, \tilde{d}^*], \\ \tilde{Q}G(x) & \text{if } x \in (\tilde{d}^*, +\infty), \end{cases} \quad (2.2.11)$$

$$\tilde{V}^\xi(x) = \begin{cases} \tilde{K}F(x) & \text{if } x \in (-\infty, \tilde{b}^*), \\ \tilde{Q}G(x) + e^x - c_s & \text{if } x \in [\tilde{b}^*, +\infty), \end{cases} \quad (2.2.12)$$

where \tilde{a}^* satisfies (2.2.8), and

$$\begin{aligned} \tilde{P} &= \tilde{K} - \frac{e^{\tilde{a}^*} + c_b}{F(\tilde{a}^*)}, \\ \tilde{K} &= \frac{e^{\tilde{d}^*}G(\tilde{d}^*) - (e^{\tilde{d}^*} + c_b)G'(\tilde{d}^*)}{F'(\tilde{d}^*)G(\tilde{d}^*) - F(\tilde{d}^*)G'(\tilde{d}^*)}, \\ \tilde{Q} &= \frac{e^{\tilde{d}^*}F(\tilde{d}^*) - (e^{\tilde{d}^*} + c_b)F'(\tilde{d}^*)}{F'(\tilde{d}^*)G(\tilde{d}^*) - F(\tilde{d}^*)G'(\tilde{d}^*)} \end{aligned}$$

There exist unique critical levels \tilde{d}^ and \tilde{b}^* which are found from the nonlinear system of equations:*

$$\frac{e^d G(d) - (e^d + c_b)G'(d)}{F'(d)G(d) - F(d)G'(d)} = \frac{e^b G(b) - (e^b - c_s)G'(b)}{F'(b)G(b) - F(b)G'(b)}, \quad (2.2.13)$$

$$\frac{e^d F(d) - (e^d + c_b)F'(d)}{F'(d)G(d) - F(d)G'(d)} = \frac{e^b F(b) - (e^b - c_s)F'(b)}{F'(b)G(b) - F(b)G'(b)}. \quad (2.2.14)$$

Moreover, the critical levels are such that $\tilde{d}^ \in (x_{b1}, x_{b2})$ and $\tilde{b}^* > x_s$.*

The optimal strategy in Theorem 2.2.7 is described by the stopping times

$\Lambda_0^* = (\nu_1^*, \tau_1^*, \nu_2^*, \tau_2^*, \dots)$, and $\Lambda_1^* = (\tau_1^*, \nu_2^*, \tau_2^*, \nu_3^*, \dots)$, with

$$\nu_1^* = \inf\{t \geq 0 : X_t \in [\tilde{a}^*, \tilde{d}^*]\},$$

$$\tau_i^* = \inf\{t \geq \nu_i^* : X_t \geq \tilde{b}^*\}, \quad \text{and} \quad \nu_{i+1}^* = \inf\{t \geq \tau_i^* : X_t \leq \tilde{d}^*\}, \quad \text{for } i \geq 1.$$

In other words, it is optimal to buy if the price is within $[e^{\tilde{a}^*}, e^{\tilde{d}^*}]$ and then sell when the price ξ reaches $e^{\tilde{b}^*}$. The structure of the buy/sell regions is similar to that in the double stopping case (see Theorems 2.2.2 and 2.2.4). In particular, \tilde{a}^* is the same as a^{ξ^*} in Theorem 2.2.4 since the equations (2.2.4) and (2.2.8) are equivalent. The level \tilde{a}^* is only relevant to the first purchase. Mathematically, \tilde{a}^* is determined separately from \tilde{d}^* and \tilde{b}^* . If we start with a zero position, then it is optimal to enter if the price ξ lies in the interval $[e^{\tilde{a}^*}, e^{\tilde{d}^*}]$. However, on all subsequent trades, we enter as soon as the price hits $e^{\tilde{d}^*}$ from above (after exiting at $e^{\tilde{b}^*}$ previously). Hence, the lower level \tilde{a}^* becomes irrelevant after the first entry.

Note that the conditions that differentiate Theorems 2.2.6 and 2.2.7 are exhaustive and mutually exclusive. If the conditions in Theorem 2.2.6 are violated, then the conditions in Theorem 2.2.7 must hold. In particular, condition (2.2.8) in Theorem 2.2.6 holds if and only if

$$\left| \int_{-\infty}^{x_{b1}} \Psi(x) e^x f_b(x) dx \right| < \int_{x_{b1}}^{x_{b2}} \Psi(x) e^x f_b(x) dx, \quad (2.2.15)$$

where

$$\Psi(x) = \frac{2F(x)}{\sigma^2 \mathcal{W}(x)}, \quad \text{and} \quad \mathcal{W}(x) = F'(x)G(x) - F(x)G'(x) > 0. \quad (2.2.16)$$

Inequality (2.2.15) can be numerically verified given the model inputs.

2.2.1.3 Numerical Examples

We numerically implement Theorems 2.2.2, 2.2.4, and 2.2.7, and illustrate the associated entry/exit thresholds. In Figure 2.1 (left), the optimal entry

levels $d^{\xi*}$ and \tilde{d}^* rise, respectively, from 0.7425 to 0.7912 and from 0.8310 to 0.8850, as the speed of mean reversion μ increases from 0.5 to 1. On the other hand, the critical exit levels $b^{\xi*}$ and \tilde{b}^* remain relatively flat over μ . As for the critical lower level $a^{\xi*}$ from the optimal double stopping problem, Figure 2.1 (right) shows that it is decreasing in μ . The same pattern holds for the optimal switching problem since the critical lower level \tilde{a}^* is identical to $a^{\xi*}$, as noted above.

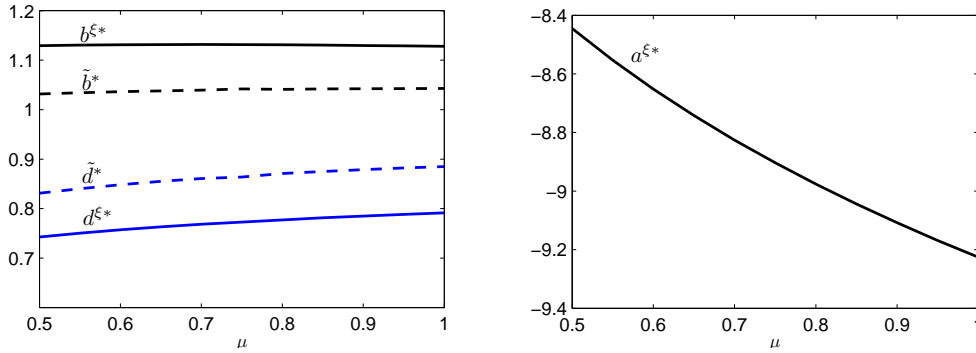


Figure 2.1: (Left) The optimal entry and exit levels vs speed of mean reversion μ . Parameters: $\sigma = 0.2$, $\theta = 1$, $r = 0.05$, $c_s = 0.02$, $c_b = 0.02$. (Right) The critical lower level of entry region $a^{\xi*}$ decreases monotonically from -8.4452 to -9.2258 as μ increases from 0.5 to 1. Parameters: $\sigma = 0.2$, $\theta = 1$, $r = 0.05$, $c_s = 0.02$, $c_b = 0.02$.

We now look at the impact of transaction cost in Figure 2.2. On the left panel, we observe that as the transaction cost c_b increases, the gap between the optimal switching entry and exit levels, \tilde{d}^* and \tilde{b}^* , widens. This means that it is optimal to delay both entry and exit. Intuitively, to counter the fall in profit margin due to an increase in transaction cost, it is necessary to buy at a lower price and sell at a higher price to seek a wider spread. In comparison, the exit level $b^{\xi*}$ from the double stopping problem is known analytically to be independent of the entry cost, so it stays constant as c_b increases in the figure. In contrast, the entry level $d^{\xi*}$, however, decreases as c_b increases but

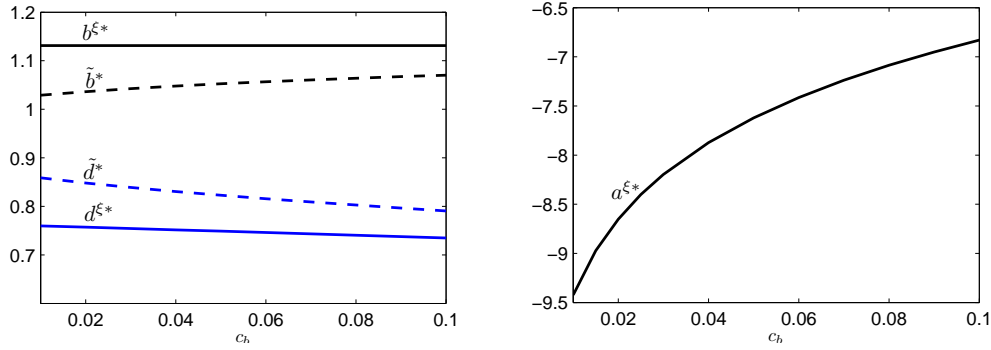


Figure 2.2: (Left) The optimal entry and exit levels vs transaction cost c_b . Parameters: $\mu = 0.6$, $\sigma = 0.2$, $\theta = 1$, $r = 0.05$, $c_s = 0.02$. (Right) The critical lower level of entry region $a^{\xi*}$ increases monotonically from -9.4228 to -6.8305 as c_b increases from 0.01 to 0.1. Parameters: $\mu = 0.6$, $\sigma = 0.2$, $\theta = 1$, $r = 0.05$, $c_s = 0.02$.

much less significantly than \tilde{d}^* . Figure 2.2 (right) shows that $a^{\xi*}$, which is the same for both the optimal double stopping and switching problems, increases monotonically with c_b .

In both Figures 2.1 and 2.2, we can see that the interval of the entry and exit levels, $(\tilde{d}^*, \tilde{b}^*)$, associated with the optimal switching problem lies within the corresponding interval $(d^{\xi*}, b^{\xi*})$ from the optimal double stopping problem. Intuitively, with the intention to enter the market again upon completing the current trade, the trader is more willing to enter/exit earlier, meaning a narrowed waiting region.

Figure 2.3 shows a simulated path and the associated entry/exit levels. As the path starts at $\xi_0 = 2.6011 > e^{\tilde{d}^*} > e^{d^{\xi*}}$, the investor waits to enter until the path reaches the lower level $e^{d^{\xi*}}$ (double stopping) or $e^{\tilde{d}^*}$ (switching) according to Theorems 2.2.4 and 2.2.7. After entry, the investor exits at the optimal level $e^{b^{\xi*}}$ (double stopping) or $e^{\tilde{b}^*}$ (switching). The optimal switching

thresholds imply that the investor first enters the market on day 188 where the underlying asset price is 2.3847. In contrast, the optimal double stopping timing yields a later entry on day 845 when the price first reaches $e^{d^{\xi^*}} = 2.1754$. As for the exit timing, under the optimal switching setting, the investor exits the market earlier on day 268 at the price $e^{\tilde{b}^*} = 2.8323$. The double stopping timing is much later on day 1160 when the price reaches $e^{b^{\xi^*}} = 3.0988$. In addition, under the optimal switching problem, the investor executes more trades within the same time span. As seen in the figure, the investor would have completed two ‘round-trip’ (buy-and-sell) trades in the market before the double stopping investor liquidates for the first time.

2.2.2 CIR model

We now turn our attention to the CIR model. We consider the optimal starting-stopping problem followed by the optimal switching problem. First, we denote the infinitesimal generator of Y as

$$\mathcal{L}^x = \frac{\sigma^2 y}{2} \frac{d^2}{dy^2} + \mu(\theta - y) \frac{d}{dy},$$

and consider the ordinary differential equation (ODE)

$$\mathcal{L}^x u(y) = ru(y), \quad \text{for } y \in \mathbb{R}_+. \quad (2.2.17)$$

To present the solutions of this ODE, we define the functions

$$F^x(y) := M\left(\frac{r}{\mu}, \frac{2\mu\theta}{\sigma^2}; \frac{2\mu y}{\sigma^2}\right), \quad \text{and} \quad G^x(y) := U\left(\frac{r}{\mu}, \frac{2\mu\theta}{\sigma^2}; \frac{2\mu y}{\sigma^2}\right),$$

where

$$M(a, b; z) = \sum_{n=0}^{\infty} \frac{a_n z^n}{b_n n!}, \quad a_0 = 1, \quad a_n = a(a+1)(a+2) \cdots (a+n-1),$$

$$U(a, b; z) = \frac{\Gamma(1-b)}{\Gamma(a-b+1)} M(a, b; z) + \frac{\Gamma(b-1)}{\Gamma(a)} z^{1-b} M(a-b+1, 2-b; z)$$

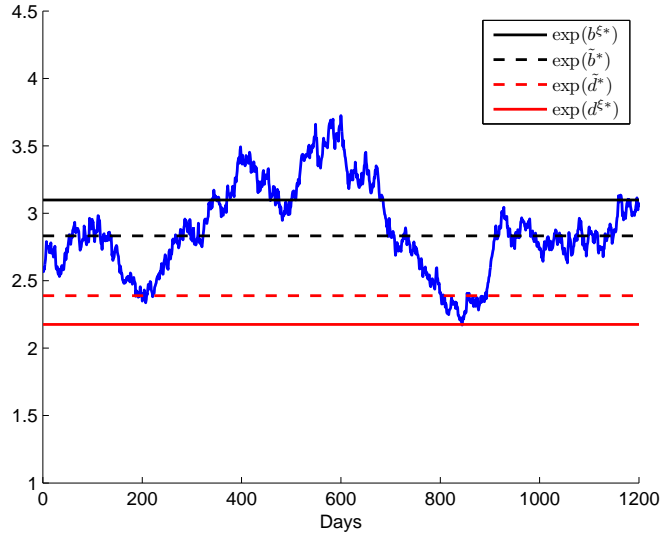


Figure 2.3: A sample XOU path, along with entry and exit levels. Under the double stopping setting, the investor enters at $\nu_{d^{\xi^*}} = \inf\{t \geq 0 : \xi_t \leq e^{d^{\xi^*}} = 2.1754\}$ with $d^{\xi^*} = 0.7772$, and exit at $\tau_{b^{\xi^*}} = \inf\{t \geq \nu_{d^{\xi^*}} : \xi_t \geq e^{b^{\xi^*}} = 3.0988\}$ with $b^{\xi^*} = 1.1310$. The optimal switching investor enters at $\nu_{\tilde{d}^*} = \inf\{t \geq 0 : \xi_t \leq e^{\tilde{d}^*} = 2.3888\}$ with $\tilde{d}^* = 0.8708$, and exit at $\tau_{\tilde{b}^*} = \inf\{t \geq \nu_{\tilde{d}^*} : \xi_t \geq e^{\tilde{b}^*} = 2.8323\}$ with $\tilde{b}^* = 1.0411$. The critical lower threshold of entry region is $e^{a^{\xi^*}} = 1.264 \cdot 10^{-4}$ with $a^{\xi^*} = -8.9760$ (not shown in this figure). Parameters: $\mu = 0.8$, $\sigma = 0.2$, $\theta = 1$, $r = 0.05$, $c_s = 0.02$, $c_b = 0.02$.

are the confluent hypergeometric functions of first and second kind, also called the Kummer's function and Tricomi's function, respectively (see Chapter 13 of Abramowitz and Stegun [1965] and Chapter 9 of Lebedev [1972]). As is well known (see Göing-Jaesche and Yor [2003]), F^x and G^x are strictly positive and, respectively, the strictly increasing and decreasing continuously differentiable solutions of the ODE (2.2.17). Also, we remark that the discounted processes $(e^{-rt}F^x(Y_t))_{t \geq 0}$ and $(e^{-rt}G^x(Y_t))_{t \geq 0}$ are martingales.

In addition, recall the reward functions defined in (2.1.9) and note that

$$(\mathcal{L}^x - r)h_b(y) \begin{cases} > 0 & \text{if } y < y_b, \\ < 0 & \text{if } y > y_b, \end{cases} \quad (2.2.18)$$

and

$$(\mathcal{L}^x - r)h_s(y) \begin{cases} > 0 & \text{if } y < y_s, \\ < 0 & \text{if } y > y_s, \end{cases} \quad (2.2.19)$$

where the critical constants y_b and y_s are defined by

$$y_b := \frac{\mu\theta - rc_b}{\mu + r} \quad \text{and} \quad y_s := \frac{\mu\theta + rc_s}{\mu + r}. \quad (2.2.20)$$

Note that y_b and y_s depend on the parameters μ , θ and r , as well as c_b and c_s respectively, but not σ .

2.2.2.1 Optimal Starting-Stopping Problem

We now present the results for the optimal starting-stopping problem (2.1.7)-(2.1.8). As it turns out, the value function V^x is expressed in terms of F^x , and J^x in terms of V^x and G^x . The functions F^x and G^x also play a role in determining the optimal starting and stopping thresholds.

First, we give a bound on the value function V^x in terms of $F^x(y)$.

Lemma 2.2.8. *There exists a positive constant K^x such that, for all $y \geq 0$, $0 \leq V^x(y) \leq K^x F^x(y)$.*

Theorem 2.2.9. *The value function for the optimal stopping problem (2.1.7) is given by*

$$V^x(y) = \begin{cases} \frac{b^{x*} - c_s}{F^x(b^{x*})} F^x(y) & \text{if } y \in [0, b^{x*}), \\ y - c_s & \text{if } y \in [b^{x*}, +\infty). \end{cases}$$

Here, the optimal stopping level $b^{x*} \in (c_s \vee y_s, \infty)$ is found from the equation

$$F^x(b) = (b - c_s)F^x'(b). \quad (2.2.21)$$

Therefore, it is optimal to stop as soon as the process Y reaches b^{x^*} from below. The stopping level b^{x^*} must also be higher than the fixed cost c_s as well as the critical level y_s defined in (2.2.20).

Now we turn to the optimal starting problem. Define the reward function

$$\hat{h}^x(y) := V^x(y) - (y + c_b).$$

Since F^x , and thus V^x , are convex, so is \hat{h}^x , we also observe that the reward function $\hat{h}^x(y)$ is decreasing in y . To exclude the scenario where it is optimal never to start, the condition stated in (2.1.10), namely, $\sup_{y \in \mathbb{R}^+} \hat{h}^x(y) > 0$, is now equivalent to

$$V^x(0) = \frac{b^{x^*} - c_s}{F^x(b^{x^*})} > c_b, \quad (2.2.22)$$

since $F^x(0) = 1$.

Lemma 2.2.10. *For all $y \geq 0$, the value function satisfies the inequality $0 \leq J^x(y) \leq (\frac{b^{x^*} - c}{F^x(b^{x^*})} - c_b)^+$.*

Theorem 2.2.11. *The optimal starting problem (2.1.8) admits the solution*

$$J^x(y) = \begin{cases} V^x(y) - (y + c_b) & \text{if } y \in [0, d^{x^*}], \\ \frac{V^x(d^{x^*}) - (d^{x^*} + c_b)}{G^x(d^{x^*})} G^x(y) & \text{if } y \in (d^{x^*}, +\infty). \end{cases}$$

The optimal starting level $d^{x^} > 0$ is uniquely determined from*

$$G^x(d)(V^{x'}(d) - 1) = G^{x'}(d)(V^x(d) - (d + c_b)).$$

As a result, it is optimal to start as soon as the CIR process Y falls below the strictly positive level d^{x^*} .

2.2.2.2 Optimal Switching Problem

Now we study the optimal switching problem under the CIR model in (2.1.2).

Lemma 2.2.12. *For all $y \geq 0$, the value functions \tilde{J}^x and \tilde{V}^x satisfy the inequalities*

$$\begin{aligned} 0 &\leq \tilde{J}^x(y) \leq \frac{\mu\theta}{r}, \\ 0 &\leq \tilde{V}^x(y) \leq y + \frac{2\mu\theta}{r}. \end{aligned}$$

We start by giving conditions under which it is optimal not to start ever.

Theorem 2.2.13. *Under the CIR model, if it holds that*

$$(i) \quad y_b \leq 0, \quad \text{or}$$

$$(ii) \quad y_b > 0 \quad \text{and} \quad c_b \geq \frac{b^{x^*} - c_s}{F^x(b^{x^*})},$$

with b^{x^} given in (2.2.21), then the optimal switching problem (2.1.13)-(2.1.14) admits the solution*

$$\tilde{J}^x(y) = 0 \quad \text{for } y \geq 0, \quad (2.2.23)$$

and

$$\tilde{V}^x(y) = \begin{cases} \frac{b^{x^*} - c_s}{F^x(b^{x^*})} F^x(y) & \text{if } y \in [0, b^{x^*}), \\ y - c_s & \text{if } y \in [b^{x^*}, +\infty). \end{cases} \quad (2.2.24)$$

Conditions (i) and (ii) depend on problem data and can be easily verified. In particular, recall that y_b is defined in (2.2.20) and is easy to compute, furthermore it is independent of σ and c_s . Since it is optimal to never enter, the switching problem is equivalent to a stopping problem and the solution in Theorem 2.2.13 agrees with that in Theorem 2.2.9. Next, we provide conditions under which it is optimal to enter as soon as the CIR process reaches some lower level.

Theorem 2.2.14. *Under the CIR model, if*

$$y_b > 0 \quad \text{and} \quad c_b < \frac{b^{x^*} - c_s}{F^x(b^{x^*})}, \quad (2.2.25)$$

with b^{x^*} given in (2.2.21), then the optimal switching problem (2.1.13)-(2.1.14) admits the solution

$$\tilde{J}^x(y) = \begin{cases} P^x F^x(y) - (y + c_b) & \text{if } y \in [0, \tilde{d}^{x^*}], \\ Q^x G^x(y) & \text{if } y \in (\tilde{d}^{x^*}, +\infty), \end{cases} \quad (2.2.26)$$

and

$$\tilde{V}^x(y) = \begin{cases} P^x F^x(y) & \text{if } y \in [0, \tilde{b}^{x^*}], \\ Q^x G^x(y) + (y - c_s) & \text{if } y \in [\tilde{b}^{x^*}, +\infty), \end{cases} \quad (2.2.27)$$

where

$$P^x = \frac{G^x(\tilde{d}^{x^*}) - (\tilde{d}^{x^*} + c_b)G^{x'}(\tilde{d}^{x^*})}{F^{x'}(\tilde{d}^{x^*})G^x(\tilde{d}^{x^*}) - F^x(\tilde{d}^{x^*})G^{x'}(\tilde{d}^{x^*})},$$

$$Q^x = \frac{F^x(\tilde{d}^{x^*}) - (\tilde{d}^{x^*} + c_b)F^{x'}(\tilde{d}^{x^*})}{F^{x'}(\tilde{d}^{x^*})G^x(\tilde{d}^{x^*}) - F^x(\tilde{d}^{x^*})G^{x'}(\tilde{d}^{x^*})}.$$

There exist unique optimal starting and stopping levels \tilde{d}^{x^*} and \tilde{b}^{x^*} , which are found from the nonlinear system of equations:

$$\frac{G^x(d) - (d + c_b)G^{x'}(d)}{F^{x'}(d)G^x(d) - F^x(d)G^{x'}(d)} = \frac{G^x(b) - (b - c_s)G^{x'}(b)}{F^{x'}(b)G^x(b) - F^x(b)G^{x'}(b)},$$

$$\frac{F^x(d) - (d + c_b)F^{x'}(d)}{F^{x'}(d)G^x(d) - F^x(d)G^{x'}(d)} = \frac{F^x(b) - (b - c_s)F^{x'}(b)}{F^{x'}(b)G^x(b) - F^x(b)G^{x'}(b)}.$$

Moreover, we have that $\tilde{d}^{x^*} < y_b$ and $\tilde{b}^{x^*} > y_s$.

In this case, it is optimal to start and stop an infinite number of times where we start as soon as the CIR process drops to \tilde{d}^{x^*} and stop when the process reaches \tilde{b}^{x^*} . Note that in the case of Theorem 2.2.13 where it is never optimal to start, the optimal stopping level b^{x^*} is the same as that of the optimal stopping problem in Theorem 2.2.9. The optimal starting level \tilde{d}^{x^*} , which only arises when it is optimal to start and stop sequentially, is in general not the same as d^{x^*} in Theorem 2.2.11.

We conclude the section with two remarks.

Remark 2.2.15. *Given the model parameters, in order to identify which of Theorem 2.2.13 or Theorem 2.2.14 applies, we begin by checking whether $y_b \leq 0$. If so, it is optimal not to enter. Otherwise, Theorem 2.2.13 still applies if $c_b \geq \frac{b^{x^*} - c_s}{F^x(b^{x^*})}$ holds. In the other remaining case, the problem is solved as in Theorem 2.2.14. In fact, the condition $c_b < \frac{b^{x^*} - c_s}{F^x(b^{x^*})}$ implies $y_b > 0$ (see the proof of Lemma 4.3 in Leung et al. [2014]). Therefore, condition (2.2.25) in Theorem 2.2.14 is in fact identical to (2.2.22) in Theorem 2.2.11.*

Remark 2.2.16. *To verify the optimality of the results in Theorems 2.2.13 and 2.2.14, one can show by direct substitution that the solutions $(\tilde{J}^x, \tilde{V}^x)$ in (2.2.23)-(2.2.24) and (2.2.26)-(2.2.27) satisfy the variational inequalities:*

$$\begin{aligned} \min\{r\tilde{J}^x(y) - \mathcal{L}^x\tilde{J}^x(y), \tilde{J}^x(y) - (\tilde{V}^x(y) - (y + c_b))\} &= 0, \\ \min\{r\tilde{V}^x(y) - \mathcal{L}^x\tilde{V}^x(y), \tilde{V}^x(y) - (\tilde{J}^x(y) + (y - c_s))\} &= 0. \end{aligned}$$

Indeed, this is the approach used by Zervos et al. [2013] for checking the solutions of their optimal switching problems.

2.2.2.3 Numerical Examples

We numerically implement Theorems 2.2.9, 2.2.11, and 2.2.14, and illustrate the associated starting and stopping thresholds. In Figure 2.4 (left), we observe the changes in optimal starting and stopping levels as speed of mean reversion increases. Both starting levels d^{x^*} and \tilde{d}^{x^*} rise with μ , from 0.0964 to 0.1219 and from 0.1460 to 0.1696, respectively, as μ increases from 0.3 to 0.85. The optimal switching stopping level \tilde{b}^{x^*} also increases. On the other hand, stopping level b^{x^*} for the starting-stopping problem stays relatively constant as μ changes.

In Figure 2.4 (right), we see that as the stopping cost c_s increases, the increase in the optimal stopping levels is accompanied by a fall in optimal starting levels. In particular, the stopping levels, b^{x^*} and \tilde{b}^{x^*} increase. In

comparison, both starting levels d^{x^*} and \tilde{d}^{x^*} fall. The lower starting level and higher stopping level mean that the entry and exit times are both delayed as a result of a higher transaction cost. Interestingly, although the cost c_s applies only when the process is stopped, it also has an impact on the timing to *start*, as seen in the changes in d^{x^*} and \tilde{d}^{x^*} in the figure.

In Figure 2.4, we can see that the continuation (waiting) region of the switching problem $(\tilde{d}^{x^*}, \tilde{b}^{x^*})$ lies within that of the starting-stopping problem (d^{x^*}, b^{x^*}) . The ability to enter and exit multiple times means it is possible to earn a smaller reward on each individual start-stop sequence while maximizing aggregate return. Moreover, we observe that optimal entry and exit levels of the starting-stopping problem is less sensitive to changes in model parameters than the entry and exit thresholds of the switching problem.

Figure 2.5 shows a simulated CIR path along with optimal entry and exit levels for both starting-stopping and switching problems. Under the starting-stopping problem, it is optimal to start once the process reaches $d^{x^*} = 0.0373$ and to stop when the process hits $b^{x^*} = 0.4316$. For the switching problem, it is optimal to start once the process values hits $\tilde{d}^{x^*} = 0.1189$ and to stop when the value of the CIR process rises to $\tilde{b}^{x^*} = 0.2078$. We note that both stopping levels b^{x^*} and \tilde{b}^{x^*} are higher than the long-run mean $\theta = 0.2$, and the starting levels d^{x^*} and \tilde{d}^{x^*} are lower than θ . The process starts at $Y_0 = 0.15 > \tilde{d}^{x^*}$, under the optimal switching setting, the first time to enter occurs on day 8 when the process falls to 0.1172 and subsequently exits on day 935 at a level of 0.2105. For the starting-stopping problem, entry takes place much later on day 200 when the process hits 0.0306 and exits on day 2671 at 0.4369. Under the optimal switching problem, two entries and two exits will be completed by the time a single entry-exit sequence is realized for the starting-stopping problem.

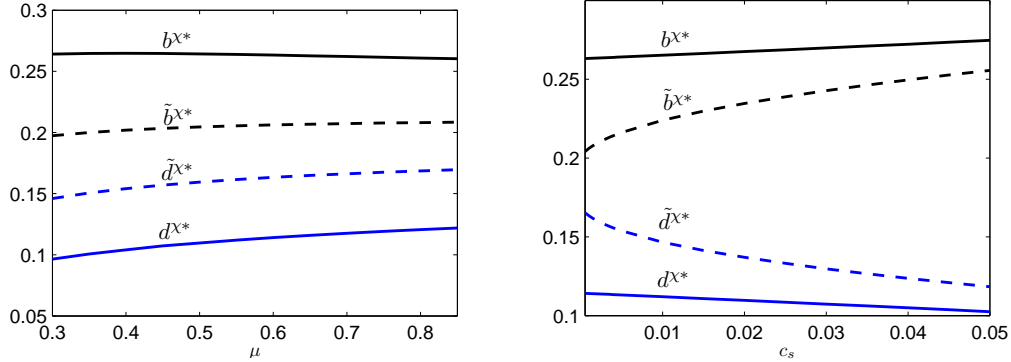


Figure 2.4: (Left) The optimal starting and stopping levels vs speed of mean reversion μ . Parameters: $\sigma = 0.15$, $\theta = 0.2$, $r = 0.05$, $c_s = 0.001$, $c_b = 0.001$. (Right) The optimal starting and stopping levels vs transaction cost c_s . Parameters: $\mu = 0.6$, $\sigma = 0.15$, $\theta = 0.2$, $r = 0.05$, $c_b = 0.001$.

2.3 Methods of Solution and Proofs

We now provide detailed proofs for our analytical results in Section 2.2 for the optimal switching problems. Using the results for the double stopping problems i.e. Theorems 2.2.2 and 2.2.4 under the XOU model and Theorems 2.2.9 and 2.2.11 under the CIR model, we can infer the structure of the buy and sell regions of the switching problems and then proceed to verify its optimality.

2.3.1 Optimal Switching Timing under the XOU Model

In this section, we provide detailed proofs for Theorems 2.2.6 and 2.2.7.

Proof of Theorem 2.2.6 (Part 1) First, with $h_s^\xi(x) = e^x - c_s$, we differentiate to get

$$\left(\frac{h_s^\xi}{F}\right)'(x) = \frac{(e^x - c_s)F'(x) - e^x F(x)}{F^2(x)}. \quad (2.3.1)$$

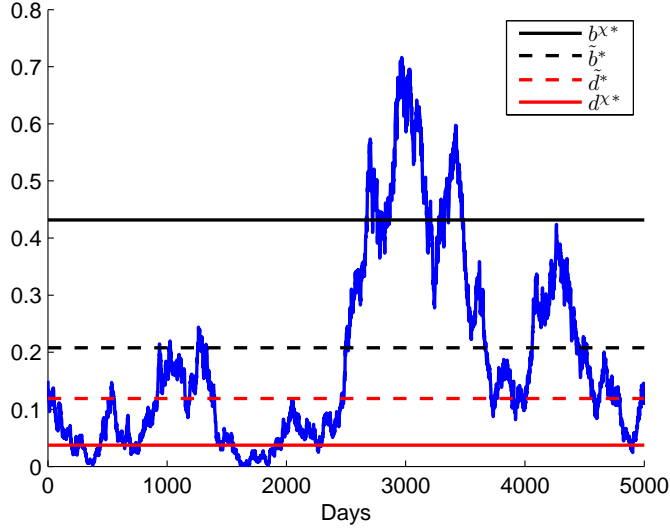


Figure 2.5: A sample CIR path, along with starting and stopping levels. Under the starting-stopping setting, a starting decision is made at $\nu_{d^{x^*}} = \inf\{t \geq 0 : Y_t \leq d^{x^*} = 0.0373\}$, and a stopping decision is made at $\tau_{b^{x^*}} = \inf\{t \geq \nu_{d^{x^*}} : Y_t \geq b^{x^*} = 0.4316\}$. Under the optimal switching problem, entry and exit take place at $\nu_{\tilde{d}^{x^*}} = \inf\{t \geq 0 : Y_t \leq \tilde{d}^{x^*} = 0.1189\}$, and $\tau_{\tilde{b}^{x^*}} = \inf\{t \geq \nu_{\tilde{d}^{x^*}} : Y_t \geq \tilde{b}^{x^*} = 0.2078\}$ respectively. Parameters: $\mu = 0.2$, $\sigma = 0.3$, $\theta = 0.2$, $r = 0.05$, $c_s = 0.001$, $c_b = 0.001$.

On the other hand, by Ito's lemma, we have

$$h_s^\xi(x) = \mathbb{E}_x\{e^{-rt}h_s^\xi(X_t)\} - \mathbb{E}_x\left\{\int_0^t e^{-ru}(\mathcal{L} - r)h_s^\xi(X_u)du\right\}.$$

Note that

$$\mathbb{E}_x\{e^{-rt}h_s^\xi(X_t)\} = e^{-rt}\left(e^{(x-\theta)e^{-\mu t} + \theta + \frac{\sigma^2}{4\mu}(1-e^{-2\mu t})} - c_s\right) \rightarrow 0 \quad \text{as } t \rightarrow +\infty.$$

This implies that

$$\begin{aligned} h_s^\xi(x) &= -\mathbb{E}_x\left\{\int_0^{+\infty} e^{-ru}(\mathcal{L} - r)h_s^\xi(X_u)du\right\} \\ &= -G(x)\int_{-\infty}^x \Psi(s)(\mathcal{L} - r)h_s^\xi(s)ds \\ &\quad - F(x)\int_x^{+\infty} \Phi(s)(\mathcal{L} - r)h_s^\xi(s)ds, \end{aligned} \tag{2.3.2}$$

where Ψ is defined in (2.2.16) and

$$\Phi(x) := \frac{2G(x)}{\sigma^2\mathcal{W}(x)}.$$

The last line follows from Theorem 50.7 in Rogers and Williams [2000, p. 293].

Dividing both sides by $F(x)$ and differentiating the RHS of (2.3.2), we obtain

$$\begin{aligned} \left(\frac{h_s^\xi}{F}\right)'(x) &= -\left(\frac{G}{F}\right)'(x) \int_{-\infty}^x \Psi(s)(\mathcal{L} - r)h_s^\xi(s)ds \\ &\quad - \frac{G}{F}(x)\Psi(x)(\mathcal{L} - r)h_s^\xi(x) - \Phi(x)(\mathcal{L} - r)h_s^\xi(x) \\ &= \frac{\mathcal{W}(x)}{F^2(x)} \int_{-\infty}^x \Psi(s)(\mathcal{L} - r)h_s^\xi(s)ds = \frac{\mathcal{W}(x)}{F^2(x)}q(x), \end{aligned}$$

where

$$q(x) := \int_{-\infty}^x \Psi(s)(\mathcal{L} - r)h_s^\xi(s)ds.$$

Since $\mathcal{W}(x), F(x) > 0$, we deduce that $\left(\frac{h_s^\xi}{F}\right)'(x) = 0$ is equivalent to $q(x) = 0$.

Using (2.3.1), we now see that (2.2.3) is equivalent to $q(b) = 0$.

Next, it follows from (2.2.6) that

$$q'(x) = \Psi(x)(\mathcal{L} - r)h_s^\xi(x) \begin{cases} > 0 & \text{if } x < x_s, \\ < 0 & \text{if } x > x_s. \end{cases} \quad (2.3.3)$$

This, together with the fact that $\lim_{x \rightarrow -\infty} q(x) = 0$, implies that there exists

a unique b^{ξ^*} such that $q(b^{\xi^*}) = 0$ if and only if $\lim_{x \rightarrow +\infty} q(x) < 0$. Next, we

show that this inequality holds. By the definition of h_s^ξ and F , we have

$$\begin{aligned} \frac{h_s^\xi(x)}{F(x)} &= \frac{e^x - c_s}{F(x)} > 0 \quad \text{for } x > \ln c_s, & \lim_{x \rightarrow +\infty} \frac{h_s^\xi(x)}{F(x)} &= 0, \\ \left(\frac{h_s^\xi}{F}\right)'(x) &= \frac{\mathcal{W}(x)}{F^2(x)} \int_{-\infty}^x \Psi(s)(\mathcal{L} - r)h_s^\xi(s)ds = \frac{\mathcal{W}(x)}{F^2(x)}q(x). \end{aligned} \quad (2.3.4)$$

Since q is strictly decreasing in $(x_s, +\infty)$, the above hold true if and only if

$\lim_{x \rightarrow +\infty} q(x) < 0$. Therefore, we conclude that there exists a unique b^{ξ^*} such

that $e^b F(b) = (e^b - c_s)F'(b)$. Using (2.3.3), we see that

$$b^{\xi^*} > x_s \quad \text{and} \quad q(x) > 0 \quad \text{for all } x < b^{\xi^*}. \quad (2.3.5)$$

Observing that $e^{b^{\xi^*}}, F(b^{\xi^*}), F'(b^{\xi^*}) > 0$, we can conclude that $h_s^\xi(b^{\xi^*}) = e^{b^{\xi^*}} - c_s > 0$, or equivalently $b^{\xi^*} > \ln c_s$.

We now verify by direct substitution that $\tilde{V}^\xi(x)$ and $\tilde{J}^\xi(x)$ in (2.2.7) satisfy the pair of variational inequalities:

$$\min\{r\tilde{J}^\xi(x) - \mathcal{L}\tilde{J}^\xi(x), \tilde{J}^\xi(x) - (\tilde{V}^\xi(x) - h_b^\xi(x))\} = 0, \quad (2.3.6)$$

$$\min\{r\tilde{V}^\xi(x) - \mathcal{L}\tilde{V}^\xi(x), \tilde{V}^\xi(x) - (\tilde{J}^\xi(x) + h_s^\xi(x))\} = 0. \quad (2.3.7)$$

First, note that $\tilde{J}^\xi(x)$ is identically 0 and thus satisfies the equality

$$(r - \mathcal{L})\tilde{J}^\xi(x) = 0. \quad (2.3.8)$$

To show that $\tilde{J}^\xi(x) - (\tilde{V}^\xi(x) - h_b^\xi(x)) \geq 0$, we look at the disjoint intervals $(-\infty, b^{\xi^*})$ and $[b^{\xi^*}, \infty)$ separately. For $x \geq b^{\xi^*}$, we have

$$\tilde{V}^\xi(x) - h_b^\xi(x) = -(c_b + c_s),$$

which implies $\tilde{J}^\xi(x) - (\tilde{V}^\xi(x) - h_b^\xi(x)) = c_b + c_s \geq 0$. When $x < b^{\xi^*}$, the inequality

$$\tilde{J}^\xi(x) - (\tilde{V}^\xi(x) - h_b^\xi(x)) \geq 0$$

can be rewritten as

$$\frac{h_b^\xi(x)}{F(x)} = \frac{e^x + c_b}{F(x)} \geq \frac{e^{b^{\xi^*}} - c_s}{F(b^{\xi^*})} = \frac{h_s^\xi(b^{\xi^*})}{F(b^{\xi^*})}. \quad (2.3.9)$$

To determine the necessary conditions for this to hold, we consider the derivative of the LHS of (2.3.9):

$$\begin{aligned} \left(\frac{h_b^\xi}{F}\right)'(x) &= \frac{\mathcal{W}(x)}{F^2(x)} \int_{-\infty}^x \Psi(s)(\mathcal{L} - r)h_b^\xi(s)ds \\ &= \frac{\mathcal{W}(x)}{F^2(x)} \int_{-\infty}^x \Psi(s)e^s f_b(s)ds. \end{aligned} \quad (2.3.10)$$

If $f_b(x) = 0$ has no roots, then $(\mathcal{L} - r)h_b^\xi(x)$ is negative for all $x \in \mathbb{R}$. On the other hand, if there is only one root \tilde{x} , then $(\mathcal{L} - r)h_b^\xi(\tilde{x}) = 0$ and $(\mathcal{L} - r)h_b^\xi(x) <$

0 for all other x . In either case, $h_b^\xi(x)/F(x)$ is a strictly decreasing function and (2.3.9) is true.

Otherwise if $f_b(x) = 0$ has two distinct roots x_{b1} and x_{b2} with $x_{b1} < x_{b2}$, then

$$(\mathcal{L} - r)h_b^\xi(x) \begin{cases} < 0 & \text{if } x \in (-\infty, x_{b1}) \cup (x_{b2}, +\infty), \\ > 0 & \text{if } x \in (x_{b1}, x_{b2}). \end{cases} \quad (2.3.11)$$

Applying (2.3.11) to (2.3.10), the derivative $(h_b^\xi/F)'(x)$ is negative on $(-\infty, x_{b1})$ since the integrand in (2.3.10) is negative. Hence, $h_b^\xi(x)/F(x)$ is strictly decreasing on $(-\infty, x_{b1})$. We further note that $b^{\xi*} > x_s > x_{b2}$. Observe that on the interval (x_{b1}, x_{b2}) , the integrand is positive. It is therefore possible for $(h_b^\xi/F)'$ to change sign at some $x \in (x_{b1}, x_{b2})$. For this to happen, the positive part of the integral must be larger than the absolute value of the negative part. In other words, (2.2.15) must hold. If (2.2.15) holds, then there must exist some $\tilde{a}^* \in (x_{b1}, x_{b2})$ such that $(h_b^\xi/F)'(\tilde{a}^*) = 0$, or equivalently (2.2.8) holds:

$$\left(\frac{h_b^\xi}{F}\right)'(\tilde{a}^*) = \frac{h_b^{\xi'}(\tilde{a}^*)}{F(\tilde{a}^*)} - \frac{h_b^\xi(\tilde{a}^*)F'(\tilde{a}^*)}{F^2(\tilde{a}^*)} = \frac{e^{\tilde{a}^*}}{F(\tilde{a}^*)} - \frac{(e^{\tilde{a}^*} + c_b)F(\tilde{a}^*)'}{F^2(\tilde{a}^*)}.$$

If (2.2.8) holds, then we have

$$\left| \int_{-\infty}^{x_{b1}} \Psi(x)e^x f_b(x) dx \right| = \int_{x_{b1}}^{\tilde{a}^*} \Psi(x)e^x f_b(x) dx.$$

In addition, since

$$\int_{\tilde{a}^*}^{x_{b2}} \Psi(x)e^x f_b(x) dx > 0,$$

it follows that

$$\left| \int_{-\infty}^{x_{b1}} \Psi(x)e^x f_b(x) dx \right| < \int_{x_{b1}}^{x_{b2}} \Psi(x)e^x f_b(x) dx.$$

This establishes the equivalence between (2.2.8) and (2.2.15). Under this condition, h_b^ξ/F is strictly decreasing on (x_{b1}, \tilde{a}^*) . Then, either it is strictly increasing on $(\tilde{a}^*, b^{\xi*})$, or there exists some $\bar{x} \in (x_{b2}, b^{\xi*})$ such that $h_b^\xi(x)/F(x)$ is

strictly increasing on (\tilde{a}^*, \bar{x}) and strictly decreasing on (\bar{x}, b^{ξ^*}) . In both cases, (2.3.9) is true if and only if (2.2.9) holds.

Alternatively, if (2.2.15) doesn't hold, then by (2.3.10), the integral $(h_b^\xi/F)'$ will always be negative. This means that the function $h_b^\xi(x)/F(x)$ is strictly decreasing for all $x \in (-\infty, b^{\xi^*})$, in which case (2.3.9) holds.

We are thus able to show that (2.3.6) holds, in particular the minimum of 0 is achieved as a result of (2.3.8). To prove (2.3.7), we go through a similar procedure. To check that

$$(r - \mathcal{L})\tilde{V}^\xi(x) \geq 0$$

holds, we consider two cases. First when $x < b^{\xi^*}$, we get

$$(r - \mathcal{L})\tilde{V}^\xi(x) = \frac{e^{b^{\xi^*}} - c_s}{F(b^{\xi^*})}(r - \mathcal{L})F(x) = 0.$$

On the other hand, when $x \geq b^{\xi^*}$, the inequality holds

$$(r - \mathcal{L})\tilde{V}^\xi(x) = (r - \mathcal{L})h_s^\xi(x) > 0,$$

since $b^{\xi^*} > x_s$ (the first inequality of (2.3.5)) and (2.2.6).

Similarly, when $x \geq b^{\xi^*}$, we have

$$\tilde{V}^\xi(x) - (\tilde{J}^\xi(x) + h_s^\xi(x)) = h_s^\xi(x) - h_s^\xi(x) = 0.$$

When $x < b^{\xi^*}$, the inequality holds:

$$\tilde{V}^\xi(x) - (\tilde{J}^\xi(x) + h_s^\xi(x)) = \frac{h_s^\xi(b^{\xi^*})}{F(b^{\xi^*})}F(x) - h_s^\xi(x) \geq 0,$$

which is equivalent to $\frac{h_s^\xi(x)}{F(x)} \leq \frac{h_s^\xi(b^{\xi^*})}{F(b^{\xi^*})}$, due to (2.3.4) and (2.3.5).

Proof of Theorem 2.2.7 (Part 1) Define the functions

$$\begin{aligned} q_G(x, z) &= \int_x^{+\infty} \Phi(s)(\mathcal{L} - r)h_b^\xi(s)ds - \int_z^{+\infty} \Phi(s)(\mathcal{L} - r)h_s^\xi(s)ds, \\ q_F(x, z) &= \int_{-\infty}^x \Psi(s)(\mathcal{L} - r)h_b^\xi(s)ds - \int_{-\infty}^z \Psi(s)(\mathcal{L} - r)h_s^\xi(s)ds. \end{aligned}$$

where We look for the points $\tilde{d}^* < \tilde{b}^*$ such that

$$q_G(\tilde{d}^*, \tilde{b}^*) = 0, \quad \text{and} \quad q_F(\tilde{d}^*, \tilde{b}^*) = 0.$$

This is because these two equations are equivalent to (2.2.13) and (2.2.14), respectively.

Now we start to solve the equations by first narrowing down the range for \tilde{d}^* and \tilde{b}^* . Observe that

$$\begin{aligned} q_G(x, z) &= \int_x^z \Phi(s)(\mathcal{L} - r)h_b^\xi(s)ds + \int_z^\infty \Phi(s)[(\mathcal{L} - r)(h_b^\xi(s) - h_s^\xi(s))]ds \\ &= \int_x^z \Phi(s)(\mathcal{L} - r)h_b^\xi(s)ds - r(c_b + c_s) \int_z^\infty \Phi(s)ds \\ &< 0, \end{aligned} \tag{2.3.12}$$

for all x and z such that $x_{b2} \leq x < z$. Therefore, $\tilde{d}^* \in (-\infty, x_{b2})$.

Since $b^{\xi*} > x_s$ satisfies $q(b^{\xi*}) = 0$ and $\tilde{a}^* < x_{b2}$ satisfies (2.2.8), we have

$$\begin{aligned} \lim_{z \rightarrow +\infty} q_F(x, z) &= \int_{-\infty}^x \Psi(s)(\mathcal{L} - r)h_b^\xi(s)ds - q(b^{\xi*}) - \int_{b^{\xi*}}^{+\infty} \Psi(s)(\mathcal{L} - r)h_s^\xi(s)ds \\ &> 0, \end{aligned}$$

for all $x \in (\tilde{a}^*, x_{b2})$. Also, we note that

$$\frac{\partial q_F}{\partial z}(x, z) = -\Psi(z)(\mathcal{L} - r)h_s^\xi(z) \begin{cases} < 0 & \text{if } z < x_s, \\ > 0 & \text{if } z > x_s, \end{cases} \tag{2.3.13}$$

and

$$\begin{aligned} q_F(x, x) &= \int_{-\infty}^x \Psi(s)(\mathcal{L} - r) \left[h_b^\xi(s) - h_s^\xi(s) \right] ds \\ &= -r(c_b + c_s) \int_{-\infty}^x \Psi(s)ds < 0. \end{aligned} \tag{2.3.14}$$

Then, (2.3.13) and (2.3.14) imply that there exists a unique function $\beta : [\tilde{a}^*, x_{b2}) \mapsto \mathbb{R}$ s.t. $\beta(x) > x_s$ and

$$q_F(x, \beta(x)) = 0. \tag{2.3.15}$$

Differentiating (2.3.15) with respect to x , we see that

$$\beta'(x) = \frac{\Psi(x)(\mathcal{L} - r)h_b^\xi(x)}{\Psi(\beta(x))(\mathcal{L} - r)h_s^\xi(\beta(x))} < 0,$$

for all $x \in (x_{b1}, x_{b2})$. In addition, by the facts that $b^{\xi*} > x_s$ satisfies $q(b^{\xi*}) = 0$, \tilde{a}^* satisfies (2.2.8), and the definition of q_F , we have

$$\beta(\tilde{a}^*) = b^{\xi*}.$$

By (2.3.12), we have $\lim_{x \uparrow x_{b2}} q_G(x, \beta(x)) < 0$. By computation, we get that

$$\begin{aligned} \frac{d}{dx} q_G(x, \beta(x)) &= -\frac{\Phi(x)\Psi(\beta(x)) - \Phi(\beta(x))\Psi(x)}{\Psi(\beta(x))} (\mathcal{L} - r)h_b^\xi(x) \\ &= -\Psi(x) \left[\frac{G(x)}{F(x)} - \frac{G(\beta(x))}{F(\beta(x))} \right] (\mathcal{L} - r)h_b^\xi(x) < 0, \end{aligned}$$

for all $x \in (x_{b1}, x_{b2})$. Therefore, there exists a unique \tilde{d}^* such that $q_G(\tilde{d}^*, \beta(\tilde{d}^*)) = 0$ if and only if

$$q_G(\tilde{a}^*, \beta(\tilde{a}^*)) > 0.$$

The above inequality holds if (2.2.10) holds. Indeed, direct computation yields the equivalence:

$$\begin{aligned} q_G(\tilde{a}^*, \beta(\tilde{a}^*)) &= \int_{\tilde{a}^*}^{+\infty} \Phi(s)(\mathcal{L} - r)h_b^\xi(s)ds - \int_{b^{\xi*}}^{+\infty} \Phi(s)(\mathcal{L} - r)h_s^\xi(s)ds \\ &= -\frac{h_b^\xi(\tilde{a}^*)}{F(\tilde{a}^*)} - \frac{G(b^{\xi*})}{F(b^{\xi*})} \int_{-\infty}^{b^{\xi*}} \Psi(s)(\mathcal{L} - r)h_s^\xi(s)ds - \int_{b^{\xi*}}^{+\infty} \Phi(s)(\mathcal{L} - r)h_s^\xi(s)ds \\ &= -\frac{e^{\tilde{a}^*} + c_b}{F(\tilde{a}^*)} + \frac{e^{b^{\xi*}} - c_s}{F(b^{\xi*})}. \end{aligned}$$

When this solution exists, we have

$$\tilde{d}^* \in (x_{b1}, x_{b2}) \text{ and } \tilde{b}^* := \beta(\tilde{d}^*) > x_s.$$

Next, we show that the functions \tilde{J}^ξ and \tilde{V}^ξ given in (2.2.11) and (2.2.12) satisfy the pair of VIs in (2.3.6) and (2.3.7). In the same vein as the proof for Theorem 2.2.6, we show

$$(r - \mathcal{L})\tilde{J}^\xi(x) \geq 0$$

by examining the 3 disjoint regions on which $\tilde{J}^\xi(x)$ assume different forms. When $x < \tilde{a}^*$,

$$(r - \mathcal{L})\tilde{J}^\xi(x) = \tilde{P}(r - \mathcal{L})F(x) = 0.$$

Next, when $x > \tilde{d}^*$,

$$(r - \mathcal{L})\tilde{J}^\xi(x) = \tilde{Q}(r - \mathcal{L})G(x) = 0.$$

Finally for $x \in [\tilde{a}^*, \tilde{d}^*]$,

$$(r - \mathcal{L})\tilde{J}^\xi(x) = (r - \mathcal{L})(\tilde{K}F(x) - h_b^\xi(x)) = -(r - \mathcal{L})h_b^\xi(x) > 0,$$

as a result of (2.3.11) since $\tilde{a}^*, \tilde{d}^* \in (x_{b1}, x_{b2})$.

Next, we verify that

$$(r - \mathcal{L})\tilde{V}^\xi(x) \geq 0.$$

Indeed, we have $(r - \mathcal{L})\tilde{V}^\xi(x) = \tilde{K}(r - \mathcal{L})F(x) = 0$ for $x < \tilde{b}^*$. When $x \geq \tilde{b}^*$, we get the inequality $(r - \mathcal{L})\tilde{V}^\xi(x) = (r - \mathcal{L})(\tilde{Q}G(x) + h_s^\xi(x)) = (r - \mathcal{L})h_s^\xi(x) > 0$ since $\tilde{b}^* > x_s$ and due to (2.2.6).

It remains to show that $\tilde{J}^\xi(x) - (\tilde{V}^\xi(x) - h_b^\xi(x)) \geq 0$ and $\tilde{V}^\xi(x) - (\tilde{J}^\xi(x) + h_s^\xi(x)) \geq 0$. When $x < \tilde{a}^*$, we have

$$\begin{aligned} \tilde{J}^\xi(x) - (\tilde{V}^\xi(x) - h_b^\xi(x)) &= (\tilde{P} - \tilde{K})F(x) + (e^x + c_b) \\ &= -F(x) \frac{e^{\tilde{a}^*} + c_b}{F(\tilde{a}^*)} + (e^x + c_b) \geq 0. \end{aligned}$$

This inequality holds since we have shown in the proof of Theorem 2.2.6 that $\frac{h_b^\xi(x)}{F(x)}$ is strictly decreasing for $x < \tilde{a}^*$. In addition,

$$\tilde{V}^\xi(x) - (\tilde{J}^\xi(x) + h_s^\xi(x)) = F(x) \frac{e^{\tilde{a}^*} + c_b}{F(\tilde{a}^*)} - (e^x - c_s) \geq 0,$$

since (2.3.3) (along with the ensuing explanation) implies that $\frac{h_s^\xi(x)}{F(x)}$ is increasing for all $x \leq \tilde{a}^*$.

In the other region where $x \in [\tilde{a}^*, \tilde{d}^*]$, we have

$$\begin{aligned} \tilde{J}^\xi(x) - (\tilde{V}^\xi(x) - h_b^\xi(x)) &= 0, \\ \tilde{V}^\xi(x) - (\tilde{J}^\xi(x) + h_s^\xi(x)) &= h_b^\xi(x) - h_s^\xi(x) = c_b + c_s \geq 0. \end{aligned}$$

When $x > \tilde{b}^*$, it is clear that

$$\begin{aligned} \tilde{J}^\xi(x) - (\tilde{V}^\xi(x) - h_b^\xi(x)) &= h_b^\xi(x) - h_s^\xi(x) = c_b + c_s \geq 0, \\ \tilde{V}^\xi(x) - (\tilde{J}^\xi(x) + h_s^\xi(x)) &= 0. \end{aligned}$$

To establish the inequalities for $x \in (\tilde{d}^*, \tilde{b}^*)$, we first denote

$$\begin{aligned} g_{\tilde{J}^\xi}(x) &:= \tilde{J}^\xi(x) - (\tilde{V}^\xi(x) - h_b^\xi(x)) = \tilde{Q}G(x) - \tilde{K}F(x) + h_b^\xi(x) \\ &= F(x) \int_{\tilde{d}^*}^x \Phi(s)(\mathcal{L} - r)h_b^\xi(s)ds - G(x) \int_{\tilde{d}^*}^x \Psi(s)(\mathcal{L} - r)h_b^\xi(s)ds, \\ g_{\tilde{V}^\xi}(x) &:= \tilde{V}^\xi(x) - (\tilde{J}^\xi(x) + h_s^\xi(x)) = \tilde{K}F(x) - \tilde{Q}G(x) - h_s^\xi(x) \\ &= F(x) \int_x^{\tilde{b}^*} \Phi(s)(\mathcal{L} - r)h_s^\xi(s)ds - G(x) \int_x^{\tilde{b}^*} \Psi(s)(\mathcal{L} - r)h_s^\xi(s)ds. \end{aligned}$$

In turn, we compute to get

$$\begin{aligned} g'_{\tilde{J}^\xi}(x) &= F'(x) \int_{\tilde{d}^*}^x \Phi(s)(\mathcal{L} - r)h_b^\xi(s)ds - G'(x) \int_{\tilde{d}^*}^x \Psi(s)(\mathcal{L} - r)h_b^\xi(s)ds, \\ g'_{\tilde{V}^\xi}(x) &= F'(x) \int_x^{\tilde{b}^*} \Phi(s)(\mathcal{L} - r)h_s^\xi(s)ds - G'(x) \int_x^{\tilde{b}^*} \Psi(s)(\mathcal{L} - r)h_s^\xi(s)ds. \end{aligned}$$

Recall the definition of x_{b2} and x_s , and the fact that $G' < 0 < F'$, we have $g'_{\tilde{J}^\xi}(x) > 0$ for $x \in (\tilde{d}^*, x_{b2})$ and $g'_{\tilde{V}^\xi}(x) < 0$ for $x \in (x_s, \tilde{b}^*)$. These, together

with the fact that $g_{\tilde{J}^\xi}(\tilde{d}^*) = g_{\tilde{V}^\xi}(\tilde{b}^*) = 0$, imply that

$$g_{\tilde{J}^\xi}(x) > 0 \text{ for } x \in (\tilde{d}^*, x_{b2}), \text{ and } g_{\tilde{V}^\xi}(x) > 0 \text{ for } x \in (x_s, \tilde{b}^*).$$

Furthermore, since we have

$$g_{\tilde{J}^\xi}(\tilde{b}^*) = c_b + c_s \geq 0, \quad g_{\tilde{V}^\xi}(\tilde{d}^*) = c_b + c_s \geq 0, \quad (2.3.16)$$

and

$$\begin{aligned} (\mathcal{L} - r)g_{\tilde{J}^\xi}(x) &= (\mathcal{L} - r)h_b^\xi(x) < 0 \text{ for all } x \in (x_{b2}, \tilde{b}^*), \\ (\mathcal{L} - r)g_{\tilde{V}^\xi}(x) &= -(\mathcal{L} - r)h_s^\xi(x) < 0 \text{ for all } x \in (\tilde{d}^*, x_s). \end{aligned} \quad (2.3.17)$$

In view of inequalities (2.3.16)–(2.3.17), the maximum principle implies that $g_{\tilde{J}^\xi}(x) \geq 0$ and $g_{\tilde{V}^\xi}(x) \geq 0$ for all $x \in (\tilde{d}^*, \tilde{b}^*)$. Hence, we conclude that $\tilde{J}(x) - (\tilde{V}(x) - h_b^\xi(x)) \geq 0$ and $\tilde{V}(x) - (\tilde{J}(x) + h_s^\xi(x)) \geq 0$ hold for $x \in (\tilde{d}^*, \tilde{b}^*)$.

Proof of Theorems 2.2.6 and 2.2.7 (Part 2) We now show that the candidate solutions in Theorems 2.2.6 and 2.2.7, denoted by \tilde{j}^ξ and \tilde{v}^ξ , are equal to the optimal switching value functions \tilde{J}^ξ and \tilde{V}^ξ in (2.1.11) and (2.1.12), respectively. First, we note that $\tilde{j}^\xi \leq \tilde{J}^\xi$ and $\tilde{v}^\xi \leq \tilde{V}^\xi$, since \tilde{J}^ξ and \tilde{V}^ξ dominate the expected discounted cash low from any admissible strategy.

Next, we show the reverse inequalities. In Part 1, we have proved that \tilde{j}^ξ and \tilde{v}^ξ satisfy the VIs (2.3.6) and (2.3.7). In particular, we know that $(r - \mathcal{L})\tilde{j}^\xi \geq 0$, and $(r - \mathcal{L})\tilde{v}^\xi \geq 0$. Then by Dynkin's formula and Fatou's lemma, as in Øksendal [2003, p. 226], for any stopping times ζ_1 and ζ_2 such that $0 \leq \zeta_1 \leq \zeta_2$ almost surely, we have the inequalities

$$\mathbb{E}_x \{e^{-r\zeta_1} \tilde{j}^\xi(X_{\zeta_1})\} \geq \mathbb{E}_x \{e^{-r\zeta_2} \tilde{j}^\xi(X_{\zeta_2})\}, \quad (2.3.18)$$

$$\mathbb{E}_x \{e^{-r\zeta_1} \tilde{v}^\xi(X_{\zeta_1})\} \geq \mathbb{E}_x \{e^{-r\zeta_2} \tilde{v}^\xi(X_{\zeta_2})\}. \quad (2.3.19)$$

For $\Lambda_0 = (\nu_1, \tau_1, \nu_2, \tau_2, \dots)$, noting that $\nu_1 \leq \tau_1$ almost surely, we have

$$\tilde{j}^\xi(x) \geq \mathbb{E}_x \{e^{-r\nu_1} \tilde{j}^\xi(X_{\nu_1})\} \quad (2.3.20)$$

$$\geq \mathbb{E}_x \{e^{-r\nu_1} (\tilde{v}^\xi(X_{\nu_1}) - h_b^\xi(X_{\nu_1}))\} \quad (2.3.21)$$

$$\geq \mathbb{E}_x \{e^{-r\tau_1} \tilde{v}^\xi(X_{\tau_1})\} - \mathbb{E}_x \{e^{-r\nu_1} h_b^\xi(X_{\nu_1})\} \quad (2.3.22)$$

$$\geq \mathbb{E}_x \{e^{-r\tau_1} (\tilde{j}^\xi(X_{\tau_1}) + h_s^\xi(X_{\tau_1}))\} - \mathbb{E}_x \{e^{-r\nu_1} h_b^\xi(X_{\nu_1})\} \quad (2.3.23)$$

$$= \mathbb{E}_x \{e^{-r\tau_1} \tilde{j}^\xi(X_{\tau_1})\} + \mathbb{E}_x \{e^{-r\tau_1} h_s^\xi(X_{\tau_1}) - e^{-r\nu_1} h_b^\xi(X_{\nu_1})\}, \quad (2.3.24)$$

where (2.3.20) and (2.3.22) follow from (2.3.18) and (2.3.19) respectively. Also, (2.3.21) and (2.3.23) follow from (2.3.6) and (2.3.7) respectively. Observe that (2.3.24) is a recursion and $\tilde{j}^\xi(x) \geq 0$ in both Theorems 2.2.6 and 2.2.7, we obtain

$$\tilde{j}^\xi(x) \geq \mathbb{E}_x \left\{ \sum_{n=1}^{\infty} [e^{-r\tau_n} h_s^\xi(X_{\tau_n}) - e^{-r\nu_n} h_b^\xi(X_{\nu_n})] \right\}.$$

Maximizing over all Λ_0 yields that $\tilde{j}^\xi(x) \geq \tilde{J}^\xi(x)$. A similar proof gives $\tilde{v}^\xi(x) \geq \tilde{V}^\xi(x)$.

Remark 2.3.1. *If there is no transaction cost for entry, i.e. $c_b = 0$, then f_b , which is now a linear function with a non-zero slope, has one root x_0 . Moreover, we have $f_b(x) > 0$ for $x \in (-\infty, x_0)$ and $f_b(x) < 0$ for $x \in (x_0, +\infty)$. This implies that the entry region must be of the form $(-\infty, d_0)$, for some number d_0 . Hence, the continuation region for entry is the connected interval (d_0, ∞) .*

Remark 2.3.2. *Let \mathcal{L}^ξ be the infinitesimal generator of the XOU process $\xi = e^X$, and define the function $H_b(\varsigma) := \varsigma + c_b \equiv h_b^\xi(\ln \varsigma)$. In other words, we have the equivalence:*

$$(\mathcal{L}^\xi - r)H_b(\varsigma) \equiv (\mathcal{L} - r)h_b^\xi(\ln \varsigma).$$

Referring to (2.2.5) and (2.2.6), we have either that

$$(\mathcal{L}^\xi - r)H_b(\varsigma) \begin{cases} > 0 & \text{for } \varsigma \in (\varsigma_{b1}, \varsigma_{b2}), \\ < 0 & \text{for } \varsigma \in (0, \varsigma_{b1}) \cup (\varsigma_{b2}, +\infty), \end{cases} \quad (2.3.25)$$

where $\varsigma_{b1} = e^{x_{b1}} > 0$ and $\varsigma_{b2} = e^{x_{b2}}$ and $x_{b1} < x_{b2}$ are two distinct roots to (2.2.5), or

$$(\mathcal{L}^\xi - r)H_b(\varsigma) < 0, \quad \text{for } \varsigma \in (0, \varsigma^*) \cup (\varsigma^*, +\infty), \quad (2.3.26)$$

where $\varsigma^* = e^{x_b}$ and x_b is the single root to (2.2.5). In both cases, Assumption 4 of Zervos et al. [2013] is violated, and their results cannot be applied. Indeed, they would require that $(\mathcal{L}^\xi - r)H_b(\varsigma)$ is strictly negative over a connected interval of the form (ς_0, ∞) , for some fixed $\varsigma_0 \geq 0$. However, it is clear from (2.3.25) and (2.3.26) that such a region is disconnected.

In fact, the approach by Zervos et al. [2013] applies to the optimal switching problems where the optimal wait-for-entry region (in log-price) is of the form (\tilde{d}^*, ∞) , rather than the disconnected region $(-\infty, \tilde{a}^*) \cup (\tilde{d}^*, \infty)$, as in our case with an XOU underlying. Using the new inferred structure of the wait-for-entry region, we have modified the arguments in Zervos et al. [2013] to solve our optimal switching problem for Theorems 2.2.6 and 2.2.7.

2.3.2 Optimal Switching Timing under the CIR Model

Proofs of Theorems 2.2.13 and 2.2.14 Zervos et al. [2013] have studied a similar problem of trading a mean-reverting asset with fixed transaction costs, and provided detailed proofs using a variational inequalities approach. In particular, we observe that y_b and y_s in (2.2.18) and (2.2.19) play the same roles as x_b and x_s in Assumption 4 in Zervos et al. [2013], respectively. However, Assumption 4 in Zervos et al. [2013] requires that $0 \leq x_b$, this is not necessarily true for y_b in our problem. We have checked and realized that

this assumption is not necessary for Theorem 2.2.13, and that $y_b < 0$ simply implies that there is no optimal starting level, i.e. it is never optimal to start.

In addition, Zervos et al. [2013] assume (in their Assumption 1) that the hitting time of level 0 is infinite with probability 1. In comparison, we consider not only the CIR case where 0 is inaccessible, but also when the CIR process has a reflecting boundary at 0. In fact, we find that the proofs in Zervos et al. [2013] apply to both cases under the CIR model. Therefore, apart from relaxation of the aforementioned assumptions, the proofs of our Theorems 2.2.13 and 2.2.14 are the same as that of Lemmas 1 and 2 in Zervos et al. [2013] respectively.

Chapter 3

Speculative Futures Trading under Mean Reversion

In this chapter, we study the problem of trading futures with transaction costs when the underlying spot price is driven by an OU, CIR or XOU model. We analytically derive the futures term structure and examine its connection to futures price dynamics. For each futures contract, we describe the evolution of the roll yield, and compute explicitly the expected roll yield. For the futures trading problem, we first consider the standard entry and exit problems and go on to incorporate a chooser option to either go long or short a futures contract upon entry. We formulate the optimal double stopping problems and solve them numerically using a finite difference method to determine the optimal trading strategies. Numerical examples are provided to illustrate the optimal entry and exit boundaries under different models and problem settings. Our results show that the option to choose between a long or short position motivates the investor to delay market entry, as compared to the case where the investor pre-commits to go either long or short.

Section 3.1 summarizes the futures prices and term structures under mean reversion. We discuss the concept of roll yield in Section 3.2. In Section 3.3,

we formulate and numerically solve the optimal double stopping problems for futures trading. The numerical algorithm is described in Appendix C.

3.1 Futures Prices and Term Structures

Throughout this chapter, we consider futures that are written on an asset whose price process is mean-reverting. In this section, we discuss the pricing of futures and their term structures under different spot models.

3.1.1 OU and CIR Spot Models

We begin with two mean-reverting models for the spot price S , namely, the OU and CIR models. As we will see, they yield the same price function for the futures contract. To start, suppose that the spot price evolves according to the OU model:

$$dS_t = \mu(\theta - S_t)dt + \sigma dB_t,$$

where $\mu, \sigma > 0$ are the speed of mean reversion and volatility of the process respectively. $\theta \in \mathbb{R}$ is the long run mean and B is a standard Brownian motion under the historical measure \mathbb{P} .

To price futures, we assume a re-parametrized OU model for the risk-neutral spot price dynamics. Hence, under the risk-neutral measure \mathbb{Q} , the spot price follows

$$dS_t = \tilde{\mu}(\tilde{\theta} - S_t) dt + \sigma dB_t^{\mathbb{Q}},$$

with constant parameters $\tilde{\mu}, \sigma > 0$, and $\tilde{\theta} \in \mathbb{R}$. This is again an OU process, albeit with a different long-run mean $\tilde{\theta}$ and speed of mean reversion $\tilde{\mu}$ under the risk-neutral measure. This involves a change of measure that connects the

two Brownian motions, as described by

$$dB_t^{\mathbb{Q}} = dB_t + \frac{\mu(\theta - S_t) - \tilde{\mu}(\tilde{\theta} - S_t)}{\sigma} dt.$$

Throughout, futures prices are computed the same as forward prices, and we do not distinguish between the two prices (see Cox et al. [1981]; Brennan and Schwartz [1990]). As such, the price of a futures contract with maturity T is given by

$$f_t^T \equiv f(t, S_t; T) := \mathbb{E}^{\mathbb{Q}}\{S_T | S_t\} = (S_t - \tilde{\theta})e^{-\tilde{\mu}(T-t)} + \tilde{\theta}, \quad t \leq T. \quad (3.1.1)$$

Note that the futures price is a deterministic function of time and the current spot price.

We now consider the CIR model for the spot price:

$$dS_t = \mu(\theta - S_t)dt + \sigma\sqrt{S_t}dB_t, \quad (3.1.2)$$

where $\mu, \theta, \sigma > 0$, and B is a standard Brownian motion under the historical measure \mathbb{P} . Under the risk-neutral measure \mathbb{Q} ,

$$dS_t = \tilde{\mu}(\tilde{\theta} - S_t)dt + \sigma\sqrt{S_t}dB_t^{\mathbb{Q}}, \quad (3.1.3)$$

where $\mu, \theta > 0$, and $B^{\mathbb{Q}}$ is a \mathbb{Q} -standard Brownian motion. In both SDEs, (3.1.2) and (3.1.3), we require $2\mu\theta \geq \sigma^2$ and $2\tilde{\mu}\tilde{\theta} \geq \sigma^2$ (Feller condition) so that the CIR process stays positive.

The two Brownian motions are related by

$$dB_t^{\mathbb{Q}} = dB_t + \frac{\mu(\theta - S_t) - \tilde{\mu}(\tilde{\theta} - S_t)}{\sigma\sqrt{S_t}} dt,$$

which preserves the CIR model, up to different parameter values across two measures.

The CIR terminal spot price S_T admits the non-central Chi-squared distribution and is positive, whereas the OU spot price is normally distributed.

Nevertheless, the futures price under the CIR model admits the same functional form as in the OU case (see (3.1.1)):

$$f_t^T = (S_t - \tilde{\theta})e^{-\tilde{\mu}(T-t)} + \tilde{\theta}, \quad t \leq T. \quad (3.1.4)$$

Proposition 3.1.1. *Under the OU or CIR spot model, the futures curve is (i) upward-sloping and concave if the current spot price $S_0 < \tilde{\theta}$, (ii) downward-sloping and convex if $S_0 > \tilde{\theta}$.*

Proof. We differentiate (3.1.4) with respect to T to get the derivatives:

$$\frac{\partial f_0^T}{\partial T} = -\tilde{\mu}(S_0 - \tilde{\theta})e^{-\tilde{\mu}T} \leq 0 \quad \text{and} \quad \frac{\partial^2 f_0^T}{\partial T^2} = \tilde{\mu}^2(S_0 - \tilde{\theta})e^{-\tilde{\mu}T} \geq 0,$$

for $S_0 \geq \tilde{\theta}$. Hence, we conclude. \square

Remark 3.1.2. *The futures price formula (3.1.4) holds more generally for other mean-reverting models with risk-neutral spot dynamics of the form:*

$$dS_t = \tilde{\mu}(\tilde{\theta} - S_t)dt + \sigma(S_t)dB_t^{\mathbb{Q}},$$

where $\sigma(\cdot)$ is a deterministic function such that $\mathbb{E}^{\mathbb{Q}}\{\int_0^T \sigma(S_t)^2 dt\} < \infty$.

Under the OU model, the futures satisfies the following SDE under the historical measure \mathbb{P} :

$$df_t^T = \left[(f_t^T - \tilde{\theta})(\tilde{\mu} - \mu) + \mu(\theta - \tilde{\theta})e^{-\tilde{\mu}(T-t)} \right] dt + \sigma e^{-\tilde{\mu}(T-t)} dB_t. \quad (3.1.5)$$

If the spot follows a CIR process, then the futures prices follows

$$\begin{aligned} df_t^T = & \left[(f_t^T - \tilde{\theta})(\tilde{\mu} - \mu) + \mu(\theta - \tilde{\theta})e^{-\tilde{\mu}(T-t)} \right] dt \\ & + \sigma e^{-\tilde{\mu}(T-t)} \sqrt{(f_t^T - \tilde{\theta})e^{\tilde{\mu}(T-t)} + \tilde{\theta}} dB_t. \end{aligned} \quad (3.1.6)$$

Notice that the same drift appears in both (3.1.5) and (3.1.6). Alternatively, we can express the drift in terms of the spot price as

$$e^{-\tilde{\mu}(T-t)}(\mu(\theta - S_t) - \tilde{\mu}(\tilde{\theta} - S_t)).$$

This involves the difference between the mean-reverting drifts of the spot price under the historical measure \mathbb{P} and the risk-neutral measure \mathbb{Q} . Therefore, the drift of the futures price SDE is positive when the drift of the spot price under \mathbb{P} is greater than that under \mathbb{Q} , i.e.

$$\mu(\theta - S_t) > \tilde{\mu}(\tilde{\theta} - S_t),$$

and vice versa.

Now, consider an investor with a long position in a single futures contract, she wishes to close out the position and is interested in determining the best time to short. We consider the *delayed liquidation premium*, which was introduced in Leung and Shirai [2015] for equity options. This premium expresses the benefit of waiting to liquidate as compared to closing the position immediately. Precisely, the delayed liquidation premium is defined as

$$L(t, s) := \sup_{\tau \in \mathcal{T}_{t,T}} \mathbb{E}_{t,s} \{ e^{-r(\tau-t)} (f(\tau, S_\tau; T) - c) \} - (f(t, s; T) - c), \quad (3.1.7)$$

where $\mathcal{T}_{t,T}$ is the set of all stopping times, with respect to the filtration generated by S , and c is the transaction cost. As we can see in (3.1.7), the optimal stopping time for $L(t, s)$, denoted by τ^* , maximizes the expected discounted value from liquidating the futures.

Proposition 3.1.3. *Let $t \in [0, T]$ be the current time, and define the function*

$$G(u, s) := e^{-\tilde{\mu}(u-t)} (\mu(\theta - s) + (r - \tilde{\mu})(\tilde{\theta} - s)) + r(c - \tilde{\theta}).$$

Under the OU spot model, if $G(u, s) \geq 0$, $\forall (u, s) \in [t, T] \times \mathbb{R}$, then it is optimal to hold the futures contract till expiry, namely, $\tau^ = T$ in (3.1.7). If $G(u, s) < 0$, $\forall (u, s) \in [t, T] \times \mathbb{R}$, then it is optimal to liquidate immediately, namely, $\tau^* = t$. The same holds under the CIR model with $G(u, s)$ defined over $[t, T] \times \mathbb{R}_+$.*

Proof. Applying Ito's formula to the process of $e^{-rt}(f_t^T - c)$ and taking expectation, we can express (3.1.7) as

$$L(t, s) = \sup_{\tau \in \mathcal{T}_{t,T}} \mathbb{E}_{t,s} \left\{ \int_t^\tau e^{-r(u-t)} \left[e^{-\tilde{\mu}(u-t)} (\mu(\theta - S_u) + (r - \tilde{\mu})(\tilde{\theta} - S_u)) + r(c - \tilde{\theta}) \right] du \right\}. \quad (3.1.8)$$

Therefore, if $G(u, s)$ (the integrand in (3.1.8)) is positive, $\forall (u, s) \in [t, T] \times \mathbb{R}$, then the delayed liquidation premium can be maximized by choosing $\tau^* = T$, which is the largest stopping time. Conversely, if $G < 0 \forall (u, s) \in [t, T] \times \mathbb{R}$, then it is optimal to take $\tau^* = t$ in (3.1.8). Note that if $G = 0 \forall (u, s) \in [t, T] \times \mathbb{R}$, then the delayed liquidation premium is zero, and the investor is indifferent toward when to liquidate. \square

3.1.2 XOU Spot Model

Under the exponential OU (XOU) model, the spot price follows the SDE:

$$dS_t = \mu(\theta - \ln(S_t))S_t dt + \sigma S_t dB_t, \quad (3.1.9)$$

with positive parameters (μ, θ, σ) , and standard Brownian motion B under the historical measure \mathbb{P} . For pricing futures, we assume that the risk-neutral dynamics of S satisfies

$$dS_t = \tilde{\mu}(\tilde{\theta} - \ln(S_t))S_t dt + \sigma S_t dB_t^{\mathbb{Q}},$$

where $\tilde{\mu}, \tilde{\theta} > 0$, and $B^{\mathbb{Q}}$ is a standard Brownian motion under the risk-neutral measure \mathbb{Q} .

For a futures contract written on S with maturity T , its price at time t is given by

$$f_t^T = \exp \left(e^{-\tilde{\mu}(T-t)} \ln(S_t) + (1 - e^{-\tilde{\mu}(T-t)}) \left(\tilde{\theta} - \frac{\sigma^2}{2\tilde{\mu}} + \frac{\sigma^2}{4\tilde{\mu}} (1 - e^{-2\tilde{\mu}(T-t)}) \right) \right). \quad (3.1.10)$$

Consequently, the dynamics of the futures price under the historical measure \mathbb{P} is given as

$$df_t^T = \left[\left(\ln(f_t^T) + (e^{-\tilde{\mu}(T-t)} - 1) \left(\tilde{\theta} - \frac{\sigma^2}{2\tilde{\mu}} \right) + \frac{\sigma^2}{4\tilde{\mu}} (e^{-2\tilde{\mu}(T-t)} - 1) \right) (\tilde{\mu} - \mu) + e^{-\tilde{\mu}(T-t)} (\mu\theta - \tilde{\mu}\tilde{\theta}) \right] f_t^T dt + \sigma e^{-\tilde{\mu}(T-t)} f_t^T dB_t. \quad (3.1.11)$$

By rearranging the first term in (3.1.11), the drift of the futures price SDE is positive iff

$$f_t^T > \exp \left[\frac{e^{-\tilde{\mu}(T-t)} (\tilde{\mu}\tilde{\theta} - \mu\theta)}{\tilde{\mu} - \mu} - (e^{-\tilde{\mu}(T-t)} - 1) \left(\tilde{\theta} - \frac{\sigma^2}{2\tilde{\mu}} \right) - \frac{\sigma^2}{4\tilde{\mu}} (e^{-2\tilde{\mu}(T-t)} - 1) \right],$$

or equivalently in terms of the spot price,

$$S_t > \exp \left(\frac{\tilde{\mu}\tilde{\theta} - \mu\theta}{\tilde{\mu} - \mu} \right). \quad (3.1.12)$$

In particular, if $\tilde{\theta} = \theta$, condition (3.1.12) reduces to $\log S_t > \theta$. Intuitively, since the futures price must converge to the spot price at maturity, the futures price tends to rise to approach the spot price when the spot price is high, as observed in this condition.

We now consider the delayed liquidation premium defined in (3.1.7) but under the XOU spot model. Applying Ito's formula, we express the optimal liquidation premium as

$$L(t, s) = \sup_{\tau \in \mathcal{T}_{t,T}} \mathbb{E}_{t,s} \left\{ \int_t^\tau e^{-r(u-t)} \tilde{G}(u, S_u) du \right\}, \quad (3.1.13)$$

where

$$\begin{aligned} \tilde{G}(u, s) := & \left\{ r + \left[\mu(\theta - \ln(s)) - \tilde{\mu}(\tilde{\theta} - \ln(s)) \right] e^{-\tilde{\mu}(u-t)} \right\} \\ & \times \exp \left(e^{-\tilde{\mu}(u-t)} \ln(s) + (1 - e^{-\tilde{\mu}(u-t)}) \left(\tilde{\theta} - \frac{\sigma^2}{2\tilde{\mu}} \right) + \frac{\sigma^2}{4\tilde{\mu}} (1 - e^{-2\tilde{\mu}(u-t)}) \right) - rc. \end{aligned}$$

By inspecting the premium definition, we obtain the condition under which immediate liquidation or waiting till maturity is optimal. The proof is identical to that of Proposition 3.1.3, so we omit it.

Proposition 3.1.4. *Let $t \in [0, T]$ be the current time. Under the XOU spot model, if $\tilde{G}(u, s) \geq 0 \forall (u, s) \in [t, T] \times \mathbb{R}_+$, then holding till maturity ($\tau^* = T$) is optimal for (3.1.13). If $\tilde{G}(u, s) < 0, \forall (u, s) \in [t, T] \times \mathbb{R}_+$, then immediate liquidation ($\tau^* = t$) is optimal for (3.1.13).*

Next, we summarize the term structure of futures under the XOU spot model.

Proposition 3.1.5. *Under the XOU spot model, the futures curve is*

(i) *downward-sloping and convex if*

$$\ln S_0 > \tilde{\theta} - \frac{\sigma^2}{2\tilde{\mu}}(1 - e^{-\tilde{\mu}T}) + \left(\frac{e^{2\tilde{\mu}T}}{4} + \frac{\sigma^2}{2\tilde{\mu}} \right)^{\frac{1}{2}} - \frac{e^{\tilde{\mu}T}}{2},$$

(ii) *downward-sloping and concave if*

$$\tilde{\theta} - \frac{\sigma^2}{2\tilde{\mu}}(1 - e^{-\tilde{\mu}T}) < \ln S_0 < \tilde{\theta} - \frac{\sigma^2}{2\tilde{\mu}}(1 - e^{-\tilde{\mu}T}) + \left(\frac{e^{2\tilde{\mu}T}}{4} + \frac{\sigma^2}{2\tilde{\mu}} \right)^{\frac{1}{2}} - \frac{e^{\tilde{\mu}T}}{2},$$

(iii) *upward-sloping and concave if*

$$\tilde{\theta} - \frac{\sigma^2}{2\tilde{\mu}}(1 - e^{-\tilde{\mu}T}) - \left(\frac{e^{2\tilde{\mu}T}}{4} + \frac{\sigma^2}{2\tilde{\mu}} \right)^{\frac{1}{2}} - \frac{e^{\tilde{\mu}T}}{2} < \ln S_0 < \tilde{\theta} - \frac{\sigma^2}{2\tilde{\mu}}(1 - e^{-\tilde{\mu}T}),$$

and

(iv) *upward-sloping and convex if*

$$\ln S_0 < \tilde{\theta} - \frac{\sigma^2}{2\tilde{\mu}}(1 - e^{-\tilde{\mu}T}) - \left(\frac{e^{2\tilde{\mu}T}}{4} + \frac{\sigma^2}{2\tilde{\mu}} \right)^{\frac{1}{2}} - \frac{e^{\tilde{\mu}T}}{2}.$$

Proof. Direct differentiation of f_0^T yields that

$$\frac{\partial f_0^T}{\partial T} = \left[\tilde{\mu} \left(\tilde{\theta} - \frac{\sigma^2}{2\tilde{\mu}} - \ln S_0 \right) e^{-\tilde{\mu}T} + \frac{\sigma^2}{2} e^{-2\tilde{\mu}T} \right] f_0^T,$$

and

$$\begin{aligned} \frac{\partial^2 f_0^T}{\partial T^2} = & \left[\tilde{\mu}^2 e^{-2\tilde{\mu}T} \left(\tilde{\theta} - \frac{\sigma^2}{2\tilde{\mu}} - \ln S_0 \right)^2 + (\tilde{\mu}\sigma^2 e^{-3\tilde{\mu}T} - \tilde{\mu}^2 e^{-\tilde{\mu}T}) \left(\tilde{\theta} - \frac{\sigma^2}{2\tilde{\mu}} - \ln S_0 \right) \right. \\ & \left. + \frac{\sigma^4}{4} e^{-4\tilde{\mu}T} - \sigma^2 \tilde{\mu} e^{-2\tilde{\mu}T} \right] f_0^T. \end{aligned}$$

The results are obtained by analyzing the signs of the first and second order derivatives. □

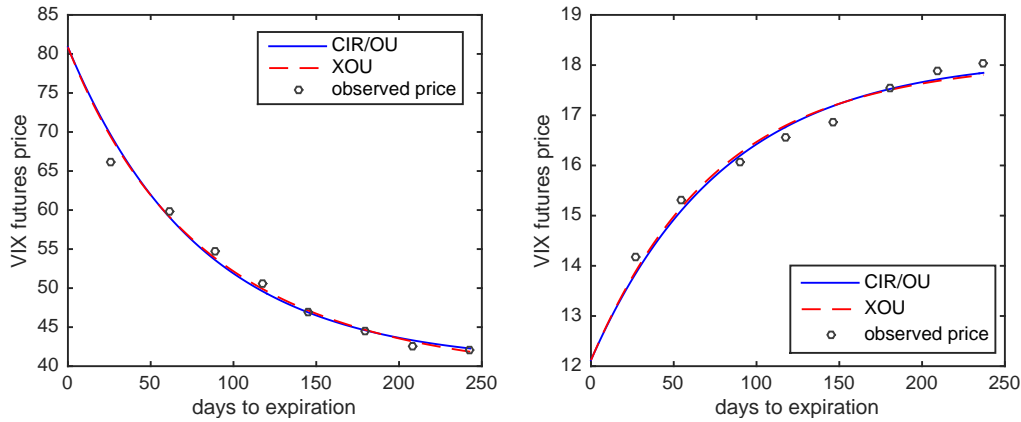


Figure 3.1: (Left) VIX futures historical prices on Nov 20, 2008 with the current VIX value at 80.86. The days to expiration range from 26 to 243 days (Dec–Jul contracts). Calibrated parameters: $\tilde{\mu} = 4.59, \tilde{\theta} = 40.36$ under the CIR/OU model, or $\tilde{\mu} = 3.25, \tilde{\theta} = 3.65, \sigma = 0.15$ under the XOU model. (Right) VIX futures historical prices on Jul 22, 2015 with the current VIX value at 12.12. The days to expiration ranges from 27 days to 237 days (Aug–Mar contracts). Calibrated parameters: $\tilde{\mu} = 4.55, \tilde{\theta} = 18.16$ under the CIR/OU model, or $\tilde{\mu} = 4.08, \tilde{\theta} = 3.06, \sigma = 1.63$ under the XOU model.

Figure 3.1 displays two characteristically different term structures observed in the VIX futures market. These futures, written on the CBOE Volatility Index (VIX) are traded on the CBOE Futures Exchange. As the VIX measures the 1-month implied volatility calculated from the prices of S&P 500 options, VIX futures provide exposure to the market’s volatility. We plot the VIX futures prices during the recent financial crisis on November 20, 2008 (left), and on a post-crisis date, July 22, 2015 (right), along with the calibrated futures curves under the OU/CIR model and XOU model. In the calibration, the model parameter values are chosen to minimize the sum of squared errors between the model and observed futures prices.

The OU/CIR/XOU model generates a decreasing convex curve for November 20, 2008 (left), and an increasing concave curve for July 22, 2015 (right),

and they all fit the observed futures prices very well. The former term structure starts with a very high spot price of 80.86 with a calibrated risk-neutral long-run mean $\tilde{\theta} = 40.36$ under the OU/CIR model, suggesting that the market's expectation of falling market volatility. In contrast, we infer from the term structure on July 25, 2015 that the market expects the VIX to raise from the current spot value of 12.12 to be closer to $\tilde{\theta} = 18.16$.

3.2 Roll Yield

By design, the value of a futures contract converges to the spot price as time approaches maturity. If the futures market is in *backwardation*, the futures price increases to reach the spot price at expiry. In contrast, when the market is in *contango*, the futures price tends to decrease to the spot price. For an investor with a long futures position, the return is positive in a backwardation market, and negative in a contango market. An investor can long the front-month contract, then short it at or before expiry, and simultaneously go long the next-month contract. This *rolling strategy* that involves repeatedly rolling an expiring contract into a new one is commonly adopted during backwardation, while its opposite is often used in a contango market. Backwardation and contango phenomena are widely observed in the energy commodities and volatility futures markets.

More generally, both the futures and spot prices vary over time. If the spot price increases/decreases, the futures price will also end up higher/lower. This leads us to consider the difference between the futures and spot returns, defined as the change in values without dividing by the initial value.¹ Let $0 \leq t_1 < t_2 \leq T$. We denote the *roll yield* over the period $[t_1, t_2]$ associated

¹See *Deconstructing Futures Returns: The Role of Roll Yield*, Campbell White Paper Series, February 2014.

with a single futures contract with maturity T by

$$\mathcal{R}(t_1, t_2, T) := (f_{t_2}^T - f_{t_1}^T) - (S_{t_2} - S_{t_1}).$$

In other words, roll yield here is the change in the futures price that is not accounted for by the change in spot price. It represents the net benefits and/or costs of owning futures rather than the underlying asset itself.

This notion of roll yield is the same as that in Moskowitz et al. [2012] where the relationship between roll yield and futures returns is studied. Gorton et al. [2013] treat roll yield as the same as futures basis, which means a negative roll yield signifies a market in contango and a positive roll yield is equivalent to backwardation. In our set-up, if one always hold a futures contract to maturity, then roll yield is the same as futures basis. Therefore, the definition of roll yield in Gorton et al. [2013] is a special case of ours. In particular, if $t_2 = T$, then the roll yield reduces to the price difference $(S_{t_1} - f_{t_1}^T)$. Furthermore, observe that if $S_{t_2} = S_{t_1}$ then roll yield becomes merely the change in futures price.

A closely related concept is the S&P-GSCI roll yield. S&P-GSCI carries out rolling of the underlying futures contracts once each month, from the fifth to the ninth business day. On each day, 20% of the current portfolio is rolled over, in a process commonly known as the *Goldman roll*. The S&P-GSCI roll yield for each commodity is defined as the difference between the average purchasing price of the new futures contracts and the average selling price of the old futures contracts. In essence, it is an indicator of the sign of the slope of the futures term structure. In comparison to the S&P-GSCI index, our definition accounts for the changes of spot price over time.

Next, we examine the cumulative roll yield across maturities. Denote by $T_1 < T_2 < T_3 < \dots$ the maturities of futures contracts. We roll over at every T_i by replacing the contract expiring at T_i with a new contract that expires at T_{i+1} . Let $i(t) := \min\{i : T_{i-1} < t \leq T_i\}$, and $i(0) = 1$. Then the roll yield up

to time $t > T_1$ is

$$\begin{aligned} \mathcal{R}(0, t) &= (f_t^{T_{i(t)}} - f_{T_{i(t)-1}}^{T_{i(t)}}) + \sum_{j=2}^{i(t)-1} (S_{T_j} - f_{T_{j-1}}^{T_j}) + (S_{T_1} - f_0^{T_1}) - (S_t - S_0) \\ &= \underbrace{(f_t^{T_{i(t)}} - S_t) - (f_0^{T_1} - S_0)}_{\text{Basis Return}} + \underbrace{\sum_{j=1}^{i(t)-1} (S_{T_j} - f_{T_j}^{T_{j+1}})}_{\text{Cumulative Roll Adjustment}}. \end{aligned} \quad (3.2.1)$$

The cumulative roll adjustment is related to the term structure of futures contracts. If $T_i - T_{i-1}$ is constant, and the term structure only moves parallel, then the cumulative roll adjustment is simply the number of roll-over times a constant (difference between spot and near-month futures contract).

3.2.1 OU and CIR Spot Models

Suppose the spot price follows the OU or CIR model described in Section 3.1.1. Inspecting (3.2.1), we can write down the SDE for the roll yield under the OU model:

$$\begin{aligned} d\mathcal{R}(0, t) &= df_t^{T_{i(t)}} - dS_t \\ &= \left[e^{-\tilde{\mu}(T_{i(t)}-t)} \left(\mu(\theta - S_t) - \tilde{\mu}(\tilde{\theta} - S_t) \right) - \mu(\theta - S_t) \right] dt \\ &\quad + \sigma \left(e^{-\tilde{\mu}(T_{i(t)}-t)} - 1 \right) dB_t. \end{aligned} \quad (3.2.2)$$

The roll yield SDE under the CIR model has the same drift as (3.2.2). Furthermore, the drift is positive iff

$$S_t > \frac{e^{-\tilde{\mu}(T_{i(t)}-t)}(\tilde{\mu}\tilde{\theta} - \mu\theta) + \mu\theta}{e^{-\tilde{\mu}(T_{i(t)}-t)}(\tilde{\mu} - \mu) + \mu}.$$

In particular, if $\theta = \tilde{\theta}$, then the drift is positive iff $S_t > \theta$. When $t = T_{i(t)}$, the drift is $\tilde{\mu}(S_t - \tilde{\theta})$ and is positive iff $S_t > \tilde{\theta}$. Furthermore, the drift term can also be expressed as

$$\tilde{\mu} \left(f_t^{T_{i(t)}} - \tilde{\theta} \right) - (1 - e^{-\tilde{\mu}(T_{i(t)}-t)}) \mu(\theta - S_t).$$

On the other hand, we observe that

$$d\mathcal{R}(0, t)dS_t = \sigma^2 (e^{-\tilde{\mu}(T_{i(t)}-t)} - 1) dt,$$

under the OU case and

$$d\mathcal{R}(0, t)dS_t = \sigma^2 (e^{-\tilde{\mu}(T_{i(t)}-t)} - 1) S_t dt,$$

under the CIR case. In other words, the instantaneous covariations between roll yield and spot price under both OU and CIR models are negative for $t < T_{i(t)}$ regardless of the spot price level.

Consider a longer horizon with rolling at multiple maturities, the expected roll yield is

$$\begin{aligned} \mathbb{E}\{\mathcal{R}(0, t)\} &= \mathbb{E}\{f_t^{T_{i(t)}} - S_t\} - (f_0^{T_1} - S_0) + \sum_{j=1}^{i(t)-1} \mathbb{E}\{S_{T_j} - f_{T_j}^{T_{j+1}}\} \\ &= ((S_0 - \theta)e^{-\mu t} + \theta - \tilde{\theta})(e^{-\tilde{\mu}(T_{i(t)}-t)} - 1) - (S_0 - \tilde{\theta})(e^{-\tilde{\mu}T_1} - 1) \\ &\quad + \sum_{j=1}^{i(t)-1} ((S_0 - \theta)e^{-\mu T_j} + \theta - \tilde{\theta})(1 - e^{-\tilde{\mu}(T_{j+1}-T_j)}). \end{aligned}$$

In summary, the expected roll yield depends not only on the risk-neutral parameters $\tilde{\mu}$ and $\tilde{\theta}$, but also their historical counterparts. It vanishes when $S_0 = \theta = \tilde{\theta}$. This is intuitive because if the current spot price is currently at the long-run mean, and the risk-neutral and historical measures coincide, then the spot and futures prices have little tendency to deviate from the long-run mean. Also, notice that neither the futures price nor the roll yield depends on the volatility parameter σ . This is true under the OU/CIR model, but not the exponential OU model, as we discuss next.

3.2.2 XOU Spot Model

We now turn to the exponential OU spot price model discussed in Section 3.1.2. Recalling the futures price in (3.1.10), the expected roll yield is given

by

$$\mathbb{E}\{\mathcal{R}(0, t)\} = Y_1(t) + Y_2(t) - (f_0^{T_1} - S_0), \quad (3.2.3)$$

where

$$\begin{aligned} Y_1(t) &= \mathbb{E}\{f_t^{T_{i(t)}} - S_t\} \\ &= \exp\left(e^{-\tilde{\mu}(T_{i(t)}-t)-\mu t} \ln(S_0) + \left(\theta - \frac{\sigma^2}{2\mu}\right)(1 - e^{-\mu t})e^{-\tilde{\mu}(T_{i(t)}-t)}\right. \\ &\quad + \frac{\sigma^2}{4\mu}e^{-2\tilde{\mu}(T_{i(t)}-t)}(1 - e^{-2\mu t}) + (1 - e^{-\tilde{\mu}(T_{i(t)}-t)})(\tilde{\theta} - \frac{\sigma^2}{2\tilde{\mu}}) \\ &\quad \left. + \frac{\sigma^2}{4\tilde{\mu}}(1 - e^{-2\tilde{\mu}(T_{i(t)}-t)})\right) \\ &\quad - \exp\left(e^{-\mu t} \ln(S_0) + (1 - e^{-\mu t})(\theta - \frac{\sigma^2}{2\mu}) + \frac{\sigma^2}{4\mu}(1 - e^{-\mu t})\right), \end{aligned}$$

and

$$\begin{aligned} Y_2(t) &= \sum_{j=1}^{i(t)-1} \mathbb{E}\{S_{T_j} - f_{T_j}^{T_{j+1}}\} \\ &= \sum_{j=1}^{i(t)-1} \left(\exp\left(e^{-\mu T_j} \ln(S_0) + (1 - e^{-\mu T_j})(\theta - \frac{\sigma^2}{2\mu}) + \frac{\sigma^2}{4\mu}(1 - e^{-\mu T_j})\right) \right. \\ &\quad - \exp\left(e^{-\tilde{\mu}(T_{j+1}-T_j)-\mu T_j} \ln(S_0) + \left(\theta - \frac{\sigma^2}{2\mu}\right)(1 - e^{-\mu T_j})e^{-\tilde{\mu}(T_{j+1}-T_j)}\right. \\ &\quad + \frac{\sigma^2}{4\mu}e^{-2\tilde{\mu}(T_{j+1}-T_j)}(1 - e^{-2\mu T_j}) \\ &\quad \left. \left. + (1 - e^{-\tilde{\mu}(T_{j+1}-T_j)})(\tilde{\theta} - \frac{\sigma^2}{2\tilde{\mu}}) + \frac{\sigma^2}{4\tilde{\mu}}(1 - e^{-2\tilde{\mu}(T_{j+1}-T_j)})\right) \right). \end{aligned}$$

The explicit formula (3.2.3) for the expected roll yield reveals the non-trivial dependence on the volatility parameter σ , as well as the risk-neutral parameters $(\tilde{\mu}, \tilde{\theta})$ and historical parameters (μ, θ) . It is useful for instantly predicting the roll yield after calibrating the risk-neutral parameters from the term structure of the futures prices, and estimating the historical parameters from past spot prices.

Referring to (3.1.9) and (3.1.11), the historical dynamics of the roll yield under an XOU spot model is given by

$$d\mathcal{R}(0, t) = h(t, s)dt + \sigma \left(e^{-\tilde{\mu}(T_{i(t)}-t)} f_t^{T_{i(t)}} - S_t \right) dB_t,$$

where

$$\begin{aligned} h(t, s) = & \left(\ln s(\tilde{\mu} - \mu) + (\mu\theta - \tilde{\mu}\tilde{\theta}) \right) \exp \left(e^{-\tilde{\mu}(T_{i(t)}-t)} \ln(s) \right. \\ & \left. + (1 - e^{-\tilde{\mu}(T_{i(t)}-t)}) \left(\tilde{\theta} - \frac{\sigma^2}{2\tilde{\mu}} \right) + \frac{\sigma^2}{4\tilde{\mu}} (1 - e^{-2\tilde{\mu}(T_{i(t)}-t)}) \right) e^{-\tilde{\mu}(T_{i(t)}-t)} \\ & - \mu(\theta - \ln(s))s, \end{aligned}$$

is the drift expressed in terms of the spot price S_t . This reduces to

$$h(T_{i(t)}, s) = s \ln(s)(\tilde{\mu} - \mu + \mu\theta) - \tilde{\mu}\tilde{\theta}s, \quad \text{if } t = T_{i(t)}.$$

Unlike the OU/CIR case, under an XOU spot model there is no explicit solution for the critical level of the spot price at which the drift changes sign.

As in the OU/CIR spot model, it is of interest to compute

$$d\mathcal{R}(0, t)dS_t = \sigma^2 \left(e^{-\tilde{\mu}(T_{i(t)}-t)} f_t^{T_{i(t)}} - S_t \right) S_t dt,$$

from which we see that the covariation between roll yield and spot price can be either positive or negative. In particular when the futures price is significantly higher than the spot price, i.e. when the market is in contango, the correlation tends to be positive.

3.3 Optimal Timing to Trade Futures

In Section 3.1, we have discussed the timing to liquidate a long futures position, and the concept of rolling discussed in Section 3.2 corresponds to holding the futures up to expiry. In this section, we further explore the timing options embedded in futures, and develop the optimal trading strategies.

3.3.1 Optimal Double Stopping Approach

Let us consider the scenario in which an investor has a long position in a futures contract with expiration date T . With a long position in the futures, the investor can hold it till maturity, but can also close the position early by taking an opposite position at the prevailing market price. At maturity, the two opposite positions cancel each other. This motivates us to investigate the best time to close.

If the investor selects to close the long position at time $\tau \leq T$, then she will receive the market value of the futures on the expiry date, denoted by $f(\tau, S_\tau; T)$, minus the transaction cost $c \geq 0$. To maximize the expected discounted value, evaluated under the investor's historical probability measure \mathbb{P} with a constant subjective discount rate $r > 0$, the investor solves the optimal stopping problem

$$\mathcal{V}(t, s) = \sup_{\tau \in \mathcal{T}_{t,T}} \mathbb{E}_{t,s} \{ e^{-r(\tau-t)} (f(\tau, S_\tau; T) - c) \},$$

where $\mathcal{T}_{t,T}$ is the set of all stopping times, with respect to the filtration generated by S , taking values between t and \hat{T} , where $\hat{T} \in (0, T]$ is the trading deadline, which can equal but not exceed the futures' maturity. Throughout this chapter, we continue to use the shorthand notation $\mathbb{E}_{t,s} \{ \cdot \} \equiv \mathbb{E} \{ \cdot | S_t = s \}$ to indicate the expectation taken under the historical probability measure \mathbb{P} .

The value function $\mathcal{V}(t, s)$ represents the expected liquidation value associated with the long futures position. Prior to taking the long position in futures, the investor, with zero position, can select the optimal timing to start the trade, or not to enter at all. This leads us to analyze the timing option inherent in the trading problem. Precisely, at time $t \leq T$, the investor faces the optimal entry timing problem

$$\mathcal{J}(t, s) = \sup_{\nu \in \mathcal{T}_{t,T}} \mathbb{E}_{t,s} \{ e^{-r(\nu-t)} (\mathcal{V}(\nu, S_\nu) - (f(\nu, S_\nu; T) + \hat{c}))^+ \},$$

where $\hat{c} \geq 0$ is the transaction cost, which may differ from c . In other words, the investor seeks to maximize the expected difference between the value function $\mathcal{V}(\nu, S_\nu)$ associated with the long position and the prevailing futures price $f(\nu, S_\nu; T)$. The value function $\mathcal{J}(t, s)$ represents the maximum expected value of the trading opportunity embedded in the futures. We refer this “long to open, short to close” strategy as the *long-short* strategy.

Alternatively, an investor may well choose to short a futures contract with the speculation that the futures price will fall, and then close it out later by establishing a long position.² Given an investor who has a unit short position in the futures contract, the objective is to minimize the expected discounted cost to close out this position at/before maturity. The optimal timing strategy is determined from

$$\mathcal{U}(t, s) = \inf_{\tau \in \mathcal{T}_{t,T}} \mathbb{E}_{t,s} \{ e^{-r(\tau-t)} (f(\tau, S_\tau; T) + \hat{c}) \}.$$

If the investor begins with a zero position, then she can decide when to enter the market by solving

$$\mathcal{K}(t, s) = \sup_{\nu \in \mathcal{T}_{t,T}} \mathbb{E}_{t,s} \{ e^{-r(\nu-t)} ((f(\nu, S_\nu; T) - c) - \mathcal{U}(\nu, S_\nu))^+ \}.$$

We call this “short to open, long to close” strategy as the *short-long* strategy.

When an investor contemplates entering the market, she can either long or short first. Therefore, on top of the timing option, the investor has an additional choice between the long-short and short-long strategies. Hence, the investor solves the market entry timing problem:

$$\mathcal{P}(t, s) = \sup_{\varsigma \in \mathcal{T}_{t,T}} \mathbb{E}_{t,s} \{ e^{-r(\varsigma-t)} \max\{\mathcal{A}(\varsigma, S_\varsigma), \mathcal{B}(\varsigma, S_\varsigma)\} \}, \quad (3.3.1)$$

²By taking a short futures position, the investor is required to sell the underlying spot at maturity at a pre-specified price. In contrast to the short sale of a stock, a short futures does not involve share borrowing or re-purchasing.

with two alternative rewards upon entry defined by

$$\begin{aligned}\mathcal{A}(\varsigma, S_\varsigma) &:= (\mathcal{V}(\varsigma, S_\varsigma) - (f(\varsigma, S_\varsigma; T) + \hat{c}))^+ \quad (\text{long-short}), \\ \mathcal{B}(\varsigma, S_\varsigma) &:= ((f(\varsigma, S_\varsigma; T) - c) - \mathcal{U}(\varsigma, S_\varsigma))^+ \quad (\text{short-long}).\end{aligned}$$

3.3.2 Variational Inequalities & Optimal Trading Strategies

In order to solve for the optimal trading strategies, we study the variational inequalities corresponding to the value functions \mathcal{J} , \mathcal{V} , \mathcal{U} , \mathcal{K} and \mathcal{P} . To this end, we first define the operators:

$$\mathcal{L}^{(1)}\{\cdot\} := -r \cdot + \frac{\partial \cdot}{\partial t} + \tilde{\mu}(\tilde{\theta} - s) \frac{\partial \cdot}{\partial s} + \frac{\sigma^2}{2} \frac{\partial^2 \cdot}{\partial s^2}, \quad (3.3.2)$$

$$\mathcal{L}^{(2)}\{\cdot\} := -r \cdot + \frac{\partial \cdot}{\partial t} + \tilde{\mu}(\tilde{\theta} - s) \frac{\partial \cdot}{\partial s} + \frac{\sigma^2 s}{2} \frac{\partial^2 \cdot}{\partial s^2},$$

$$\mathcal{L}^{(3)}\{\cdot\} := -r \cdot + \frac{\partial \cdot}{\partial t} + \tilde{\mu}(\tilde{\theta} - \ln s) \frac{\partial \cdot}{\partial s} + \frac{\sigma^2 s^2}{2} \frac{\partial^2 \cdot}{\partial s^2}, \quad (3.3.3)$$

corresponding to, respectively, the OU, CIR, and XOU models.

The optimal exit and entry problems \mathcal{J} and \mathcal{V} associated with the *long-short* strategy are solved from the following pair of variational inequalities:

$$\max \{ \mathcal{L}^{(i)}\mathcal{V}(t, s), (f(t, s; T) - c) - \mathcal{V}(t, s) \} = 0, \quad (3.3.4)$$

$$\max \{ \mathcal{L}^{(i)}\mathcal{J}(t, s), (\mathcal{V}(t, s) - (f(t, s; T) + \hat{c}))^+ - \mathcal{J}(t, s) \} = 0, \quad (3.3.5)$$

for $(t, s) \in [0, T] \times \mathbb{R}$, with $i \in \{1, 2, 3\}$ representing the OU, CIR, or XOU model respectively.³ Similarly, the reverse *short-long* strategy can be determined by numerically solving the variational inequalities satisfied by \mathcal{U} and

³The spot price is positive, thus $s \in \mathbb{R}_+$, under the CIR and XOU models.

\mathcal{K} :

$$\min \{ \mathcal{L}^{(i)}\mathcal{U}(t, s), (f(t, s; T) + \hat{c}) - \mathcal{U}(t, s) \} = 0, \quad (3.3.6)$$

$$\max \{ \mathcal{L}^{(i)}\mathcal{K}(t, s), ((f(t, s; T) - c) - \mathcal{U}(t, s))^+ - \mathcal{K}(t, s) \} = 0. \quad (3.3.7)$$

As \mathcal{V} , \mathcal{J} , \mathcal{U} , and \mathcal{K} are numerically solved, they become the input to the final problem represented by the value function \mathcal{P} . To determine the optimal timing to enter the futures market, we solve the variational inequality

$$\max \{ \mathcal{L}^{(i)}\mathcal{P}(t, s), \max\{\mathcal{A}(t, s), \mathcal{B}(t, s)\} - \mathcal{P}(t, s) \} = 0. \quad (3.3.8)$$

The optimal timing strategies are described by a series of boundaries representing the time-varying critical spot price at which the investor should establish a long/short futures position. In the “long to open, short to close” trading problem, where the investor pre-commits to taking a long position first, the market entry timing is described by the “ \mathcal{J} ” boundary in Figure 3.2(a). The subsequent timing to exit the market is represented by the “ \mathcal{V} ” boundary in Figure 3.2(a). As we can see, the investor will long the futures when the spot price is low, and short to close the position when the spot price is high, confirming the buy-low-sell-high intuition.

If the investor adopts the *short-long* strategy, by which she will first short a futures and subsequently close out with a long position, then the optimal market entry and exit timing strategies are represented, respectively, by the “ \mathcal{K} ” and “ \mathcal{U} ” boundaries in Figure 3.2(c). The investor will enter the market by shorting a futures when the spot price is sufficiently high (at the “ \mathcal{K} ” boundary), and close it out when the spot price is low. Thus, the boundaries reflect a sell-high-buy-low strategy.

When there are no transaction costs (see Figure 3.2(b) and 3.2(d)), the waiting region shrinks for both strategies. Practically, this means that the investor tends to enter and exit the market earlier, resulting in more rapid

trades. This is intuitive as transaction costs discourage trades, especially near expiry.

In the market entry problem represented by $\mathcal{P}(t, s)$ in (3.3.1), the investor decides at what spot price to open a position. The corresponding timing strategy is illustrated by two boundaries in Figure 3.2(e). The boundary labeled as “ $\mathcal{P} = \mathcal{A}$ ” (resp. “ $\mathcal{P} = \mathcal{B}$ ”) indicates the critical spot price (as a function of time) at which the investor enters the market by taking a *long* (resp. *short*) futures position. The area above the “ $\mathcal{P} = \mathcal{B}$ ” boundary is the “short-first” region, whereas the area below the “ $\mathcal{P} = \mathcal{A}$ ” boundary is the “long-first” region. The area between the two boundaries is the region where the investor should wait to enter. The ordering of the regions is intuitive – the investor should long the futures when the spot price is currently low and short it when the spot price is high. As time approaches maturity, the value of entering the market diminishes. The investor will not start a long/short position unless the spot is very low/high close to maturity. Therefore, the waiting region expands significantly near expiry.

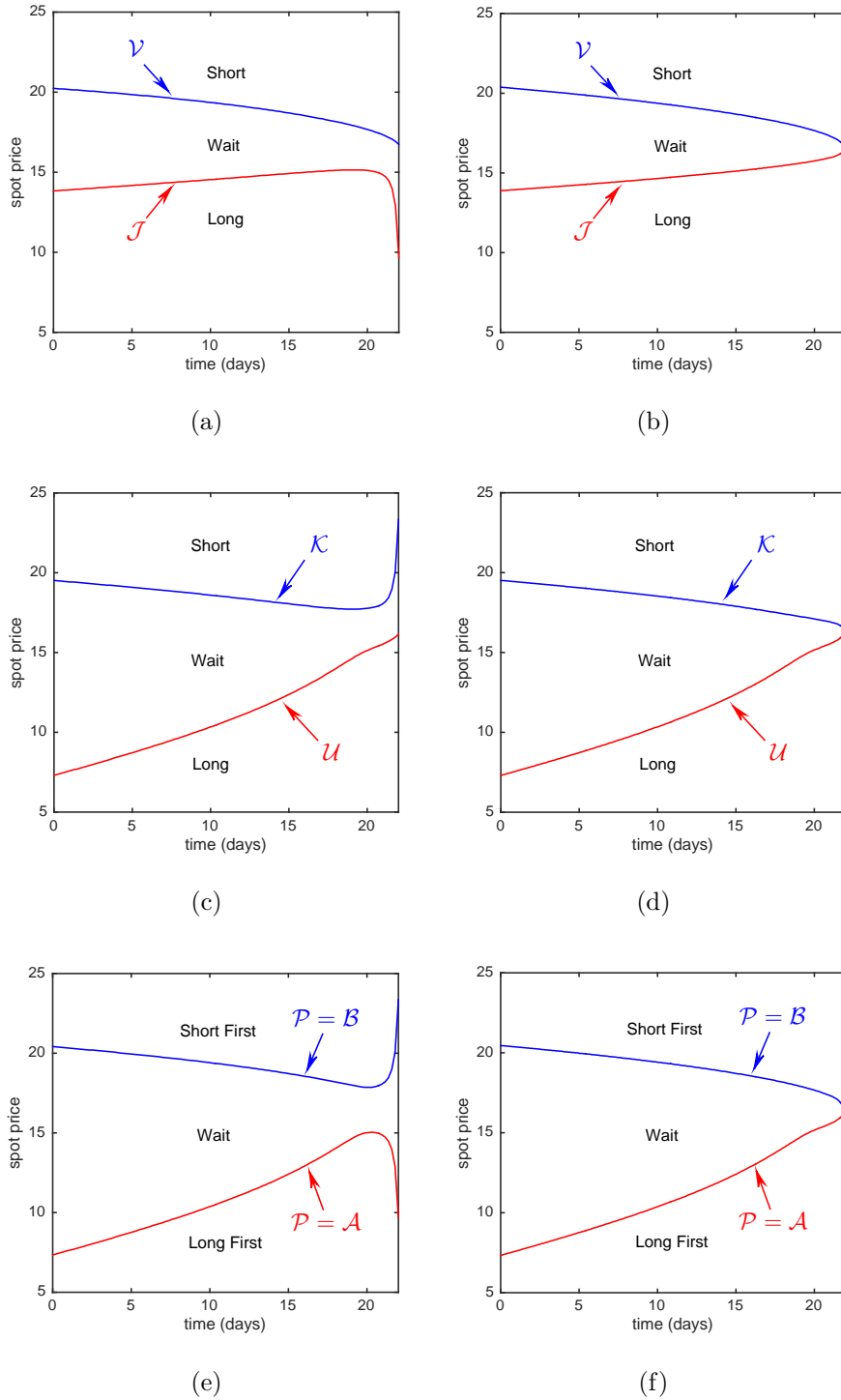
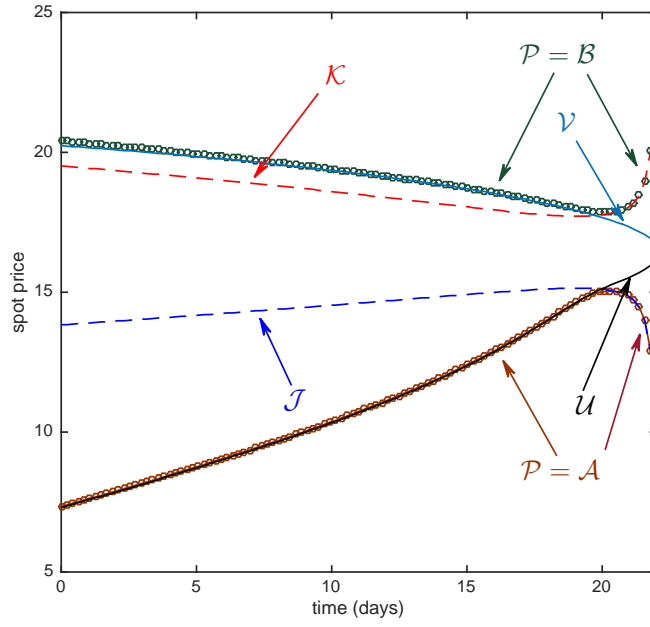
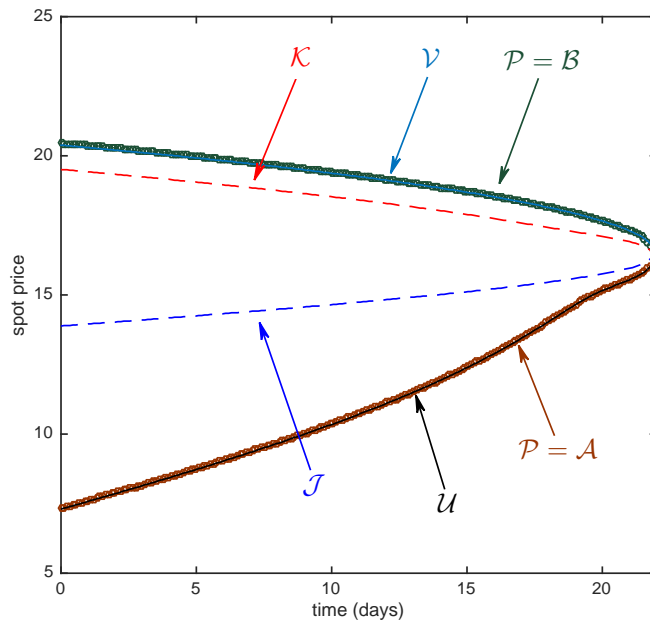


Figure 3.2: Optimal long-short boundaries with/without transaction costs for futures trading under the CIR model in (a) and (b) respectively, optimal short-long boundaries with/without transaction costs in (c) and (d) respectively, and optimal boundaries with/without transaction costs in (e) and (f) respectively. Parameters: $\hat{T} = \frac{22}{252}$, $T = \frac{66}{252}$, $r = 0.05$, $\sigma = 5.33$, $\theta = 17.58$, $\tilde{\theta} = 18.16$, $\mu = 8.57$, $\tilde{\mu} = 4.55$, $c = \hat{c} = 0.005$.

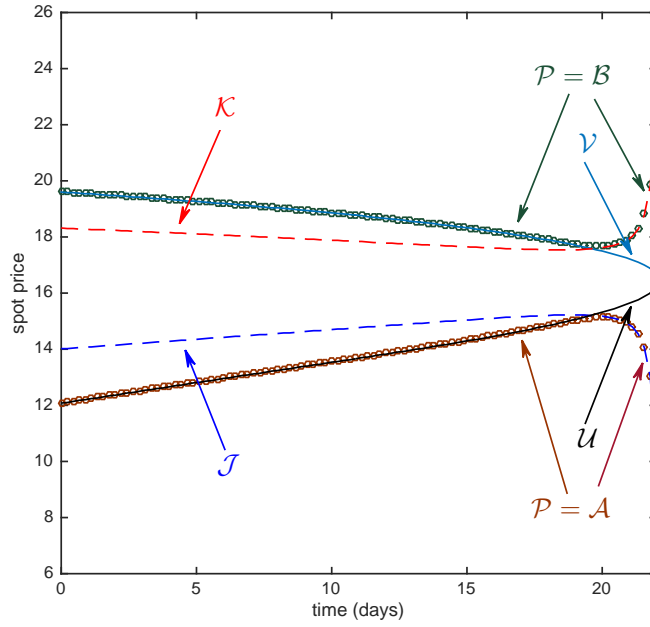


(a)

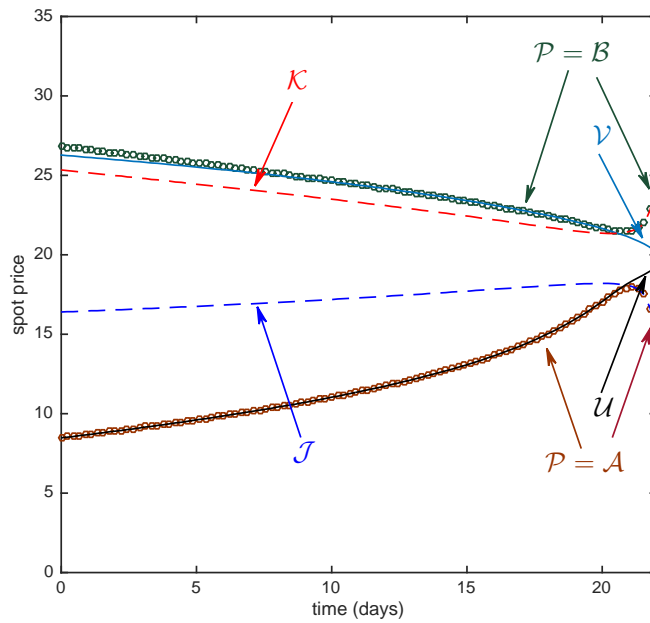


(b)

Figure 3.3: Optimal boundaries with and without transaction costs for futures trading under the CIR model in (a) and (b) respectively. Parameters: $\hat{T} = \frac{22}{252}$, $T = \frac{66}{252}$, $r = 0.05$, $\sigma = 5.33$, $\theta = 17.58$, $\tilde{\theta} = 18.16$, $\mu = 8.57$, $\tilde{\mu} = 4.55$, $c = \hat{c} = 0.005$.



(a)



(b)

Figure 3.4: Optimal boundaries with transaction costs for futures trading. (a) OU spot model with $\sigma = 18.7, \theta = 17.58, \tilde{\theta} = 18.16, \mu = 8.57, \tilde{\mu} = 4.55$. (b) XOU spot model with $\sigma = 1.63, \theta = 3.03, \tilde{\theta} = 3.06, \mu = 8.57, \tilde{\mu} = 4.08$. Common parameters: $\hat{T} = \frac{22}{252}, T = \frac{66}{252}, c = \hat{c} = 0.005$.

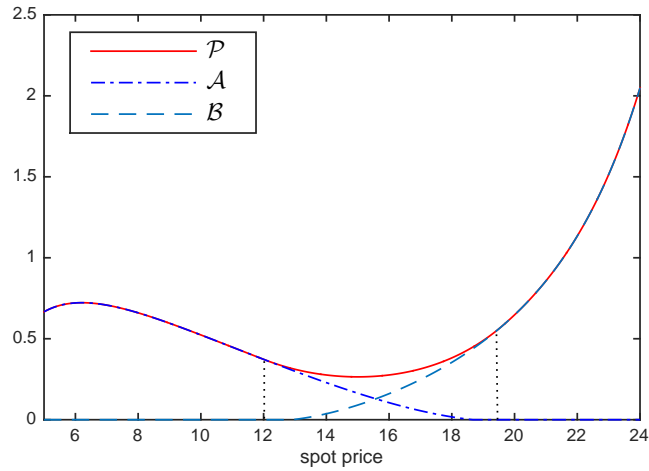


Figure 3.5: The value functions \mathcal{P} , \mathcal{A} , and \mathcal{B} plotted against the spot price at time 0. The parameters are the same as those in Figure 3.4.

The investor's exit strategy depends on the initial entry position. If the investor enters by taking a long position (at the " $\mathcal{P} = \mathcal{A}$ " boundary), then the optimal exit timing to close her position is represented by the upper boundary with label " \mathcal{V} " in Figure 3.2(a). If the investor's initial position is short, then the optimal time to close by going long the futures is described by the lower boundary with label " \mathcal{U} " in Figure 3.2(c).

Since the value function \mathcal{P} dominates both \mathcal{J} and \mathcal{K} due to the additional flexibility, it is not surprising that the " $\mathcal{P} = \mathcal{A}$ " boundary is lower than the " \mathcal{J} " boundary, and the " $\mathcal{P} = \mathcal{B}$ " boundary is higher than the " \mathcal{K} " boundary, as seen in Figure 3.3(a). This means that the embedded timing option to choose between the two strategies ("long to open, short to close" or "short to open, long to close") induces the investor to delay market entry to wait for better prices. This phenomenon is also observed for both OU and XOU spot models in Figure 3.4. Figure 3.5 shows that the value function \mathcal{P} dominates \mathcal{B} and \mathcal{A} for all values of spot price. We can also see the regions where the " $\mathcal{P} = \mathcal{A}$ " (when the spot price is low) and " $\mathcal{P} = \mathcal{B}$ " (when the spot price is

high).

We see that Figure 3.4(b) is similar to Figure 3.3(a), in both CIR and XOU cases, the difference between “ \mathcal{U} ” boundary and the “ \mathcal{J} ” boundary is much larger than the difference between the “ \mathcal{V} ” boundary and the “ \mathcal{K} ” boundary. This means that the decision to choose either *long-short* or *short-long* has a larger impact on the optimal price level to long futures compared to the optimal level to short. On the other hand, in Figure 3.4(a), we observe a more symmetric relationship between the *long-short* and *short-long* optimal exercise boundaries. In particular, choosing one strategy or the other does not affect the optimal price levels as much as CIR and XOU cases.

3.4 Conclusion

We have studied an optimal double stopping approach for trading futures under a number of mean-reverting spot models. Our model yields trading decisions that are consistent with the spot price dynamics and futures term structure. Accounting for the timing options as well as the option to choose between a long or short position, we find that it is optimal to delay market entry, as compared to the case of committing to either go long or short *a priori*.

A natural direction for future research is to investigate the trading strategies under a multi-factor or time-varying mean-reverting spot price model. To this end, we include here some references that discuss the pricing aspect of futures under such models, for example, Detemple and Osakwe [2000]; Lu and Zhu [2009]; Zhu and Lian [2012]; Mencía and Sentana [2013] for VIX futures, Schwartz [1997]; Ribeiro and Hodges [2004] for commodities, and Monoyios and Sarno [2002] for equity index futures. It is also of practical interest to develop similar optimal multiple stopping approaches to trading commodities under mean-reverting spot models (Leung et al. [2015, 2014]), and credit

derivatives trading (Leung and Liu [2012]).

Chapter 4

Optimal Risk Averse Timing of an Asset Sale

In this chapter, we incorporate risk preference into optimal stopping problems. We consider a risk-averse investor who has an exponential, power, or log utility. We analyze the optimal timing to sell an asset when prices are driven by a GBM or XOU process – to account for, respectively, the trending and mean-reverting price dynamics. This gives rise to a total of six different scenarios. In all cases, we derive the optimal thresholds to liquidate the asset and the certainty equivalents associated with the timing option to sell. We compare these results across models and utilities, with emphasis on their dependence on asset price, risk aversion, and quantity. We find that the timing option may render the investor's value function and certainty equivalent non-concave in price. Numerical results are presented to illustrate the investor's strategies and the premium associated with optimally timing to sell.

In Section 4.1, the asset sale problems are formulated for different utilities and price dynamics. In Section 4.2, we present the solutions of the problems and discuss the optimal selling strategies. We analyze the certainty equivalents in Section 4.3. All proofs are included in Section 4.4.

4.1 Problem Overview

We consider a risk-averse asset holder (investor) with a subjective probability measure \mathbb{P} . For our optimal asset sale problems, we will study two models for the risky asset price, namely, the geometric Brownian motion (GBM) model and the exponential Ornstein-Uhlenbeck (XOU) model. First, the GBM price process S satisfies

$$dS_t = \mu S_t dt + \sigma S_t dB_t,$$

with constant parameters $\mu \in \mathbb{R}$ and $\sigma > 0$, where $(B_t)_{t \geq 0}$ is a standard Brownian motion under \mathbb{P} . Under the second model, the XOU price process ξ is defined by

$$\begin{aligned} \xi_t &= e^{X_t}, \\ dX_t &= \kappa(\theta - X_t) dt + \eta dB_t, \end{aligned} \tag{4.1.1}$$

where the log-price X is an OU process with constant parameters $\kappa, \eta > 0$, $\theta \in \mathbb{R}$.

The investor's risk preference is modeled by three utility functions:

(1) Exponential utility

$$U_e(w) = 1 - e^{-\gamma w}, \quad \text{for } w \in \mathbb{R},$$

with the risk aversion parameter $\gamma > 0$;

(2) Log utility

$$U_l(w) = \log(w), \quad \text{for } w > 0;$$

(3) Power utility

$$U_p(w) = \frac{w^p}{p}, \quad \text{for } w \geq 0,$$

where $p := 1 - \varrho$, with the risk aversion parameter $\varrho \in [0, 1)$. In particular, when $p = 1$, the power utility is linear, corresponding to zero risk aversion.

Denote by \mathbb{F} the filtration generated by the Brownian motion B , and \mathcal{T} the set of all \mathbb{F} -stopping times. The investor seeks to maximize the expected discounted utility from asset sale by selecting the optimal stopping time. Denote by $\nu > 0$ the quantity of the risky asset to be sold. For simplicity, we limit our analysis to *simultaneous* liquidation of all ν units. The investor will receive the utility value of $U_i(\nu S_\tau)$ or $U_i(\nu \xi_\tau)$, $i \in \{e, l, p\}$, under the GBM and XOU model respectively, when all units are sold at time τ .

Therefore, the investor solves the optimal stopping problems under two different price dynamics:

$$\text{(GBM)} \quad V_i(s, \nu) = \sup_{\tau \in \mathcal{T}} \mathbb{E}_s \{ e^{-r\tau} U_i(\nu S_\tau) \}, \quad (4.1.2)$$

$$\text{(XOU)} \quad \tilde{V}_i(z, \nu) = \sup_{\tau \in \mathcal{T}} \mathbb{E}_z \{ e^{-r\tau} U_i(\nu \xi_\tau) \},$$

for $i \in \{e, l, p\}$, where $r > 0$ is the constant subjective discount rate. We have used the shorthand notations: $\mathbb{E}_s \{ \cdot \} \equiv \mathbb{E} \{ \cdot | S_0 = s \}$ and $\mathbb{E}_z \{ \cdot \} \equiv \mathbb{E} \{ \cdot | \xi_0 = z \}$. By the standard theory of optimal stopping (see e.g. Chapter 1 of Peskir and Shiryaev [2006] and Chapter 10 of Øksendal [2003]), the optimal stopping times are of the form

$$\tau_i^* = \inf \{ t \geq 0 : V_i(S_t, \nu) = U_i(\nu S_t) \}, \quad (4.1.3)$$

$$\tilde{\tau}_i^* = \inf \{ t \geq 0 : \tilde{V}_i(\xi_t, \nu) = U_i(\nu \xi_t) \}. \quad (4.1.4)$$

In this chapter, we analytically derive the value functions and show they satisfy their associated variational inequalities. Under the GBM model, for any fixed ν , the value functions $V_i(s) \equiv V_i(s, \nu)$, for $i \in \{e, l, p\}$, satisfy the variational inequalities

$$\max \{ (\mathcal{L}^S - r)V_i(s), U_i(\nu s) - V_i(s) \} = 0, \quad \forall s \in \mathbb{R}_+, \quad (4.1.5)$$

for $i \in \{e, l, p\}$, where \mathcal{L}^S is the infinitesimal generator of S defined by

$$\mathcal{L}^S = \frac{\sigma^2 s^2}{2} \frac{d^2}{ds^2} + \mu s \frac{d}{ds}. \quad (4.1.6)$$

Likewise, under the XOU model the value functions $\tilde{V}_i(z) \equiv \tilde{V}_i(z, \nu)$, $i \in \{e, l, p\}$, solve the variational inequalities

$$\max\{(\mathcal{L}^X - r)\tilde{V}_i(e^x), U_i(\nu e^x) - \tilde{V}_i(e^x)\} = 0, \quad \forall x \in \mathbb{R}, \quad (4.1.7)$$

for $i \in \{e, l, p\}$, where

$$\mathcal{L}^X = \frac{\eta^2}{2} \frac{d^2}{dx^2} + \kappa(\theta - x) \frac{d}{dx}, \quad (4.1.8)$$

is the infinitesimal generator of the OU process X (see (4.1.1)). For optimal stopping problems driven by an XOU process, we find it more convenient to work with the log-price X .

To better understand the value of the risky asset under optimal liquidation, we study the *certainty equivalent* associated with each utility maximization problem. The certainty equivalent is defined as the guaranteed cash amount that generates the same utility as the maximal expected utility from optimally timing to sell the risky asset. Precisely, we define

$$\text{(GBM)} \quad C_i(s, \nu) = U_i^{-1}(V_i(s, \nu)), \quad (4.1.9)$$

$$\text{(XOU)} \quad \tilde{C}_i(z, \nu) = U_i^{-1}(\tilde{V}_i(z, \nu)), \quad (4.1.10)$$

for $i \in \{e, l, p\}$, under the GBM and XOU models respectively. Certainty equivalent gives us a common (cash) unit to compare the values of timing to sell under different utilities, dynamics, and quantities.

Moreover, the certainty equivalent can shed light on the investor's optimal strategy. Indeed, applying (4.1.9) and (4.1.10) to (4.1.3) and (4.1.4) respectively, we obtain an alternative expression for the optimal stopping time under each model:

$$\tau_i^* = \inf\{t \geq 0 : C_i(S_t, \nu) = \nu S_t\},$$

$$\tilde{\tau}_i^* = \inf\{t \geq 0 : \tilde{C}_i(\xi_t, \nu) = \nu \xi_t\}.$$

In other words, it is optimal for the investor to sell when the certainty equivalent is equal to the total cash amount of νS_t or $\nu \xi_t$, under the GBM or XOU model respectively, received from the sale.

4.2 Optimal Timing Strategies

In this section, we present the analytical results and discuss the value functions and optimal selling strategies under the GBM and XOU models. The methods of solution and detailed proofs are presented in Section 4.4.

4.2.1 The GBM Model

To prepare for our results for the GBM model, we first consider an increasing general solution to the ODE:

$$\mathcal{L}^S f(s) = rf(s), \quad s \in \mathbb{R}_+, \quad (4.2.1)$$

with \mathcal{L}^S defined in (4.1.6). This solution is $f(s) = s^\alpha$ with

$$\alpha = \left(\frac{1}{2} - \frac{\mu}{\sigma^2} \right) + \sqrt{\left(\frac{\mu}{\sigma^2} - \frac{1}{2} \right)^2 + \frac{2r}{\sigma^2}}. \quad (4.2.2)$$

By inspection, we see that $0 < \alpha < 1$ when $r < \mu$, and $\alpha \geq 1$ when $r \geq \mu$.

Theorem 4.2.1. *Consider the optimal asset sale problem (4.1.2) under the GBM model with exponential utility.*

(i) *If $r \geq \mu$, then it is optimal to sell immediately, and the value function is*

$$V_e(s, \nu) = 1 - e^{-\gamma \nu s}.$$

(ii) *If $r < \mu$, then the value function is given by*

$$V_e(s, \nu) = \begin{cases} (1 - e^{-\gamma \nu a_e})(a_e)^{-\alpha} s^\alpha & \text{if } s \in [0, a_e), \\ 1 - e^{-\gamma \nu s} & \text{if } s \in [a_e, +\infty), \end{cases}$$

where the optimal threshold $a_e \in (0, +\infty)$ is uniquely determined by the equation

$$\alpha(e^{\gamma\nu a_e} - 1) - \gamma\nu a_e = 0. \quad (4.2.3)$$

The optimal time to sell is

$$\tau_e^* = \inf\{t \geq 0 : S_t \geq a_e\}.$$

Under the GBM model with exponential utility, the optimal selling strategy can be either trivial or non-trivial. When the subjective discount rate r equals or exceeds the drift μ of the GBM process, it is optimal to sell immediately. This is intuitive as the asset net discounting tends to lose value. On the other hand, when $r < \mu$, the investor should sell when the unit price exceeds a finite threshold. At the optimal sale time τ_e^* , the investor receives the cash amount νa_e from the sale of ν units of S . In other words, a_e is the per-unit price received upon sale, but according to (4.2.3) it varies depending on the quantity ν and risk aversion parameter γ .

Theorem 4.2.2. *Consider the optimal stopping problem (4.1.2) under the GBM model with log utility. The value function is given by*

$$V_l(s, \nu) = \begin{cases} \frac{\nu^\alpha}{\alpha e} s^\alpha & \text{if } s \in [0, a_l), \\ \log(\nu s) & \text{if } s \in [a_l, +\infty), \end{cases}$$

where $a_l := \nu^{-1} \exp(\alpha^{-1})$ is the unique optimal threshold. The optimal time to sell is

$$\tau_l^* = \inf\{t \geq 0 : S_t \geq a_l\}.$$

With log utility, the optimal strategy is to sell as soon as the unit price of the risky asset, S , enters the upper interval $[a_l, +\infty)$. Note that the optimal

threshold a_l is inversely proportional to quantity, so the total cash amount received upon sale, $\nu a_l = \exp(\alpha^{-1})$, remains the same regardless of quantity. In other words, the log-utility investor is not financially better off by holding more units of S . Under exponential utility, the optimal selling price is implicitly defined by (4.2.3) in Theorem 4.2.1 and must be evaluated numerically. In contrast, the optimal threshold under log utility is fully explicit.

Turning to the value functions, a natural question is whether they preserve the concavity of the utilities. Indeed, if the investor sells at a pre-determined fixed time T , then the expected utility $W(s) := \mathbb{E}_s\{e^{-rT}U(\nu S_T)\}$ is concave in s for any concave utility function U . From Theorem 4.2.1, we see that $V_e(s, \nu)$ is concave in s for all $s \in \mathbb{R}_+$. On the other hand, $V_l(s, \nu)$ is concave in s when $\alpha < 1$, but it is neither convex nor concave in s when $\alpha \geq 1$. In other words, the timing option to sell gives rise to the possibility of non-concave value function. In Figure 4.1, we plot the value functions associated with the exponential and log utilities when the investor is holding a single unit of the asset. The value functions dominate the utility functions, and coincide smoothly at the optimal selling thresholds. In Figure 4.1(b), the value function $V_l(s, 1)$ under log utility is shown to have two possible shapes. For $\mu = 0.01 < 0.02 = r$, i.e. $\alpha < 1$, the value function $V_l(s, 1)$ is convex when s is lower than a_l , and concave for $s \geq a_l$. In the other scenario, $\mu > r$, i.e. $\alpha > 1$, the value function $V_l(s, 1)$ is concave.

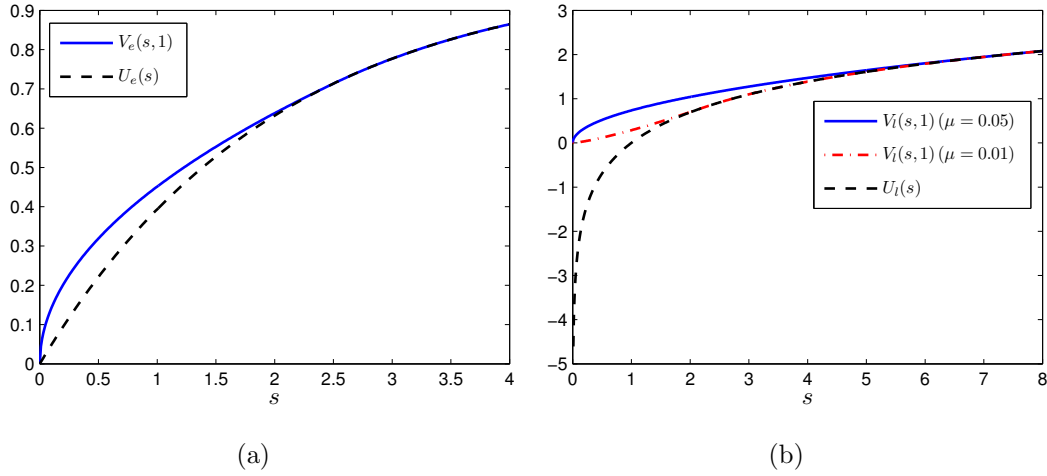


Figure 4.1: Value functions smooth-paste the utility function under the GBM model. (a) The value function $V_e(s,1)$ dominates the exponential utility $U_e(s)$ (with $\gamma = 0.5$ and $\mu = 0.05$) and coincides for $s \geq a_e = 2.5129$. (b) The value functions $V_l(s,1)$ (with $\mu = 0.05$) and $V_l(s,1)$ (with $\mu = 0.01$) dominate the log utility $U_l(s)$ and coincide for $s \geq a_l = 7.3891$ and $s \geq a_l = 2.1832$ respectively. Common parameters: $\sigma = 0.2, \nu = 1, r = 2\%$.

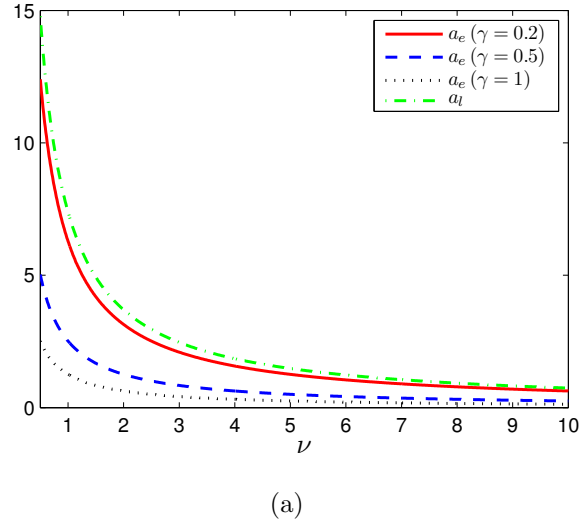


Figure 4.2: Optimal selling thresholds, a_e (with $\gamma = 0.2, 0.5, 1$) and a_l , under the GBM model vs quantity ν . Parameters: $\mu = 0.05, \sigma = 0.2, r = 2\%$.

Figure 4.2 illustrates the effect of quantity ν on optimal selling thresholds a_e and a_l under exponential and log utilities respectively. The optimal strategy under power utility is trivial and thus omitted from the figure. The optimal threshold a_e is decreasing in ν for each fixed risk aversion $\gamma = 0.2, 0.5$ and 1 . Moreover, for any fixed quantity, a higher γ lowers the optimal selling price. The quantity ν effectively scales up the risk aversion to the value $\nu\gamma$ instead of γ . Increase in either of these parameters results in higher risk aversion, inducing the investor to sell at a lower price. In comparison, the log-utility optimal threshold a_l is explicit and inversely proportional to ν , as seen in the figure.

We conclude this section with a discussion on the optimal liquidation strategy under power utility. First, observe that for any $p \in (0, 1]$, the power process S_t^p is also a GBM satisfying

$$dS_t^p = \tilde{\mu}S_t^p dt + \tilde{\sigma}S_t^p dB_t,$$

with new parameters

$$\tilde{\mu} = p\mu + \frac{1}{2}p(p-1)\sigma^2 \quad \text{and} \quad \tilde{\sigma} = p\sigma.$$

Then, the process $(e^{-rt}S_t^p)_{t \geq 0}$ is a submartingale (resp. supermartingale) if $\tilde{\mu} > r$ (resp. $\tilde{\mu} \leq r$). As a result, the optimal timing to sell is trivial, as we summarize next.

Theorem 4.2.3. *Consider the optimal asset sale problem (4.1.2) under the GBM model with power utility.*

- (i) *If $\tilde{\mu} \leq r$, then it is optimal to sell immediately, and the value function*

$$V_p(s, \nu) = U_p(\nu s).$$
- (ii) *If $\tilde{\mu} > r$, then it is optimal to wait indefinitely, and the value function*

$$V_p(s, \nu) = +\infty.$$

4.2.2 The XOU Model

In this section, we discuss the optimal asset sale problems under the XOU model. Recall from Chapter 2 that the classical solutions of the ODE

$$\mathcal{L}^X f(x) = rf(x), \quad (4.2.4)$$

for $x \in \mathbb{R}$, are

$$F(x) \equiv F(x; \kappa, \theta, \eta, r) := \int_0^\infty v^{\frac{r}{\kappa}-1} e^{\sqrt{\frac{2\kappa}{\eta^2}}(x-\theta)v - \frac{v^2}{2}} dv, \quad (4.2.5)$$

$$G(x) \equiv G(x; \kappa, \theta, \eta, r) := \int_0^\infty v^{\frac{r}{\kappa}-1} e^{\sqrt{\frac{2\kappa}{\eta^2}}(\theta-x)v - \frac{v^2}{2}} dv. \quad (4.2.6)$$

Alternatively, the functions F and G can be expressed as

$$F(x) = e^{\frac{\kappa}{2\eta^2}(x-\theta)^2} D_{-r/\kappa} \left(\sqrt{\frac{2\kappa}{\eta^2}}(\theta - x) \right),$$

and

$$G(x) = e^{\frac{\kappa}{2\eta^2}(x-\theta)^2} D_{-r/\kappa} \left(\sqrt{\frac{2\kappa}{\eta^2}}(x - \theta) \right),$$

where $D_\nu(\cdot)$ is the parabolic cylinder function or Weber function (see Erdélyi et al. [1953]). The strictly positive and convex function F plays a central role in the solution of the optimal asset sale problems under the XOU model.

Theorem 4.2.4. *Under an XOU model with exponential utility, the optimal asset sale problem admits the solution*

$$\tilde{V}_e(z, \nu) = \begin{cases} KF(\log(z)) & \text{if } z \in [0, e^{b_e}), \\ 1 - e^{-\gamma\nu z} & \text{if } z \in [e^{b_e}, +\infty), \end{cases} \quad (4.2.7)$$

with the constant

$$K = \frac{1 - \exp(-\gamma\nu e^{b_e})}{F(b_e)} > 0.$$

The critical log-price level $b_e \in (-\infty, +\infty)$ satisfies

$$(1 - \exp(-\gamma\nu e^{b_e})) F'(b_e) = \gamma\nu e^{b_e} \exp(-\gamma\nu e^{b_e}) F(b_e). \quad (4.2.8)$$

The optimal time to sell is

$$\tilde{\tau}_e^* = \inf\{t \geq 0 : \xi_t \geq e^{b_e}\}.$$

According to Theorem 4.2.4, the investor should sell all ν units as soon as the asset price ξ reaches e^{b_e} or above. The optimal price level e^{b_e} depends on both the investor's risk aversion and quantity, but it stays the same as long as the product $\nu\gamma$ remains unchanged.

Theorem 4.2.5. *Under an XOU model with log utility, the optimal asset sale problem admits the solution*

$$\tilde{V}_l(z, \nu) = \begin{cases} DF(\log(z)) & \text{if } z \in [0, e^{b_l}), \\ \log(\nu z) & \text{if } z \in [e^{b_l}, +\infty), \end{cases}$$

with the coefficient

$$D = \frac{b_l + \log(\nu)}{F(b_l)} > 0. \quad (4.2.9)$$

The finite critical log-price level b_l is uniquely determined from the equation

$$F(b_l) = (b_l + \log(\nu))F'(b_l). \quad (4.2.10)$$

The optimal time to sell is

$$\tilde{\tau}_l^* = \inf\{t \geq 0 : \xi_t \geq e^{b_l}\}.$$

In Figure 4.3(d), we see that the optimal unit selling price e^{b_l} is decreasing in ν but when multiplied by the quantity ν , the total cash amount νe^{b_l} received from the sale increases.

For the case of power utility, we observe that $\tilde{\xi} := \xi^p$ is again an XOU process, satisfying

$$\tilde{\xi}_t = e^{\tilde{X}_t}, \quad \text{where} \quad d\tilde{X}_t = \kappa(\tilde{\theta} - \tilde{X}_t) dt + \tilde{\eta} dB_t, \quad t \geq 0,$$

with the new parameters $\tilde{\eta} := p\eta > 0$, and $\tilde{\theta} := p\theta \in \mathbb{R}$. In particular, both the original long-run mean θ and volatility parameter η have been scaled by a factor of p , while the speed of mean reversion remains unchanged. Therefore, the value function admits the separable form:

$$\tilde{V}_p(z, \nu) = \sup_{\tau \in \mathcal{T}} \mathbb{E}_z \left\{ e^{-r\tau} \frac{\nu^p \xi_\tau^p}{p} \right\} = U_p(\nu) \tilde{V}(\tilde{z}, 1), \quad (4.2.11)$$

where

$$\tilde{V}(\tilde{z}, 1) := \sup_{\tau \in \mathcal{T}} \mathbb{E}_z \left\{ e^{-r\tau} \tilde{\xi}_\tau \right\}. \quad (4.2.12)$$

Hence, without loss of generality, the optimal timing to sell can be determined from the optimal stopping problem in (4.2.12), and the corresponding value function \tilde{V}_p can be recovered from (4.2.11).

Theorem 4.2.6. *Under the XOOU model with power utility, the solution to the optimal asset sale problem is given by*

$$\tilde{V}_p(z, \nu) = \begin{cases} MF(p \log(z)) & \text{if } z \in [0, e^{b_p}), \\ \frac{\nu^p}{p} z^p & \text{if } z \in [e^{b_p}, +\infty), \end{cases}$$

where

$$M = \frac{\nu^p e^{pb_p}}{pF(pb_p)} > 0.$$

The critical log-price threshold $b_p \in (-\infty, +\infty)$ satisfies the equation

$$F'(pb_p) = F(pb_p), \quad (4.2.13)$$

where $F(x) \equiv F(x; \kappa, \tilde{\theta}, \tilde{\eta}, r)$. The optimal asset sale timing is

$$\tilde{\tau}_p^* = \inf\{t \geq 0 : \xi_t \geq e^{b_p}\}.$$

The investor should sell all ν units the first time the asset price reaches the level e^{b_p} . According to (4.2.13), the optimal price level is independent of quantity ν , as we can see in Figure 4.3(d).

Under the XOU model, the value functions $\tilde{V}_i(z, \nu), i \in \{e, l, p\}$ are not necessarily concave in z due to the convex nature of F and the timing option to sell. Let's inspect the value functions in Figure 4.3. In each of these three cases, the value function is initially convex before smooth-pasting on the concave utility.

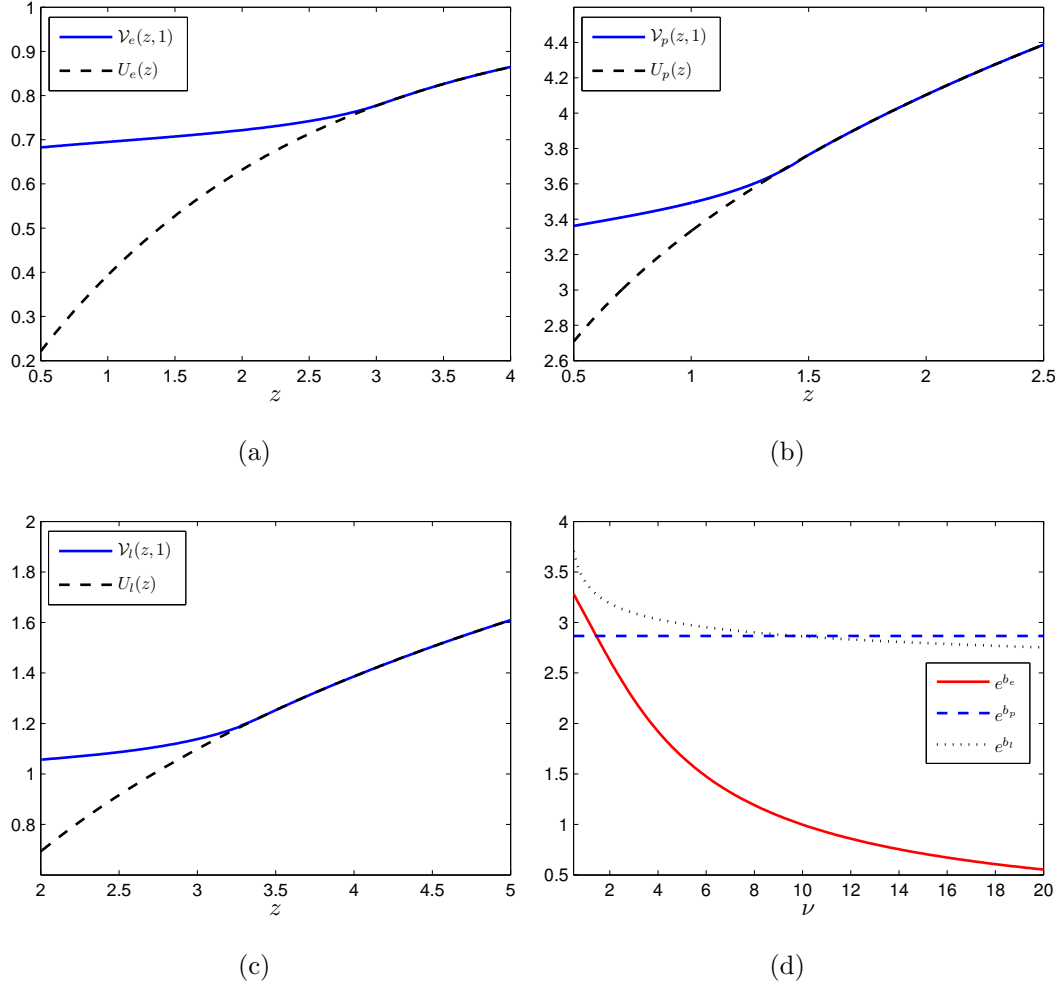


Figure 4.3: Under the XOU model, (a) the value function $\tilde{V}_e(z, 1)$ dominates the exponential utility $U_e(z)$ (with $\gamma = 0.5$) and coincides for $z \geq e^{b_e} = e^{1.1188} = 3.0612$. (b) The value function $\tilde{V}_p(z, 1)$ dominates the power utility $U_p(z)$ (with $p = 0.3$) and coincides for $z \geq e^{b_p} = e^{0.3519} = 1.3715$. (c) The value function $\tilde{V}_l(z, 1)$ dominates the log utility $U_l(z)$ and coincides for $z \geq e^{b_l} = e^{1.2227} = 3.3963$. (d) Optimal selling thresholds vs quantity ν . $\gamma = 0.5, p = 0.3$. Common Parameters: $\kappa = 0.6, \theta = 1, \eta = 0.2, r = 2\%$.

In Table 4.1, we summarize the results from Sections 4.2.1 and 4.2.2 and list the optimal thresholds for all the cases we have discussed. All thresholds, except a_l , are implicitly determined by the equations referenced in the table. The asset price model plays a crucial role in the structure of the optimal strategy. Under the GBM model with exponential utility, immediate liquidation may be optimal in one scenario regardless of the current asset price. On the contrary, with the same utility under the XOU model, immediate liquidation is never optimal and the investor should wait till the asset price rises to level e^{b_e} . With power utility, the GBM model implies a trivial optimal strategy, whereas the XOU model results in a threshold-type strategy. Lastly, even though both GBM and XOU price processes lead to non-trivial strategies for log utility, the optimal threshold a_l is explicit while e^{b_l} must be computed numerically.

	Exponential utility	Log utility	Power utility
GBM	0 / a_e in (4.2.3)	$a_l := \frac{e^{1/\alpha}}{\nu}$	0 / $+\infty$
XOU	e^{b_e} in (4.2.8)	e^{b_l} in (4.2.10)	e^{b_p} in (4.2.13)

Table 4.1: Optimal thresholds for asset sale under different models and utilities.

4.3 Certainty Equivalents

Having derived the value functions analytically, we now state as corollaries the certainty equivalents $C_i(s, \nu)$ and $\tilde{C}_i(z, \nu)$, $i \in \{e, l, p\}$, defined respectively in (4.1.9) and (4.1.10) under the GBM and XOU models. Furthermore, to quantify the value gained from waiting to sell the asset compared to immediate

liquidation, we define the *optimal liquidation premium* under each model:

$$\text{(GBM)} \quad L(s, \nu) := C_i(s, \nu) - \nu s,$$

$$\text{(XOU)} \quad L(z, \nu) := \tilde{C}_i(z, \nu) - \nu z,$$

for $i \in \{e, l, p\}$. We will examine the dependence of this premium on the asset price and quantity.

Corollary 4.3.1. *Under the GBM model, the certainty equivalents under different utilities are given as follows:*

(1) *Exponential utility:*

$$C_e(s, \nu) = \begin{cases} -\frac{1}{\gamma} \log \left(1 - \frac{1 - e^{-\gamma \nu a_e}}{a_e^\alpha} s^\alpha \right) & \text{if } s \in [0, a_e), \\ \nu s & \text{if } s \in [a_e, +\infty). \end{cases}$$

(2) *Log utility:*

$$C_l(s, \nu) = \begin{cases} \exp \left(\frac{\nu^\alpha s^\alpha}{\alpha e} \right) & \text{if } s \in [0, a_l), \\ \nu s & \text{if } s \in [a_l, +\infty). \end{cases}$$

(3) *Power utility:*

$$C_p(s, \nu) = \begin{cases} \nu s & \text{if } \tilde{\mu} \leq r, \\ +\infty & \text{if } \tilde{\mu} > r. \end{cases}$$

With exponential and log utilities, the certainty equivalents dominate νs – the value from immediate sale, and they coincide when the asset price exceeds the corresponding optimal selling thresholds. With power utility, the investor either sells immediately or waits indefinitely, corresponding to the certainty equivalents of value νs and $+\infty$, respectively.

The impact of ν on C_e is both direct in its certainty equivalent's expression, but also indirect in the derivation of a_e . As a result, the relationship between

C_e and ν is rather intricate. In comparison, the explicit formula for the optimal threshold a_l under log utility facilitates our analysis on the behavior of the certainty equivalent C_l . Fix any price s , $C_l(s, \nu)$ is convex in ν when $r \geq \mu$. Consequently, the liquidation premium is maximized at $\nu = 0$. However, when $r < \mu$, then $C_l(s, \nu)$ is concave on the price interval $(0, \log(\frac{1-\alpha}{s^\alpha}) + 1)$ and convex on $(\log(\frac{1-\alpha}{s^\alpha}) + 1, \exp(\alpha^{-1})/s)$. This implies that there exists an optimal quantity $\nu^* \in (0, \log(\frac{1-\alpha}{s^\alpha}) + 1)$ that maximizes the liquidation premium. This is useful when the investor can also choose the initial position in S .

Next, we state the certainty equivalents under the XOU model.

Corollary 4.3.2. *Under the XOU model, the certainty equivalents under different utilities are given as follows:*

(1) *Exponential utility:*

$$\tilde{C}_e(z, \nu) = \begin{cases} -\frac{1}{\gamma} \log \left[1 - \frac{1 - \exp(-\gamma \nu e^{b_e})}{F(b_e)} F(\log(z)) \right] & \text{if } z \in [0, e^{b_e}), \\ \nu z & \text{if } z \in [e^{b_e}, +\infty). \end{cases}$$

(2) *Log utility:*

$$\tilde{C}_l(z, \nu) = \begin{cases} \exp \left[\frac{b_l + \log(\nu)}{F(b_l)} F(\log(z)) \right] & \text{if } z \in [0, e^{b_l}), \\ \nu z & \text{if } z \in [e^{b_l}, +\infty). \end{cases}$$

(3) *Power utility:*

$$\tilde{C}_p(z, \nu) = \begin{cases} \left[\frac{e^{pb_p}}{F(pb_p)} F(p \log(z)) \right]^{1/p} \nu & \text{if } z \in [0, e^{b_p}), \\ \nu z & \text{if } z \in [e^{b_p}, +\infty). \end{cases}$$

For all three utilities, the certainty equivalents are equal to the immediate sale value, νz , when the asset price z is in the exercise region, where all units

are sold. In addition, we emphasize that both b_e and b_l are dependent on ν , which can be observed from (4.2.8) and (4.2.10). In contrast, the optimal log-price threshold under power utility b_p is *independent* of ν . Consequently, if we consider any fixed z in the continuation region $(0, e^{b_p})$, then the certainty equivalent $\tilde{C}_p(z, \nu) - \nu z$ is linear and strictly increasing in ν . This is interesting since under exponential and log utilities, increasing quantity has the effect of making the investor more risk-averse. In other words, as long as quantity is large enough, the investor will liquidate everything immediately even if the current price appears unattractive.

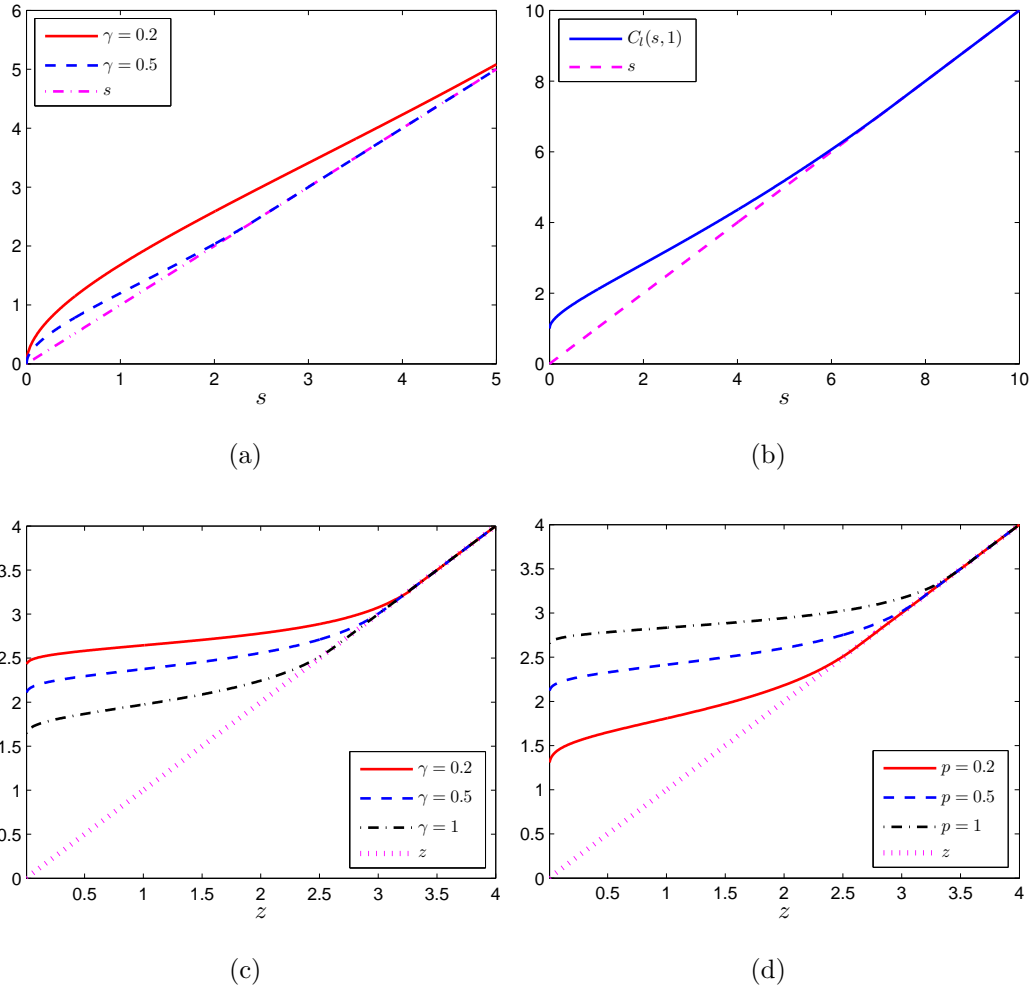


Figure 4.4: Certainty equivalent vs price. (a) $C_e(s,1)$ under the GBM model ($\mu = 0.05, \sigma = 0.2$). (b) $C_l(s,1)$ under the GBM model ($\mu = 0.05, \sigma = 0.2$). (c) $\tilde{C}_e(z,1)$ under the XOU model ($\kappa = 0.6, \theta = 1, \eta = 0.2$). (d) $\tilde{C}_p(z,1)$ under the XOU model ($\kappa = 0.6, \theta = 1, \eta = 0.2$). Note that $p := 1 - \varrho$, where ϱ is the risk aversion parameter. Common parameter: $r = 2\%$.

Let us now examine the certainty equivalents' dependence on the asset price. Under the GBM model, we plot the certainty equivalents, $C_e(s,1)$ and $C_l(s,1)$, against prices, respectively, in Figures 4.4(a) and 4.4(b), with a single unit of asset held. The optimal selling strategy for power utility is trivial, and thus, not presented. From Section 4.2.1, we know that for sufficiently

large s , it is optimal to sell and thus the certainty equivalents will eventually coincide with s and be linear. Notice that in both Figures 4.4(a) and 4.4(b), the certainty equivalents are concave for small s and subsequently convex for large s . In general, the certainty equivalents are neither concave nor convex functions of asset price, especially since the value functions V_i and \tilde{V}_i , $i \in \{e, l, p\}$ are not necessarily concave.

In Figure 4.4(a), we have also shown $C_e(s, 1)$ for different values of risk aversion level γ . As the investor becomes more risk-averse, it becomes optimal to sell the asset earlier. This is reflected by the certainty equivalent's convergence to the linear price line s at a lower price. Moreover, a less risk-averse certainty equivalent dominates a more risk-averse one at all prices. Similar effects of risk aversion is also seen in Figure 4.4(c) for exponential utility and Figure 4.4(d) for power utility under the XOU model.

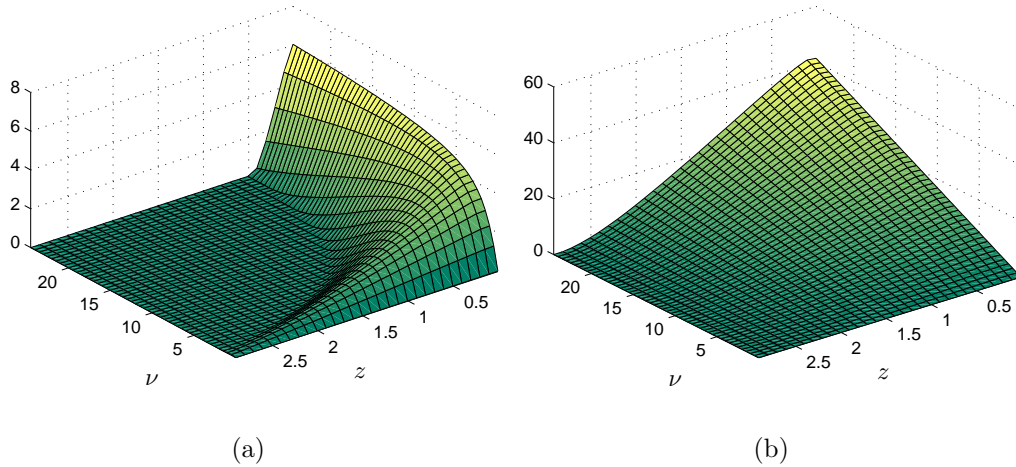


Figure 4.5: Liquidation premium $L(z, \nu)$ under the XOU model plotted against quantity ν and price z . (a) Exponential utility with $\gamma = 0.5$. (b) Power utility with $p = 0.3$. Common parameters: $\kappa = 0.6, \theta = 1, \eta = 0.2, r = 2\%$.

Figures 4.5(a) and 4.5(b), respectively, illustrate the liquidation premia for exponential and power utilities under the XOU model. The liquidation pre-

mium for power utility is linear in ν for any fixed value of z , but the exponential utility liquidation premium is nonlinear. In general, the liquidation premium vanishes when z is sufficiently high when the asset price is in the exercise region. As we can see from Figures 4.5(a) and 4.5(b) and Figures 4.4(a)-(d), the optimal liquidation premium tends to be large and may increase when the asset price is very low. This suggests that there is a high value of waiting to sell the asset later if the current price is low. As the asset price rises, the premium shrinks to zero. The investor finds no value in waiting any longer, resulting in an immediate sale.

4.4 Methods of Solution and Proofs

In this section, we present the detailed proofs for our analytical results in Section 4.2, from Theorems 4.2.1 - 4.2.2 for the GBM model to Theorems 4.2.4 - 4.2.6 for the XOU model. Our method of solution is to first construct candidate solutions using the classical solutions to ODEs (4.2.1) and (4.2.4), corresponding to the GBM and XOU models respectively, and then verify that the candidate solutions indeed satisfy the associated variational inequalities (4.1.5) and (4.1.7).

4.4.1 GBM Model

Proof of Theorem 4.2.1 (Exponential Utility). To prove that the value functions in Theorem 4.2.1 satisfy the variational inequality in (4.1.5), we consider the two cases, $r \geq \mu$ and $r < \mu$, separately.

When $r \geq \mu$, it is optimal to sell immediately. To see this, for any fixed ν we verify that $V_e(s, \nu) = 1 - e^{-\gamma\nu s}$ satisfies (4.1.5). Since $V_e(s, \nu) = U_e(\nu s)$ for

all $s \in \mathbb{R}_+$, we only need to check that the inequality

$$(\mathcal{L}^S - r)(1 - e^{-\gamma\nu s}) = e^{-\gamma\nu s} \left(\mu\gamma\nu s - \frac{\sigma^2\gamma^2\nu^2 s^2}{2} - re^{\gamma\nu s} + r \right) \leq 0, \quad (4.4.1)$$

holds for all $s \in \mathbb{R}_+$. First, we observe that the sign of the LHS of (4.4.1) depends solely on

$$g(s) := \mu\gamma\nu s - \frac{\sigma^2\gamma^2\nu^2 s^2}{2} - re^{\gamma\nu s} + r. \quad (4.4.2)$$

The first and order second derivatives g are, respectively,

$$g' = \mu\gamma\nu - \sigma^2\gamma^2\nu^2 s - r\gamma\nu e^{\gamma\nu s}, \quad \text{and} \quad g'' = -\sigma^2\gamma^2\nu^2 - r\gamma^2\nu^2 e^{\gamma\nu s},$$

from which we observe that g is strictly concave on \mathbb{R}_+ . Furthermore, $g(0) = 0$ and the fact $\lim_{s \rightarrow +\infty} g(s) = -\infty$ imply that g has a global maximum. Since $g'_+(0) = (\mu - r)\gamma\nu > 0$ (resp. < 0) if $\mu > r$ (resp. $\mu < r$), the maximum of g is non-positive if $r \geq \mu$. As a result, g is non-positive for all $s \in \mathbb{R}_+$, which yields inequality (4.4.1), as desired.

For an arbitrary $\nu > 0$, we can view $\nu\gamma$ together as the risk aversion parameter for the exponential utility, and equivalently consider the asset sale problem with $\nu = 1$ and risk aversion $\nu\gamma$ without loss of generality. When $r < \mu$, we consider a candidate solution V_e of the form As^α , where $A > 0$ is a constant to be determined. Recall that α is less than 1 when $r < \mu$, and hence s^α is an increasing concave function. We solve for the optimal threshold a_e and coefficient A from the value-matching and smooth-pasting conditions

$$\begin{aligned} Aa_e^\alpha &= U_e(a_e) = 1 - e^{-\gamma\nu a_e}, \\ A\alpha a_e^{\alpha-1} &= U'_e(a_e) = \gamma\nu e^{-\gamma\nu a_e}. \end{aligned} \quad (4.4.3)$$

This leads to the following equation satisfied by the optimal threshold a_e :

$$\alpha(e^{\gamma\nu a_e} - 1) - \gamma\nu a_e = 0. \quad (4.4.4)$$

We now show that there exists a unique and positive root to (4.4.4). Our approach involves establishing a relationship between (4.4.4) and $(\mathcal{L}^S - r)(1 - e^{-\gamma\nu s})$. To this end, first observe that the exponential utility $1 - e^{-\gamma\nu s}$ has the following properties:

$$\lim_{s \rightarrow 0} \frac{1 - e^{-\gamma\nu s}}{s^\beta} = \lim_{s \rightarrow +\infty} \frac{1 - e^{-\gamma\nu s}}{s^\alpha} = 0, \quad (4.4.5)$$

where

$$\beta = \left(\frac{1}{2} - \frac{\mu}{\sigma^2} \right) - \sqrt{\left(\frac{\mu}{\sigma^2} - \frac{1}{2} \right)^2 + \frac{2r}{\sigma^2}},$$

and s^β is a decreasing and convex solution to (4.2.1). In addition, we have

$$\begin{aligned} & E_s \left\{ \int_0^\infty e^{-rt} |(\mathcal{L}^S - r)(1 - e^{-\gamma\nu st})| dt \right\} \\ &= \mathbb{E}_s \left\{ \int_0^\infty e^{-rt} \left| e^{-\gamma\nu st} \left(\mu\gamma\nu st - \frac{\sigma^2\gamma^2\nu^2 s^2}{2} - r e^{\gamma\nu st} + r \right) \right| dt \right\} \\ &< \mathbb{E}_s \left\{ \int_0^\infty e^{-rt} \left(1 + \frac{\sigma^2}{2} + r \right) dt \right\} = \frac{1}{r} + \frac{\sigma^2}{2r} + 1 < \infty. \end{aligned} \quad (4.4.6)$$

The limits in (4.4.5) and condition (4.4.6) together imply that the function $1 - e^{-\gamma\nu s}$ admits the following analytic representation:

$$\begin{aligned} 1 - e^{-\gamma\nu s} &= -s^\beta \int_0^s \Psi^S(v) (\mathcal{L}^S - r) (1 - e^{-\gamma\nu v}) dv \\ &\quad - s^\alpha \int_s^{+\infty} \Phi^S(v) (\mathcal{L}^S - r) (1 - e^{-\gamma\nu v}) dv, \end{aligned} \quad (4.4.7)$$

where

$$\Psi^S(s) = \frac{2s^\alpha}{\sigma^2 s^2 \mathcal{W}^S(s)}, \quad \Phi^S(s) = \frac{2s^\beta}{\sigma^2 s^2 \mathcal{W}^S(s)},$$

and

$$\mathcal{W}^S(s) = \frac{2\sqrt{\left(\mu - \frac{\sigma^2}{2}\right)^2 + 2\sigma^2 r}}{\sigma^2} s^{-\frac{2\mu}{\sigma^2}} > 0, \quad \forall s \in \mathbb{R}_+.$$

We refer the reader to Section 2 of Zervos et al. [2013] and Chapter 2 of Borodin and Salminen [2002] for details on the representation.

Next, dividing $1 - e^{-\gamma\nu s}$ by s^α and differentiating in s , we have

$$\left(\frac{1 - e^{-\gamma\nu s}}{s^\alpha}\right)' = \frac{\gamma\nu e^{-\gamma\nu s} s^\alpha - (1 - e^{-\gamma\nu s}) \alpha s^{\alpha-1}}{s^{2\alpha}}. \quad (4.4.8)$$

The crucial step is to recognize that finding the root to the derivative in (4.4.8) is equivalent to solving (4.4.4). Furthermore, appealing to (4.4.7), the LHS of (4.4.8) becomes

$$\begin{aligned} \left(\frac{1 - e^{-\gamma\nu s}}{s^\alpha}\right)' &= -\left(\frac{s^\beta}{s^\alpha}\right)' \int_0^s \Psi^S(v)(\mathcal{L}^S - r)(1 - e^{-\gamma\nu v}) dv \\ &\quad - \frac{s^\beta}{s^\alpha} \Psi^S(s)(\mathcal{L}^S - r)(1 - e^{-\gamma\nu s}) + \Phi^S(s)(\mathcal{L}^S - r)(1 - e^{-\gamma\nu s}) \\ &= \frac{\mathcal{W}^S(s)}{s^{2\alpha}} \int_0^s \Psi^S(v)(\mathcal{L}^S - r)(1 - e^{-\gamma\nu v}) dv = \frac{\mathcal{W}^S(s)}{s^{2\alpha}} q_e(s), \end{aligned}$$

where

$$q_e(s) := \int_0^s \Psi^S(v)(\mathcal{L}^S - r)(1 - e^{-\gamma\nu v}) dv.$$

Since both $s^{2\alpha}$ and $\mathcal{W}^S(s)$ are strictly positive for $s > 0$, we conclude that (4.4.4) is equivalent to the equation $q_e(a_e) = 0$. By differentiating, we obtain $q_e'(s) = \Psi^S(s)(\mathcal{L}^S - r)(1 - e^{-\gamma\nu s})$. Since $\Psi^S(s) > 0$ for all $s \in \mathbb{R}_+$, the sign of $q_e'(s)$ depends solely on $(\mathcal{L}^S - r)(1 - e^{-\gamma\nu s})$, and thus on g defined in (4.4.2). The function g is strictly concave on \mathbb{R}_+ . Since $g'_+(0) = (\mu - r)\gamma\nu > 0$, the maximum of g is strictly positive. This implies that there exists a unique positive φ such that $g(\varphi) = 0$. Consequently, we have

$$q_e'(s) \begin{cases} > 0 & \text{if } s < \varphi, \\ < 0 & \text{if } s > \varphi. \end{cases}$$

This together with the fact that $q_e(0) = 0$, lead us to conclude that there exists a unique $a_e > 0$ such that $q_e(a_e) = 0$ if and only if $\lim_{s \rightarrow +\infty} q_e(s) < 0$. The latter holds due to the facts:

$$\begin{aligned} q_e(s) &= \frac{s^{2\alpha}}{\mathcal{W}^S(s)} \left(\frac{1 - e^{-\gamma\nu s}}{s^\alpha}\right)', & \frac{1 - e^{-\gamma\nu s}}{s^\alpha} > 0, \quad \forall s \in [0, +\infty), \\ \lim_{s \rightarrow +\infty} \frac{1 - e^{-\gamma\nu s}}{s^\alpha} &= 0. \end{aligned}$$

Therefore, we conclude that there exists a unique finite root a_e to equation (4.4.4). Furthermore, by the nature of q_e we have

$$a_e > \varphi \quad \text{and} \quad q_e(s) > 0, \quad \forall s < a_e.$$

Finally, from (4.4.3) we deduce that $A = (1 - e^{-\gamma\nu a_e})a_e^{-\alpha} > 0$.

Next, we verify the optimality of the candidate solution using the variational inequality (4.1.5). First, observe that $1 - e^{-\gamma\nu s} - V_e(s) = 0$ on $[a_e, +\infty)$, and $V_e(s) \geq 1 - e^{-\gamma\nu s}$ for all $s \in [0, a_e)$. Lastly, the inequality $(\mathcal{L}^S - r)(1 - e^{-\gamma\nu s}) \leq 0$ follows from

$$\begin{aligned} (\mathcal{L}^S - r)(1 - e^{-\gamma\nu s}) &= (\mathcal{L}^S - r)As^\alpha = 0, \quad \text{for } s \in [0, a_e), \\ (\mathcal{L}^S - r)(1 - e^{-\gamma\nu s}) &\leq 0, \quad \text{for } s \in [a_e, +\infty). \end{aligned}$$

Hence, $V_e(s, \nu)$ given in Theorem 4.2.1 is indeed optimal.

Proof of Theorem 4.2.2 (Log Utility). For any fixed ν , νS follows a GBM process with the same drift and volatility parameters as S . In other words, we can reduce the problem to that of selling a *single* unit of a risky asset whose price process is $\tilde{S} := \nu S$ with initial value $\tilde{S}_0 = \tilde{s} := \nu s$. Therefore, we construct a candidate solution of the form $V_l(s, \nu) = V_l(\tilde{s}, 1) = B\tilde{s}^\alpha$, where B is a positive constant. The value-matching and smooth-pasting conditions are

$$\begin{aligned} B\tilde{a}^\alpha &= U_l(\tilde{a}) = \log(\tilde{a}), \\ B\alpha\tilde{a}^{\alpha-1} &= U'_l(\tilde{a}) = \frac{1}{\tilde{a}}. \end{aligned} \tag{4.4.9}$$

These equations can be solved explicitly to give a unique solution $\tilde{a} = \exp(\alpha^{-1})$ and consequently the coefficient $B = 1/\alpha e > 0$. The optimal aggregate selling price \tilde{a} translates into the optimal unit selling price $a_l = \tilde{a}/\nu = \nu^{-1} \exp(\alpha^{-1})$.

Next, we show that $V_l(s, \nu) = V_l(\tilde{s}, 1) \equiv V_l(\tilde{s})$ given in Theorem 4.2.2 indeed satisfies the variational inequality

$$\max\{(\mathcal{L}^{\tilde{S}} - r)V_l(\tilde{s}), \log(\tilde{s}) - V_l(\tilde{s})\} = 0, \quad \tilde{s} \in \mathbb{R}_+,$$

where $\mathcal{L}^{\tilde{S}}$ is the infinitesimal generator of the GBM process \tilde{S} . This is equivalent to showing that $V_l(s, \nu)$ in (4.2.2) satisfies the variational inequality (4.1.5). First, on $[0, \tilde{a})$ we have $(\mathcal{L}^{\tilde{S}} - r)V_l(\tilde{s}) = (\mathcal{L}^{\tilde{S}} - r)B\tilde{s}^\alpha = 0$. Next, observe that the function

$$(\mathcal{L}^{\tilde{S}} - r) \log(\tilde{s}) = -\frac{\sigma^2}{2} + \mu - r \log(\tilde{s}),$$

has a unique root at $\tilde{\varphi} = e^{\frac{\mu - \sigma^2/2}{r}}$ such that

$$(\mathcal{L}^{\tilde{S}} - r) \log(\tilde{s}) \begin{cases} > 0 & \text{if } \tilde{s} < \tilde{\varphi}, \\ < 0 & \text{if } \tilde{s} > \tilde{\varphi}. \end{cases}$$

On $[\tilde{a}, +\infty)$, we have $(\mathcal{L}^{\tilde{S}} - r)V_l(\tilde{s}, 1) = (\mathcal{L}^{\tilde{S}} - r) \log(\tilde{s})$. To show that $(\mathcal{L}^{\tilde{S}} - r)V_l(\tilde{s}, 1) \leq 0$ we need to prove that $\tilde{a} > \tilde{\varphi}$, or equivalently,

$$\frac{1}{\alpha} > \frac{\mu - \sigma^2/2}{r}.$$

This follows directly from the definition of α in (4.2.2).

Next, we check that $V_l(\tilde{s}, 1) \geq \log(\tilde{s})$ for all $\tilde{s} \in \mathbb{R}_+$. Since $V_l(\tilde{s}, 1) = \log(\tilde{s})$ on $[\tilde{a}, +\infty)$, it remains to show that $\log(\tilde{s}) \leq V_l(\tilde{s}, 1)$ on $[0, \tilde{a})$. Using (4.4.9), the desired inequality is equivalent to

$$\frac{\log(\tilde{s})}{\tilde{s}^\alpha} \leq \frac{\log(\tilde{a})}{\tilde{a}^\alpha}. \quad (4.4.10)$$

Differentiating the left-hand side, we get

$$\left(\frac{\log(\tilde{s})}{\tilde{s}^\alpha} \right)' = \frac{\tilde{s}^{\alpha-1} - \alpha \tilde{s}^{\alpha-1} \log(\tilde{s})}{\tilde{s}^{2\alpha}} = \frac{1 - \alpha \log(\tilde{s})}{\tilde{s}^{\alpha+1}}.$$

The function $\frac{\log(\tilde{s})}{\tilde{s}^\alpha}$ is strictly increasing for $\tilde{s} < \exp(\alpha^{-1})$. Hence, inequality (4.4.10) follows.

4.4.2 XOU Model

Proof of Theorem 4.2.4 (Exponential Utility). Recall that the functions F and G (see (4.2.5) and (4.2.6)) are respectively increasing and decreasing. Since the exponential utility U_e is strictly increasing, we postulate that the solution to the variational inequality (4.1.7) is of the form $KF(x)$, where K is a positive coefficient to be determined. By grouping ν with γ , the problem of selling ν units of the risky asset can be reduced to that of selling a single unit. The value-matching and smooth-pasting conditions are

$$KF(b_e) = 1 - \exp(-\gamma\nu e^{b_e}), \quad (4.4.11)$$

$$KF'(b_e) = \gamma\nu e^{b_e} \exp(-\gamma\nu e^{b_e}). \quad (4.4.12)$$

Using (4.4.11), we have $K = (1 - \exp(-\gamma\nu e^{b_e}))F(b_e)^{-1} > 0$. Combining (4.4.11) and (4.4.12), we obtain (4.2.8) for b_e .

Next, we want to establish that

$$\mathbb{E}_x \left\{ \int_0^\infty e^{-rt} |(\mathcal{L}^X - r)(1 - \exp(-\gamma\nu e^{X_t}))| dt \right\} < \infty. \quad (4.4.13)$$

First, using (4.1.8) we compute

$$\begin{aligned} (\mathcal{L}^X - r)(1 - \exp(-\gamma\nu e^x)) &= \frac{\eta^2}{2} \gamma\nu e^x \exp(-\gamma\nu e^x)(1 - \gamma\nu e^x) \\ &\quad + \kappa(\theta - x)\gamma\nu e^x \exp(-\gamma\nu e^x) \\ &\quad - r(1 - \exp(-\gamma\nu e^x)). \end{aligned}$$

Then, for any $T > 0$,

$$\begin{aligned} &\mathbb{E}_x \left\{ \int_0^T e^{-rt} |(\mathcal{L}^X - r)(1 - \exp(-\gamma\nu e^{X_t}))| dt \right\} \\ &< \mathbb{E}_x \left\{ \int_0^T e^{-rt} \left(\frac{\eta^2}{2} (1 + \gamma\nu e^{X_t}) + \kappa|\theta| + \kappa|X_t| + r \right) dt \right\} \\ &= \int_0^T e^{-rt} \left(\frac{\eta^2}{2} + \frac{\eta^2\gamma\nu}{2} \mathbb{E}_x \{e^{X_t}\} + \kappa|\theta| + \kappa\mathbb{E}_x \{|X_t|\} + r \right) dt \\ &< \frac{\eta^2}{2r} + \frac{\eta^2\gamma\nu}{2r} e^{|x|+|\theta|+\frac{\eta^2}{4\kappa}} + \frac{\kappa|\theta|}{r} + \frac{\kappa}{r} \left(\sqrt{\frac{\eta^2}{\pi\kappa}} + |x| + |\theta| \right) + 1, \end{aligned}$$

where we have used the fact that $|X_t|$ conditioned on $X_0 = x$ has a folded normal distribution. Furthermore, since this bound is time-independent and finite, we deduce that (4.4.13) is indeed true. We follow the arguments in Section 2 of Zervos et al. [2013] to obtain the representation

$$\begin{aligned} 1 - \exp(-\gamma\nu e^x) &= -G(x) \int_{-\infty}^x \Psi^X(v)(\mathcal{L}^X - r)(1 - \exp(-\gamma\nu e^v)) dv \\ &\quad - F(x) \int_x^{+\infty} \Phi^X(v)(\mathcal{L}^X - r)(1 - \exp(-\gamma\nu e^v)) dv, \end{aligned} \quad (4.4.14)$$

where

$$\Psi^X(x) := \frac{2F(x)}{\eta^2 \mathcal{W}^X(x)}, \quad \Phi^X(x) := \frac{2G(x)}{\eta^2 \mathcal{W}^X(x)}, \quad (4.4.15)$$

and

$$\mathcal{W}^X(x) = F'(x)G(x) - F(x)G'(x) > 0, \quad \forall x \in \mathbb{R}.$$

To see the connection between (4.4.14) and (4.2.8), we divide both sides of (4.4.14) by $F(x)$ and differentiate with respect to x , and get the derivative

$$\begin{aligned} &\left(\frac{1 - \exp(-\gamma\nu e^x)}{F(x)} \right)' \\ &= \frac{\gamma\nu e^x \exp(-\gamma\nu e^x) F(x) - (1 - \exp(-\gamma\nu e^x)) F'(x)}{F^2(x)} \end{aligned} \quad (4.4.16)$$

$$\begin{aligned} &= - \left(\frac{G(x)}{F(x)} \right)' \int_{-\infty}^x \Psi^X(v)(\mathcal{L}^X - r) (1 - e^{-\gamma\nu e^v}) dv \\ &\quad - \frac{G(x)}{F(x)} \Psi^X(x)(\mathcal{L}^X - r) (1 - e^{-\gamma\nu e^x}) \\ &\quad + \Phi^X(x)(\mathcal{L}^X - r) (1 - e^{-\gamma\nu e^x}) \\ &= \frac{\mathcal{W}^X(x)}{F^2(x)} \int_{-\infty}^x \Psi^X(v)(\mathcal{L}^X - r) (1 - e^{-\gamma\nu e^v}) dv \\ &= \frac{\mathcal{W}^X(x)}{F^2(x)} \tilde{q}_e(x), \end{aligned} \quad (4.4.17)$$

where

$$\tilde{q}_e(x) := \int_{-\infty}^x \Psi^X(v)(\mathcal{L}^X - r) (1 - \exp(-\gamma\nu e^v)) dv. \quad (4.4.18)$$

By comparing (4.2.8) to the numerator on the RHS of (4.4.16), and given that $\frac{\mathcal{W}^X(x)}{F^2(x)}$ in (4.4.17) is strictly positive, we see that the equation satisfied by b_e in (4.2.8) is equivalent to $\tilde{q}_e(b_e) = 0$. Therefore, our goal is to show that $\tilde{q}_e(x)$ has a unique and finite root.

Differentiating (4.4.18) with respect to x yields

$$\tilde{q}'_e(x) = \Psi^X(x)(\mathcal{L}^X - r)(1 - \exp(-\gamma\nu e^x)).$$

This implies that the sign of \tilde{q}'_e depends solely on $(\mathcal{L}^X - r)(1 - \exp(-\gamma\nu e^x))$. We proceed to show that $\tilde{q}'_e(x)$ has a unique root. To facilitate computation, we define a new function

$$\begin{aligned} h(x) &:= \frac{\tilde{q}'_e(x)}{\Psi^X(x)} \times \frac{\exp(\gamma\nu e^x)}{\gamma\nu e^x} = (\mathcal{L}^X - r)(1 - \exp(-\gamma\nu e^x)) \frac{\exp(\gamma\nu e^x)}{\gamma\nu e^x} \\ &= \frac{\eta^2}{2} (1 - \gamma\nu e^x) + \kappa(\theta - x) \\ &\quad - r \left(\frac{\exp(\gamma\nu e^x)}{\gamma\nu e^x} - \frac{1}{\gamma\nu e^x} \right). \end{aligned}$$

Since h is obtained through dividing and multiplying \tilde{q}'_e by strictly positive terms, any root of \tilde{q}'_e must also be a root of h and vice-versa.

To find the root of h , we solve

$$-\frac{\eta^2\gamma\nu}{2}e^x - \frac{r}{\gamma\nu}e^{-x}(\exp(\gamma\nu e^x) - 1) = \kappa x - \kappa\theta - \frac{\eta^2\gamma\nu}{2}. \quad (4.4.19)$$

The RHS of (4.4.19) is a strictly increasing linear function. As for the LHS, we observe that

$$\begin{aligned} \lim_{x \rightarrow +\infty} -\frac{\eta^2\gamma\nu}{2}e^x - \frac{r}{\gamma\nu}e^{-x}(\exp(\gamma\nu e^x) - 1) &= -\infty, \\ \lim_{x \rightarrow -\infty} -\frac{\eta^2\gamma\nu}{2}e^x - \frac{r}{\gamma\nu}e^{-x}(\exp(\gamma\nu e^x) - 1) &= r. \end{aligned}$$

Hence, in order for h to have a unique root, it suffices to show that the LHS of (4.4.19) is strictly decreasing. Given that $r, \gamma, \nu > 0$ and e^x is strictly

increasing, it remains to show that the function $e^{-x} (\exp(\gamma\nu e^x) - 1)$ is strictly increasing for all $x \in \mathbb{R}$. The quotient rule gives

$$\left(\frac{\exp(\gamma\nu e^x) - 1}{e^x} \right)' = \frac{\exp(\gamma\nu e^x) (\gamma\nu e^x - 1) + 1}{e^x}.$$

The numerator $\exp(\gamma\nu e^x) (\gamma\nu e^x - 1) + 1$ goes to $+\infty$ as x goes to $+\infty$ and goes to 0 as x goes to $-\infty$. Moreover, the derivative of $\exp(\gamma\nu e^x) (\gamma\nu e^x - 1) + 1$ is $\gamma^2\nu^2 e^{2x} \exp(\gamma\nu e^x)$ which is strictly positive. This proves that the function $e^{-x} (\exp(\gamma\nu e^x) - 1)$ is indeed strictly increasing and as a result, h has a unique root, denoted by ζ . Finally, observe that

$$\tilde{q}'_e(x) = \begin{cases} > 0 & \text{if } x < \zeta, \\ < 0 & \text{if } x > \zeta. \end{cases} \quad (4.4.20)$$

Combining (4.4.20) with $\lim_{x \rightarrow -\infty} \tilde{q}_e(x) = 0$, we now see that a unique root, b_e , such that $\tilde{q}_e(b_e) = 0$, exists if and only if $\lim_{x \rightarrow +\infty} \tilde{q}_e(x) < 0$. To examine this limit, we apply the definition of F to get

$$\tilde{q}_e(x) = \frac{F^2(x)}{\mathcal{W}^X(x)} \left(\frac{1 - \exp(-\gamma\nu e^x)}{F(x)} \right)', \quad (4.4.21)$$

$$\frac{1 - \exp(-\gamma\nu e^x)}{F(x)} > 0, \quad \forall x \in \mathbb{R}, \quad \lim_{x \rightarrow +\infty} \frac{1 - \exp(-\gamma\nu e^x)}{F(x)} = \frac{1}{+\infty} = 0. \quad (4.4.22)$$

Since \tilde{q}_e is strictly decreasing in $(\zeta, +\infty)$, (4.4.21) and (4.4.22) hold if and only if $\lim_{x \rightarrow +\infty} \tilde{q}_e(x) < 0$. This shows, as desired, that there exists a unique and finite b_e such that

$$\gamma\nu e^{b_e} \exp(-\gamma\nu e^{b_e}) F(b_e) = (1 - \exp(-\gamma\nu e^{b_e})) F'(b_e).$$

Moreover, by (4.4.20), we see that

$$b_e > \zeta \quad \text{and} \quad \tilde{q}_e(x) > 0, \quad \forall x < b_e. \quad (4.4.23)$$

Now, in order to ascertain the optimality of \tilde{V}_e presented in (4.2.7), we re-express \tilde{V}_e in terms of the variable x , and show that it satisfies the following variational inequality:

$$\max\{(\mathcal{L}^X - r)\tilde{V}_e(e^x), (1 - \exp(-\gamma\nu e^x)) - \tilde{V}_e(e^x)\} = 0, \quad \forall x \in \mathbb{R}.$$

Indeed, this follows from direct substitution. First, on $[b_e, +\infty)$, we have

$$(1 - \exp(-\gamma\nu e^x)) - \tilde{V}_e(e^x) = (1 - \exp(-\gamma\nu e^x)) - (1 - \exp(-\gamma\nu e^x)) = 0.$$

On $(-\infty, b_e)$, we apply (4.4.21) and (4.4.23) to conclude that

$$(1 - \exp(-\gamma\nu e^x)) - \tilde{V}_e(e^x) = (1 - \exp(-\gamma\nu e^x)) - \frac{1 - \exp(-\gamma\nu e^{b_e})}{F(b_e)}F(x) \leq 0.$$

Next, we verify that $(\mathcal{L}^X - r)\tilde{V}_e(e^x) \leq 0, \forall x \in \mathbb{R}$. To this end, we have

$$(\mathcal{L}^X - r)\tilde{V}_e(e^x) = (\mathcal{L}^X - r)KF(x) = 0, \quad \text{on } (-\infty, b_e),$$

$$(\mathcal{L}^X - r)\tilde{V}_e(e^x) = (\mathcal{L}^X - r)(1 - \exp(-\gamma\nu e^x)) \leq 0, \quad \text{on } [b_e, +\infty),$$

as a consequence of (4.2.4) and (4.4.20). Hence, we conclude the optimality of \tilde{V}_e in (4.2.7).

Proof of Theorem 4.2.5 (Log Utility). Since $\log(\nu\xi) = X + \log(\nu)$ where X is an OU process, the optimal asset sale problem can be viewed as that under an OU process with a linear utility and a transaction cost (resp. reward) of value $\log(\nu)$ if $\nu < 1$ (resp. $\nu > 1$) (see Leung and Li [2015]).

The functions F and G given in (4.2.5) and (4.2.6) are respectively strictly increasing and decreasing functions. For any given ν , $X + \log(\nu)$ is also a strictly increasing function. This prompts us to postulate a solution to the variational inequality (4.1.7) of the form $DF(x)$ where $D > 0$ is a constant to be determined. Consequently, the optimal log-price threshold b_l is determined from the following value-matching and smooth-pasting conditions:

$$DF(b_l) = b_l + \log(\nu), \quad \text{and} \quad DF'(b_l) = 1.$$

Combining these equations leads to (4.2.9) and (4.2.10). Straightforward computation yields

$$(\mathcal{L}^X - r)(x + \log(\nu)) = -(\kappa + r)x + \kappa\theta - r \log(\nu),$$

which is a strictly decreasing linear function with a unique root ℓ . For any $T > 0$,

$$\begin{aligned} & \mathbb{E}_x \left\{ \int_0^T e^{-rt} |(\mathcal{L}^X - r)(X_t + \log(\nu))| dt \right\} \\ & < \mathbb{E}_x \left\{ \int_0^T e^{-rt} ((\kappa + r)|X_t| + \kappa|\theta| + r|\log(\nu)|) dt \right\} \\ & = \int_0^T e^{-rt} ((\kappa + r)\mathbb{E}_x\{|X_t|\} + \kappa|\theta| + r|\log(\nu)|) dt \\ & < \frac{\kappa + r}{r} \left(\sqrt{\frac{\eta^2}{\pi\kappa}} + |x| + |\theta| \right) + \frac{\kappa|\theta|}{r} + |\log(\nu)|, \end{aligned}$$

which implies that

$$\mathbb{E}_x \left\{ \int_0^\infty e^{-rt} |(\mathcal{L}^X - r)(X_t + \log(\nu))| dt \right\} < \infty.$$

With this, we follow the arguments in Section 2 of Zervos et al. [2013] to obtain the representation

$$\begin{aligned} x + \log(\nu) = & -G(x) \int_{-\infty}^x \Psi^X(v)(\mathcal{L}^X - r)(v + \log(\nu)) dv \quad (4.4.24) \\ & -F(x) \int_x^{+\infty} \Phi^X(v)(\mathcal{L}^X - r)(v + \log(\nu)) dv, \end{aligned}$$

where Ψ^X and Φ^X are as defined in (4.4.15). We relate (4.4.24) to (4.2.10) by first dividing both sides of (4.4.24) by $F(x)$ and differentiating with respect to

x . This yields

$$\begin{aligned}
& \left(\frac{x + \log(\nu)}{F(x)} \right)' \\
&= \frac{F(x) - F'(x)(x + \log(\nu))}{F^2(x)} \\
&= - \left(\frac{G(x)}{F(x)} \right)' \int_{-\infty}^x \Psi^X(v)(\mathcal{L}^X - r)(v + \log(\nu)) dv \\
&\quad - \frac{G(x)}{F(x)} \Psi^X(x)(\mathcal{L}^X - r)(x + \log(\nu)) + \Phi^X(x)(\mathcal{L}^X - r)(x + \log(\nu)) \\
&= \frac{\mathcal{W}^X(x)}{F^2(x)} \int_{-\infty}^x \Psi^X(v)(\mathcal{L}^X - r)(v + \log(\nu)) dv = \frac{\mathcal{W}^X(x)}{F^2(x)} \tilde{q}_l(x),
\end{aligned} \tag{4.4.25}$$

where

$$\tilde{q}_l(x) := \int_{-\infty}^x \Psi^X(v)(\mathcal{L}^X - r)(v + \log(\nu)) dv.$$

Comparing (4.2.10) and the RHS of (4.4.25), along with the facts that $F > 0$ and $\mathcal{W}^X > 0$, we see that solving equation (4.2.10) for the log-price threshold is equivalent to solving

$$\tilde{q}_l(x) = 0.$$

Direct differentiation yields that

$$\tilde{q}'_l(x) = \Psi^X(x)(\mathcal{L}^X - r)(x + \log(\nu)) \begin{cases} > 0 & \text{if } x < \ell, \\ < 0 & \text{if } x > \ell. \end{cases} \tag{4.4.26}$$

The fact that $\lim_{x \rightarrow -\infty} \tilde{q}_l(x) = 0$ implies that there exists a unique b_l such that $\tilde{q}_l(b_l) = 0$ if and only if $\lim_{x \rightarrow +\infty} \tilde{q}_l(x) < 0$. By the definition of F , we have

$$\begin{aligned}
\tilde{q}_l(x) &= \frac{F^2(x)}{\mathcal{W}^X(x)} \left(\frac{x + \log(\nu)}{F(x)} \right)', \quad \frac{x + \log(\nu)}{F(x)} > 0, \quad \forall x > -\log(\nu) \\
\lim_{x \rightarrow +\infty} \frac{x + \log(\nu)}{F(x)} &= 0.
\end{aligned} \tag{4.4.27}$$

Given that \tilde{q}_l is strictly decreasing in $(\ell, +\infty)$, we conclude that in order for (4.4.27) to hold, we must have $\lim_{x \rightarrow +\infty} \tilde{q}_l(x) < 0$. This means that there

exists a unique and finite b_l such that $(b_l + \log(\nu))F'(b_l) = F(b_l)$. Moreover, given (4.4.26), we have

$$b_l > \ell \quad \text{and} \quad \tilde{q}_l(x) > 0, \quad \forall x < b_l. \quad (4.4.28)$$

Furthermore, since both F and F' are strictly positive, $b_l + \log(\nu)$ must also be positive.

Lastly, we need to check that the following variational inequality holds for any fixed ν :

$$\max\{(\mathcal{L}^X - r)\tilde{V}_l(e^x), (x + \log(\nu)) - \tilde{V}_l(e^x)\} = 0, \quad \forall x \in \mathbb{R}.$$

To begin, on the interval $[b_l, +\infty)$, we have $(x + \log(\nu)) - \tilde{V}_l(e^x) = (x + \log(\nu)) - (x + \log(\nu)) = 0$. Next, on the region $(-\infty, b_l)$, we have

$$(x + \log(\nu)) - \tilde{V}_l(e^x) = (x + \log(\nu)) - \frac{b_l + \log(\nu)}{F(b_l)}F(x) \leq 0$$

since the function $\frac{x + \log(\nu)}{F(x)}$ is increasing on $(-\infty, b_l)$ due to (4.4.27) and (4.4.28).

Also, we note that

$$\begin{aligned} (\mathcal{L}^X - r)\tilde{V}_l(e^x) &= (\mathcal{L}^X - r)DF(x) = 0, & \text{on } (-\infty, b_l), \\ (\mathcal{L}^X - r)\tilde{V}_l(e^x) &= (\mathcal{L}^X - r)(x + \log(\nu)) \leq 0, & \text{on } [b_l, +\infty). \end{aligned}$$

The latter inequality is true due to (4.4.26) and (4.4.28). \tilde{V}_l defined in Theorem 4.2.5 is therefore the optimal solution to the optimal asset sale problem under log utility.

Proof of Theorem 4.2.6 (Power Utility). Since the powered XOU process, ξ^p , is still an XOU process, the asset sale problem is an optimal stopping problem driven by an XOU process, which has been solved by the author's prior work; see Theorem 3.1.1 of Leung et al. [2015]. The theorem is also presented in this dissertation as Theorem 2.2.2 of Chapter 2. Therefore, we omit the proof.

Bibliography

- Abramowitz, M. and Stegun, I. (1965). *Handbook of Mathematical Functions: with Formulas, Graphs, and Mathematical Tables*, volume 55. Dover Publications.
- Acworth, W. (2016). 2015 annual survey: Global derivatives volume. [Online; posted 15-March-2016].
- Alili, L., Patie, P., and Pedersen, J. (2005). Representations of the first hitting time density of an Ornstein-Uhlenbeck process. *Stochastic Models*, 21(4):967–980.
- Anthony, M. and MacDonald, R. (1998). On the mean-reverting properties of target zone exchange rates: Some evidence from the ERM. *European Economic Review*, 42(8):1493–1523.
- Bali, T. G. and Demirtas, K. O. (2008). Testing mean reversion in financial market volatility: Evidence from S&P 500 index futures. *Journal of Futures Markets*, 28(1):1–33.
- Balvers, R., Wu, Y., and Gilliland, E. (2000). Mean reversion across national stock markets and parametric contrarian investment strategies. *The Journal of Finance*, 55(2):745–772.
- Benth, F. E. and Karlsen, K. H. (2005). A note on Merton’s portfolio selection

- problem for the Schwartz mean-reversion model. *Stochastic Analysis and Applications*, 23(4):687–704.
- Bessembinder, H., Coughenour, J. F., Seguin, P. J., and Smoller, M. M. (1995). Mean reversion in equilibrium asset prices: Evidence from the futures term structure. *The Journal of Finance*, 50(1):361–375.
- Borodin, A. and Salminen, P. (2002). *Handbook of Brownian Motion: Facts and Formulae*. Birkhauser, 2nd edition.
- Brennan, M. J. and Schwartz, E. S. (1990). Arbitrage in stock index futures. *Journal of Business*, 63(1):S7–S31.
- Carmona, J. and León, A. (2007). Investment option under CIR interest rates. *Finance Research Letters*, 4(4):242–253.
- Cartea, A., Jaimungal, S., and Penalva, J. (2015). *Algorithmic and High-Frequency Trading*. Cambridge University Press, Cambridge, England.
- Casassus, J. and Collin-Dufresne, P. (2005). Stochastic convenience yield implied from commodity futures and interest rates. *The Journal of Finance*, 60(5):2283–2331.
- Chiu, M. C. and Wong, H. Y. (2012). Dynamic cointegrated pairs trading: Time-consistent mean-variance strategies. Technical report, working paper.
- Cox, J. C., Ingersoll, J., and Ross, S. A. (1981). The relation between forward prices and futures prices. *Journal of Financial Economics*, 9(4):321–346.
- Cox, J. C., Ingersoll, J. E., and Ross, S. A. (1985). A theory of the term structure of interest rates. *Econometrica*, 53(2):385–408.
- Dai, M., Zhong, Y., and Kwok, Y. K. (2011). Optimal arbitrage strategies on stock index futures under position limits. *Journal of Futures Markets*, 31(4):394–406.

- Detemple, J. and Osakwe, C. (2000). The valuation of volatility options. *European Finance Review*, 4(1):21–50.
- Ekström, E., Lindberg, C., and Tysk, J. (2011). Optimal liquidation of a pairs trade. In Nunno, G. D. and Øksendal, B., editors, *Advanced Mathematical Methods for Finance*, chapter 9, pages 247–255. Springer-Verlag.
- Ekström, E. and Vaicenavicius, J. (2016). Optimal liquidation of an asset under drift uncertainty. *Working Paper*.
- Elton, E. J., Gruber, M. J., Brown, S. J., and Goetzmann, W. N. (2009). *Modern Portfolio Theory and Investment Analysis*. Wiley, 8th edition.
- Engel, C. and Hamilton, J. D. (1989). Long swings in the exchange rate: Are they in the data and do markets know it? Technical report, National Bureau of Economic Research.
- Erdélyi, A., Magnus, W., Oberhettinger, F., and Tricomi, F. G. (1953). *Higher Transcendental Functions*, volume 2. McGraw-Hill.
- Evans, J., Henderson, V., and Hobson, D. (2008). Optimal timing for an indivisible asset sale. *Mathematical Finance*, 18(4):545–567.
- Ewald, C.-O. and Wang, W.-K. (2010). Irreversible investment with Cox-Ingersoll-Ross type mean reversion. *Mathematical Social Sciences*, 59(3):314–318.
- Feller, W. (1951). Two singular diffusion problems. *The Annals of Mathematics*, 54(1):173–182.
- Geman, H. (2007). Mean reversion versus random walk in oil and natural gas prices. In Fu, M. C., Jarrow, R. A., Yen, J.-Y. J., and Elliot, R. J., editors, *Advances in Mathematical Finance*, Applied and Numerical Harmonic Analysis, pages 219–228. Birkhuser Boston.

- Göing-Jaeschke, A. and Yor, M. (2003). A survey and some generalizations of Bessel processes. *Bernoulli*, 9(2):313–349.
- Gorton, G. B., Hayashi, F., and Rouwenhorst, K. G. (2013). The fundamentals of commodity futures returns. *Review of Finance*, 17(1):35–105.
- Gropp, J. (2004). Mean reversion of industry stock returns in the US, 1926–1998. *Journal of Empirical Finance*, 11(4):537–551.
- Grübichler, A. and Longstaff, F. (1996). Valuing futures and options on volatility. *Journal of Banking and Finance*, 20(6):985–1001.
- Guo, X. and Zervos, M. (2010). π options. *Stochastic processes and their applications*, 120(7):1033–1059.
- Henderson, V. (2007). Valuing the option to invest in an incomplete market. *Mathematics and Financial Economics*, 1(2):103–128.
- Henderson, V. (2012). Prospect theory, liquidation, and the disposition effect. *Management Science*, 58(2):445–460.
- Henderson, V. and Hobson, D. (2011). Optimal liquidation of derivative portfolios. *Mathematical Finance*, 21(3):365–382.
- Heston, S. L. (1993). A closed form solution for options with stochastic volatility with applications to bond and currency options. *Review of Financial Studies*, 6:327–343.
- Irwin, S. H., Zulauf, C. R., and Jackson, T. E. (1996). Monte Carlo analysis of mean reversion in commodity futures prices. *American Journal of Agricultural Economics*, 78(2):387–399.
- Itô, K. and McKean, H. (1965). *Diffusion processes and their sample paths*. Springer Verlag.

- Jurek, J. W. and Yang, H. (2007). Dynamic portfolio selection in arbitrage. Working Paper, Princeton University.
- Karlin, S. and Taylor, H. M. (1981). *A Second Course in Stochastic Processes*, volume 2. Academic Press.
- Kong, H. T. and Zhang, Q. (2010). An optimal trading rule of a mean-reverting asset. *Discrete and Continuous Dynamical Systems*, 14(4):1403 – 1417.
- Larsen, K. S. and Sørensen, M. (2007). Diffusion models for exchange rates in a target zone. *Mathematical Finance*, 17(2):285–306.
- Lebedev, N. (1972). *Special Functions & Their Applications*. Dover Publications.
- Leung, T., Li, J., Li, X., and Wang, Z. (2016). Speculative futures trading under mean reversion. *Asia-Pacific Financial Markets*, pages 1–24.
- Leung, T. and Li, X. (2015). Optimal mean reversion trading with transaction costs and stop-loss exit. *International Journal of Theoretical & Applied Finance*, 18(3):15500.
- Leung, T., Li, X., and Wang, Z. (2014). Optimal starting–stopping and switching of a CIR process with fixed costs. *Risk and Decision Analysis*, 5(2):149–161.
- Leung, T., Li, X., and Wang, Z. (2015). Optimal multiple trading times under the exponential OU model with transaction costs. *Stochastic Models*, 31(4):554–587.
- Leung, T. and Liu, P. (2012). Risk premia and optimal liquidation of credit derivatives. *International Journal of Theoretical & Applied Finance*, 15(8):1250059.

- Leung, T. and Ludkovski, M. (2012). Accounting for risk aversion in derivatives purchase timing. *Mathematics & Financial Economics*, 6(4):363–386.
- Leung, T. and Shirai, Y. (2015). Optimal derivative liquidation timing under path-dependent risk penalties. *Journal of Financial Engineering*, 2(1):1550004.
- Leung, T. and Wang, Z. (2016). Optimal risk-averse timing of an asset sale: Trending vs mean-reverting price dynamics. *Working Paper*.
- Lu, Z. and Zhu, Y. (2009). Volatility components: The term structure dynamics of VIX futures. *Journal of Futures Markets*, 30(3):230–256.
- Malliaropulos, D. and Priestley, R. (1999). Mean reversion in Southeast Asian stock markets. *Journal of Empirical Finance*, 6(4):355–384.
- Mencía, J. and Sentana, E. (2013). Valuation of VIX derivatives. *Journal of Financial Economics*, 108(2):367–391.
- Metcalf, G. E. and Hassett, K. A. (1995). Investment under alternative return assumptions comparing random walks and mean reversion. *Journal of Economic Dynamics and Control*, 19(8):1471–1488.
- Monoyios, M. and Sarno, L. (2002). Mean reversion in stock index futures markets: a nonlinear analysis. *The Journal of Futures Markets*, 22(4):285–314.
- Moskowitz, T. J., Ooi, Y. H., and Pedersen, L. H. (2012). Time series momentum. *Journal of Financial Economics*, 104(2):228–250.
- Øksendal, B. (2003). *Stochastic Differential Equations: an Introduction with Applications*. Springer.

- Pedersen, J. L. and Peskir, G. (2016). Optimal mean-variance selling strategies. *Mathematics and Financial Economics*, 10(2):203–220.
- Peskir, G. and Shiryaev, A. N. (2006). *Optimal Stopping and Free-boundary problems*. Birkhauser-Verlag, Lectures in Mathematics, ETH Zurich.
- Poterba, J. M. and Summers, L. H. (1988). Mean reversion in stock prices: Evidence and implications. *Journal of Financial Economics*, 22(1):27–59.
- Ribeiro, D. R. and Hodges, S. D. (2004). A two-factor model for commodity prices and futures valuation. EFMA 2004 Basel Meetings Paper.
- Rogers, L. and Williams, D. (2000). *Diffusions, Markov Processes and Martingales*, volume 2. Cambridge University Press, UK, 2nd edition.
- Schwartz, E. (1997). The stochastic behavior of commodity prices: Implications for valuation and hedging. *The Journal of Finance*, 52(3):923–973.
- Shiryaev, A., Xu, Z., and Zhou, X. (2008). Thou shalt buy and hold. *Quantitative Finance*, 8(8):765–776.
- Song, Q., Yin, G., and Zhang, Q. (2009). Stochastic optimization methods for buying-low-and-selling-high strategies. *Stochastic Analysis and Applications*, 27(3):523–542.
- Song, Q. and Zhang, Q. (2013). An optimal pairs-trading rule. *Automatica*, 49(10):3007–3014.
- Tourin, A. and Yan, R. (2013). Dynamic pairs trading using the stochastic control approach. *Journal of Economic Dynamics and Control*, 37(10):1972–1981.
- Wang, Z. and Daigler, R. T. (2011). The performance of VIX option pricing models: Empirical evidence beyond simulation. *Journal of Futures Markets*, 31(3):251–281.

- Wilmott, P., Howison, S., and Dewynne, J. (1995). *The Mathematics of Financial Derivatives: A Student Introduction*. Cambridge University Press, 1st edition.
- Zervos, M., Johnson, T., and Alazemi, F. (2013). Buy-low and sell-high investment strategies. *Mathematical Finance*, 23(3):560–578.
- Zhang, H. and Zhang, Q. (2008). Trading a mean-reverting asset: Buy low and sell high. *Automatica*, 44(6):1511–1518.
- Zhang, J. E. and Zhu, Y. (2006). VIX futures. *Journal of Futures Markets*, 26(6):521–531.
- Zhu, S.-P. and Lian, G.-H. (2012). An analytical formula for VIX futures and its applications. *Journal of Futures Markets*, 32(2):166–190.

Appendix A

Appendix for GBM Example

Let S be a geometric Brownian motion with drift and volatility parameters (μ, σ) . In this case, the optimal exit problem is trivial. Indeed, if $\mu > r$, then

$$\begin{aligned} \mathcal{V}(s) &:= \sup_{\tau \in \mathcal{T}} \mathbb{E}_s \{ e^{-r\tau} (S_\tau - c_s) \} \\ &\geq \sup_{t \geq 0} (\mathbb{E}_s \{ e^{-rt} S_t \} - e^{-rt} c_s) \geq \sup_{t \geq 0} s e^{(\mu-r)t} - c_s = +\infty. \end{aligned}$$

Therefore, it is optimal to take $\tau = +\infty$ and the value function is infinite.

If $\mu = r$, then the value function is given by

$$\begin{aligned} \mathcal{V}(s) &= \sup_{t \geq 0} \sup_{\tau \in \mathcal{T}} \mathbb{E}_s \{ e^{-r(\tau \wedge t)} (S_{\tau \wedge t} - c_s) \} \\ &= s - c_s \inf_{t \geq 0} \inf_{\tau \in \mathcal{T}} \mathbb{E}_s \{ e^{-r(\tau \wedge t)} \} = s, \end{aligned} \tag{A.0.1}$$

where the second equality follows from the optional sampling theorem and that $(e^{-rt} S_t)_{t \geq 0}$ is a martingale. Again, the optimal value is achieved by choosing $\tau = +\infty$, but $\mathcal{V}(s)$ is finite in (A.0.1).

On the other hand, if $\mu < r$, then we have a non-trivial solution and exit timing:

$$\mathcal{V}(s) = \begin{cases} \left(\frac{c_s}{\eta-1} \right)^{1-\eta} \left(\frac{s}{\eta} \right)^\eta & \text{if } x < s^*, \\ s - c_s & \text{if } x \geq s^*, \end{cases}$$

where

$$\eta = \frac{\sqrt{2r\sigma^2 + (\mu - \frac{1}{2}\sigma^2)^2} - (\mu - \frac{1}{2}\sigma^2)}{\sigma^2} \quad \text{and} \quad s^* = \frac{c_s\eta}{\eta - 1} > c_s.$$

Therefore, it is optimal to liquidate as soon as S reaches level s^* . However, it is optimal *not* to enter because $\sup_{s \in \mathbb{R}_+} (\mathcal{V}(s) - s - c_b) \leq 0$, giving a zero value for the entry timing problem. Guo and Zervos [2010] provide a detailed study on this problem and its variation in the context of π options.

Appendix B

Appendix for Chapter 2

B.1 Proof of Lemma 2.2.5 (Bounds of \tilde{J}^ξ and \tilde{V}^ξ)

By definition, both $\tilde{J}^\xi(x)$ and $\tilde{V}^\xi(x)$ are nonnegative. Using Dynkin's formula, we have

$$\begin{aligned} \mathbb{E}_x\{e^{-r\tau_n}e^{X_{\tau_n}}\} - \mathbb{E}_x\{e^{-r\nu_n}e^{X_{\nu_n}}\} &= \mathbb{E}_x\left\{\int_{\nu_n}^{\tau_n} e^{-rt}(\mathcal{L} - r)e^{X_t} dt\right\} \\ &= \mathbb{E}_x\left\{\int_{\nu_n}^{\tau_n} e^{-rt}e^{X_t}\left(\frac{\sigma^2}{2} + \mu\theta - r - \mu X_t\right) dt\right\}. \end{aligned}$$

The function $e^x\left(\frac{\sigma^2}{2} + \mu\theta - r - \mu x\right)$ is bounded above on \mathbb{R} . Let M be an upper bound, it follows that

$$\mathbb{E}_x\{e^{-r\tau_n}e^{X_{\tau_n}}\} - \mathbb{E}_x\{e^{-r\nu_n}e^{X_{\nu_n}}\} \leq M\mathbb{E}_x\left\{\int_{\nu_n}^{\tau_n} e^{-rt} dt\right\}.$$

Since $e^x - c_s \leq e^x$ and $e^x + c_b \geq e^x$, we have

$$\begin{aligned} & \mathbb{E}_x \left\{ \sum_{n=1}^{\infty} [e^{-r\tau_n} h_s^\xi(X_{\tau_n}) - e^{-r\nu_n} h_b^\xi(X_{\nu_n})] \right\} \\ & \leq \sum_{n=1}^{\infty} (E\{e^{-r\tau_n} e^{X_{\tau_n}}\} - \mathbb{E}_x\{e^{-r\nu_n} e^{X_{\nu_n}}\}) \\ & \leq \sum_{n=1}^{\infty} M \mathbb{E}_x \left\{ \int_{\nu_n}^{\tau_n} e^{-rt} dt \right\} \leq M \int_0^{\infty} e^{-rt} dt = \frac{M}{r} := C_1, \end{aligned}$$

which implies that $0 \leq \tilde{J}^\xi(x) \leq C_1$. Similarly,

$$\begin{aligned} & \mathbb{E}_x \left\{ e^{-r\tau_1} h_s^\xi(X_{\tau_1}) + \sum_{n=2}^{\infty} [e^{-r\tau_n} h_s^\xi(X_{\tau_n}) - e^{-r\tau_n} h_b^\xi(X_{\tau_n})] \right\} \\ & \leq C_1 + \mathbb{E}_x\{e^{-r\tau_1} h_b^\xi(X_{\tau_1})\}. \end{aligned}$$

Letting $\nu_1 = 0$ and using Dynkin's formula again, we have

$$\mathbb{E}_x\{e^{-r\tau_1} e^{X_{\tau_1}}\} - e^x \leq \frac{M}{r}.$$

This implies that

$$\tilde{V}^\xi(x) \leq C_1 + e^x + \frac{M}{r} := e^x + C_2.$$

B.2 Proof of Lemma 2.2.12 (Bounds of \tilde{J}^χ and \tilde{V}^χ)

By definition, both $\tilde{J}^\chi(y)$ and $\tilde{V}^\chi(y)$ are nonnegative. Using Dynkin's formula, we have

$$\begin{aligned} \mathbb{E}_y\{e^{-r\tau_n} Y_{\tau_n}\} - \mathbb{E}_y\{e^{-r\nu_n} Y_{\nu_n}\} &= \mathbb{E}_y \left\{ \int_{\nu_n}^{\tau_n} e^{-rt} (\mathcal{L}^\chi - r) Y_t dt \right\} \\ &= \mathbb{E}_y \left\{ \int_{\nu_n}^{\tau_n} e^{-rt} (\mu\theta - (r + \mu)Y_t) dt \right\}. \end{aligned}$$

For $y \geq 0$, the function $\mu\theta - (r + \mu)y$ is bounded by $\mu\theta$. It follows that

$$\mathbb{E}_y\{e^{-r\tau_n} Y_{\tau_n}\} - \mathbb{E}_y\{e^{-r\nu_n} Y_{\nu_n}\} \leq \mu\theta \mathbb{E}_y \left\{ \int_{\nu_n}^{\tau_n} e^{-rt} dt \right\}.$$

Since $y - c_s \leq y$ and $y + c_b \geq y$, we have

$$\begin{aligned} & \mathbb{E}_y \left\{ \sum_{n=1}^{\infty} [e^{-r\tau_n} h_s^X(Y_{\tau_n}) - e^{-r\nu_n} h_b^X(Y_{\nu_n})] \right\} \\ & \leq \sum_{n=1}^{\infty} (E\{e^{-r\tau_n} Y_{\tau_n}\} - \mathbb{E}_y\{e^{-r\nu_n} Y_{\nu_n}\}) \\ & \leq \sum_{n=1}^{\infty} \mu\theta \mathbb{E}_y \left\{ \int_{\nu_n}^{\tau_n} e^{-rt} dt \right\} \leq \mu\theta \int_0^{\infty} e^{-rt} dt = \frac{\mu\theta}{r}. \end{aligned}$$

This implies that $0 \leq \tilde{J}^X(y) \leq \frac{\mu\theta}{r}$. Similarly,

$$\mathbb{E}_y \left\{ e^{-r\tau_1} h_s^X(Y_{\tau_1}) + \sum_{n=2}^{\infty} [e^{-r\tau_n} h_s^X(Y_{\tau_n}) - e^{-r\tau_n} h_b^X(Y_{\tau_n})] \right\} \leq \frac{\mu\theta}{r} + \mathbb{E}_y \{ e^{-r\tau_1} h_b^X(Y_{\tau_1}) \}.$$

Letting $\nu_1 = 0$ and using Dynkin's formula again, we have

$$\mathbb{E}_y \{ e^{-r\tau_1} Y_{\tau_1} \} - y \leq \frac{\mu\theta}{r}.$$

This implies that

$$\tilde{V}^X(y) \leq \frac{\mu\theta}{r} + y + \frac{\mu\theta}{r} := y + \frac{2\mu\theta}{r}.$$

Appendix C

Appendix for Chapter 3

C.1 Numerical Implementation

We apply a finite difference method to compute the optimal boundaries in Figures 3.2, 3.3 and 3.4. The operators $\mathcal{L}^{(i)}$, $i \in \{1, 2, 3\}$, defined in (3.3.2)-(3.3.3) correspond to the OU, CIR, and XOU models, respectively. To capture these models, we define the generic differential operator

$$\mathcal{L}\{\cdot\} := -r \cdot + \frac{\partial \cdot}{\partial t} + \varphi(s) \frac{\partial \cdot}{\partial s} + \frac{\sigma^2(s)}{2} \frac{\partial^2 \cdot}{\partial s^2},$$

then the variational inequalities (3.3.4), (3.3.5), (3.3.6), (3.3.7) and (3.3.8) admit the same form as the following variational inequality problem:

$$\left\{ \begin{array}{l} \mathcal{L}g(t, s) \leq 0, \quad g(t, s) \geq \xi(t, s), \quad (t, s) \in [0, \hat{T}] \times \mathbb{R}_+, \\ (\mathcal{L}g(t, s))(\xi(t, s) - g(t, s)) = 0, \quad (t, s) \in [0, \hat{T}] \times \mathbb{R}_+, \\ g(\hat{T}, s) = \xi(\hat{T}, s), \quad s \in \mathbb{R}_+. \end{array} \right.$$

Here, $g(t, s)$ represents the value functions $\mathcal{V}(t, s)$, $\mathcal{J}(t, s)$, $-\mathcal{U}(t, s)$, $\mathcal{K}(t, s)$, or $\mathcal{P}(t, s)$. The function $\xi(t, s)$ represents $f(t, s; T) - c$, $(\mathcal{V}(t, s) - (f(t, s; T) + \hat{c}))^+$, $-(f(t, s; T) + \hat{c})$, $(f(t, s; T) - c) - \mathcal{U}(t, s)^+$, or $\max\{\mathcal{A}(t, s), \mathcal{B}(t, s)\}$. The futures

price $f(t, s; T)$, with $\hat{T} \leq T$, is given by (3.1.1), (3.1.4), and (3.1.10) under the OU, CIR, and XOU models, respectively.

We now consider the discretization of the partial differential equation $\mathcal{L}g(t, s) = 0$, over an uniform grid with discretizations in time ($\delta t = \frac{\hat{T}}{N}$), and space ($\delta s = \frac{S_{\max}}{M}$). We apply the Crank-Nicolson method, which involves the finite difference equation:

$$-\alpha_i g_{i-1,j-1} + (1 - \beta_i) g_{i,j-1} - \gamma_i g_{i+1,j-1} = \alpha_i g_{i-1,j} + (1 + \beta_i) g_{i,j} + \gamma_i g_{i+1,j},$$

where

$$g_{i,j} = g(j\delta t, i\delta s), \quad \xi_{i,j} = \xi(j\delta t, i\delta s), \quad \varphi_i = \varphi(i\delta s), \quad \sigma_i = \sigma(i\delta s). \\ \alpha_i = \frac{\delta t}{4\delta s} \left(\frac{\sigma_i^2}{\delta s} - \varphi_i \right), \quad \beta_i = -\frac{\delta t}{2} \left(r + \frac{\sigma_i^2}{(\delta s)^2} \right), \quad \gamma_i = \frac{\delta t}{4\delta s} \left(\frac{\sigma_i^2}{\delta s} + \varphi_i \right),$$

for $i = 1, 2, \dots, M-1$ and $j = 1, 2, \dots, N-1$. The system to be solved backward in time is

$$\mathbf{M}_1 \mathbf{g}_{j-1} = \mathbf{r}_j,$$

where the right-hand side is

$$\mathbf{r}_j = \mathbf{M}_2 \mathbf{g}_j + \alpha_1 \begin{bmatrix} g_{0,j-1} + g_{0,j} \\ 0 \\ \vdots \\ 0 \end{bmatrix} + \gamma_{M-1} \begin{bmatrix} 0 \\ \vdots \\ 0 \\ g_{M,j-1} + g_{M,j} \end{bmatrix},$$

and

$$\mathbf{M}_1 = \begin{bmatrix} 1 - \beta_1 & -\gamma_1 & & & & \\ -\alpha_2 & 1 - \beta_2 & -\gamma_2 & & & \\ & -\alpha_3 & 1 - \beta_3 & -\gamma_3 & & \\ & & \ddots & \ddots & \ddots & \\ & & & -\alpha_{M-2} & 1 - \beta_{M-2} & -\gamma_{M-2} \\ & & & & -\alpha_{M-1} & 1 - \beta_{M-1} \end{bmatrix},$$

$$\mathbf{M}_2 = \begin{bmatrix} 1 + \beta_1 & \gamma_1 & & & & \\ \alpha_2 & 1 + \beta_2 & \gamma_2 & & & \\ & \alpha_3 & 1 + \beta_3 & \gamma_3 & & \\ & & \ddots & \ddots & \ddots & \\ & & & \alpha_{M-2} & 1 + \beta_{M-2} & \gamma_{M-2} \\ & & & & \alpha_{M-1} & 1 + \beta_{M-1} \end{bmatrix},$$

$$\mathbf{g}_j = \begin{bmatrix} g_{1,j}, g_{2,j}, \dots, g_{M-1,j} \end{bmatrix}^T.$$

This leads to a sequence of stationary complementarity problems. Hence, at

each time step $j \in \{1, 2, \dots, N-1\}$, we need to solve

$$\left\{ \begin{array}{l} \mathbf{M}_1 \mathbf{g}_{j-1} \geq \mathbf{r}_j, \\ \mathbf{g}_{j-1} \geq \boldsymbol{\xi}_{j-1}, \\ (\mathbf{M}_1 \mathbf{g}_{j-1} - \mathbf{r}_j)^T (\boldsymbol{\xi}_{j-1} - \mathbf{g}_{j-1}) = 0. \end{array} \right.$$

To solve the optimal problem, our algorithm enforces the constraint explicitly as follows

$$g_{i,j-1}^{new} = \max \{g_{i,j-1}^{old}, \xi_{i,j-1}\}.$$

The projected SOR method is used to solve the linear system.¹ At each time j , we iteratively solve

$$\begin{aligned} g_{1,j-1}^{(k+1)} &= \max \left\{ \xi_{1,j-1}, g_{1,j-1}^{(k)} + \frac{\omega}{1-\beta_1} [r_{1,j} - (1-\beta_1)g_{1,j-1}^{(k)} + \gamma_1 g_{2,j-1}^{(k)}] \right\}, \\ g_{2,j-1}^{(k+1)} &= \max \left\{ \xi_{2,j-1}, g_{2,j-1}^{(k)} + \frac{\omega}{1-\beta_2} [r_{2,j} + \alpha_2 g_{1,j-1}^{(k+1)} - (1-\beta_2)g_{2,j-1}^{(k)} + \gamma_2 g_{3,j-1}^{(k)}] \right\}, \\ &\vdots \\ g_{M-1,j-1}^{(k+1)} &= \max \left\{ \xi_{M-1,j-1}, g_{M-1,j-1}^{(k)} \right. \\ &\quad \left. + \frac{\omega}{1-\beta_{M-1}} [r_{M-1,j} + \alpha_{M-1} g_{M-2,j-1}^{(k+1)} - (1-\beta_{M-1})g_{M-1,j-1}^{(k)}] \right\}, \end{aligned}$$

where k is the iteration counter and ω is the overrelaxation parameter. The iterative scheme starts from an initial point $\mathbf{g}_j^{(0)}$ and proceeds until a convergence criterion is met, such as $\|\mathbf{g}_{j-1}^{(k+1)} - \mathbf{g}_{j-1}^{(k)}\| < \epsilon$, where ϵ is a tolerance parameter. The optimal boundary $S_f(t)$ can be identified by locating the boundary that separates the regions where $g(t, s) = \xi(t, s)$, or $g(t, s) \geq \xi(t, s)$.

¹For a detailed discussion on the projected SOR method, we refer to Wilmott et al. [1995].